

---

# Systematics of Lutetian larger foraminifera and magneto-biostratigraphy from the South Pyrenean Basin (Sierras Exteriores, Spain)

---

Roi Silva-Casal<sup>1</sup>   Josep Serra-Kiel<sup>2</sup>   Adriana Rodríguez-Pintó<sup>3</sup>   Emilio L. Pueyo<sup>4,5</sup>   Marc Aurell<sup>6</sup>   Aitor Payros<sup>7</sup>

<sup>1</sup>Institut de Recerca Geomodels, Departament de Dinàmica de la Terra i de l'Oceà, Universitat de Barcelona  
Martí i Franquès s/n, 08028 Barcelona, Spain. Silva-Casal E-mail: roi.silva.casal@gmail.com

<sup>2</sup>Museu de Ciències Naturals de Barcelona, Departament de Paleontologia  
Passeig Picasso s/n, 08003 Barcelona, Spain (Deceased)

<sup>3</sup>Freelance Geologist consultor  
Rodríguez-Pintó E-mail: adrianaropi14@gmail.com

<sup>4</sup>Instituto Geológico y Minero de España, Unidad de Zaragoza  
Manuel Lasala 44, 50009 Zaragoza, Spain. Pueyo E-mail: unaim@igme.es

<sup>5</sup>Associated Unit in Earth Sciences IGME/Universidad de Zaragoza  
Spain. Pueyo E-mail: unaim@igme.es

<sup>6</sup>Department of Earth Science, University of Zaragoza  
Pedro Cerbuna 12, E50009 Zaragoza, Spain. Aurell E-mail: maurell@unizar.es

<sup>7</sup>Department of Stratigraphy and Paleontology, Faculty of Science and Technology, University of the Basque Country (UPV/EHU)  
PO Box 644, E48080 Bilbao, Spain. Payros E-mail: a.payros@ehu.eus

---

## | A B S T R A C T |

---

A systematic description of the Eocene larger foraminifera recorded in the South Pyrenean Basin (Sierras Exteriores) is presented herein. The large dataset provided in this work includes *Nummulites* and *Alveolina* species, along with a variety of other porcellaneous and hyaline taxa with lesser biostratigraphic relevance. Most of the larger foraminifera described in this work correspond to the Lutetian (SBZ13 to SBZ16 biozones) interval, but late Ypresian (SBZ11, Cuisian) and early Bartonian (SBZ17) shallow benthic zones have also been identified. A new species, *Idalina osquetaensis*, is described. The systematic revision of middle to late Lutetian alveolines led to a reassessment of *Alveolina fusiformis* and the finding of two new precursor forms, described as *Alveolina* aff. *fragilis* and *Alveolina* aff. *elongata*. The new taxa fill in the gap existing so far in the middle to late Lutetian alveolinid biostratigraphy. Despite not being exclusive to SBZ16, these forms provide reliable biostratigraphic information in facies where *Nummulites* are not present. This reliability lies on the correlation of *Nummulites* and *Alveolina* biostratigraphic markers in the same sections and their calibration to the global time scale through magnetostratigraphy.

Magnetostratigraphic calibration of described taxa is provided, along with an update of the SBZ calibration to the Geological Time Scale (Gradstein *et al.*, 2012).

**KEYWORDS** | SBZ recalibration; middle Eocene; southern Pyrenees; Paleogene biostratigraphy.

## INTRODUCTION

Larger foraminifera are a widely distributed polyphyletic group of marine benthic organisms. These taxa are the result of a stepwise evolutionary trend towards highly adapted k-strategist organisms in stable ecological conditions (Hallock, 1985). Indeed, the variety of morphological adaptations in the shallow marine symbiont-bearing larger foraminifera is related to the specific energy levels, water depths and substrate types of the carbonate shelves where they thrive (Hottinger, 1983). The facies specificity of larger foraminifera determines their usefulness in facies analysis and palaeoenvironmental reconstructions. However, this may be disadvantageous for biostratigraphic purposes.

The facies dependence of single taxa is avoided in larger foraminifera biostratigraphy (Shallow Benthic Zones (SBZ), Serra-Kiel *et al.*, 1998) through the usage of Oppelzones, characterized by an assemblage of selected taxa. The lower parts of these zones are largely marked by the first appearances of certain taxa, whereas their upper parts are marked by last appearances (Pignatti and Papazzoni, 2017). The quality of SBZs, thus, relies on the accuracy of correlations from stratigraphic sections where different sedimentary environments are represented. As pointed out by Serra-Kiel in Mochales *et al.* (2012), Costa *et al.* (2013) and Rodríguez-Pintó *et al.* (2012a, b), magnetostratigraphy has extensively been used for this purpose, also providing chronostratigraphic calibration to the SBZs. At a regional scale, the lithostratigraphic correlation of distinct sections, located in different positions of the carbonate shelf, can also improve the reliability of the biostratigraphic dataset.

The study of larger foraminifera biostratigraphy in the Pyrenean area has been of great importance for the definition of SBZ biozones (Canudo *et al.*, 1988; Hottinger, 1960; Samsó *et al.*, 1994; Schaub, 1981; Serra-Kiel, 1984; Tosquella, 1995). The Lutetian biozones (SBZ13 to SBZ16) of Serra-Kiel *et al.* (1998) are mostly based on data from this area. The magnetostratigraphic recalibration of this Lutetian biozones by Rodríguez-Pintó *et al.* (2012a) was also performed in the South-Pyrenean area (Guara Formation), focusing on Isuela and Gabardiella sections. However, the available data obtained by previous authors from the Guara Formation (Fm.) (Canudo *et al.*, 1988; Rodríguez-Pintó *et al.*, 2012a; Samsó *et al.*, 1994) shows the need for further studies of its larger foraminiferal content. Recently, Silva-

Casal (2017) and Silva-Casal *et al.* (2019) studied the lithostratigraphy, biostratigraphy and magnetostratigraphy of the Eocene shallow marine limestone units (Boltaña, Guara and Arguis formations) of the westernmost sector of the Sierras Exteriores in the Southern Pyrenees (west of Isuela section), and a correlation with the outcrops of the Sierra de Guara further to the east was proposed. Based on these earlier studies, the work presented herein comprises an extensive biostratigraphic dataset obtained from 11 sections of the Sierras Exteriores (Fig. 1), which were correlated by lithostratigraphic and magnetostratigraphic means. Thus, we provide a magnetostratigraphically correlated and calibrated regional study of the Lutetian biozones (SBZ13-SBZ16) of the Guara Formation, including some data for the Bartonian Arguis Fm. (SBZ 17) and the upper Ypresian Boltaña Fm. (SBZ 11).

## GEOLOGICAL AND STRATIGRAPHIC SETTING

The Pyrenean chain is a double vergence orogen formed by the antiformal stacking of basement thrust sheets during the Santonian to Miocene N-S convergence of the Iberian and European plates (Muñoz, 1992). In middle Eocene times, this orogen developed foreland basins on both North-Pyrenean and South-Pyrenean sides, with a turbiditic succession deposited in the proximal foredeep, flanked by a shallow marine carbonate ramp in the more distal margin of the South Pyrenean Basin (Garcés *et al.*, 2020; Plaziat, 1981).

The Sierras Exteriores are located in the South Pyrenean western zone (Jaca-Pamplona basin) and include syntectonic materials involved in the Pyrenean orogeny (Barnolas and Pujalte, 2004). They represent the emergence of the South Pyrenean sole thrust in the southwestern part of the chain. Variable along-strike shortening estimates of this basal thrust range between 35 to 10km (Millán *et al.*, 1996) allowing for the exposure of Lutetian platform rocks in the hangingwall block that rides over the 4000m thick Oligocene molasse of the Ebro foreland basin (Oliva-Urcia *et al.*, 2019). The middle Eocene limestones exposed in the Sierras Exteriores were deposited in the distal, shallow marine margin of the South Pyrenean foreland basin (Fig. 1).

The stratigraphic record of the Sierras Exteriores is represented by Triassic to Neogene materials

(Puigdefàbregas and Souquet, 1986). Overlying a very condensed and incomplete Mesozoic succession, the Upper Cretaceous-Paleogene transition is represented by continental deposits, which are part of the Tremp Fm. (Mey et al., 1968). The Eocene limestone succession has been divided into the following lithostratigraphic formations:

The Boltaña Formation (Barnolas et al., 1991), lying unconformably on top of the Tremp Formation, represents the beginning of the shallow marine carbonate sedimentation associated with the evolution of the foreland basin. In the study area this unit only occurs in the Gabardiella section (eastern part of the study area). There, the Boltaña Formation is characterized by a 30m thick alternation of limestones and marls. The limestones contain abundant porcellaneous foraminifera (*Alveolina*, *Idalina*) and conical agglutinated forms (*Coskinolina*). In the study area, this unit has been attributed to the late Ypresian (Cuisian) SBZ11 (Rodríguez-Pintó et al., 2012a) and correlated to magnetic polarity Chron C22r (Rodríguez-

Pintó et al., 2017). The thicker Ara River section in the east, at the core of the Boltaña anticline spans from the upper part of chron C24n to chron C22r (Mochales et al., 2012).

The Guara Fm. (Puigdefàbregas, 1975) characterizes the Lutetian succession of the Sierras Exteriores. It consists of shallow marine carbonates lying unconformably on the top of the Boltaña Fm. in the Gabardiella section and on the top of the Tremp Fm. further to the west. The lowermost deposits of the Guara Fm. are also highly diachronous, becoming younger westwards. The Guara Fm. spans from chron C22n to C18r, from SBZ 11 (middle Cuisian) to SBZ 16 (late Lutetian) (Rodríguez-Pintó et al., 2012a, 2013a; Silva-Casal, 2017; Silva-Casal et al., 2019).

The Guara Fm. was divided into three non-formal lithostratigraphic units, Lower, Middle and Upper Guara units (Rodríguez-Pintó et al., 2012a; Samsó et al., 1992, 1994). In this work we regard these units as members of the Guara Fm. (see also Silva-Casal et al., 2019). The Isuela

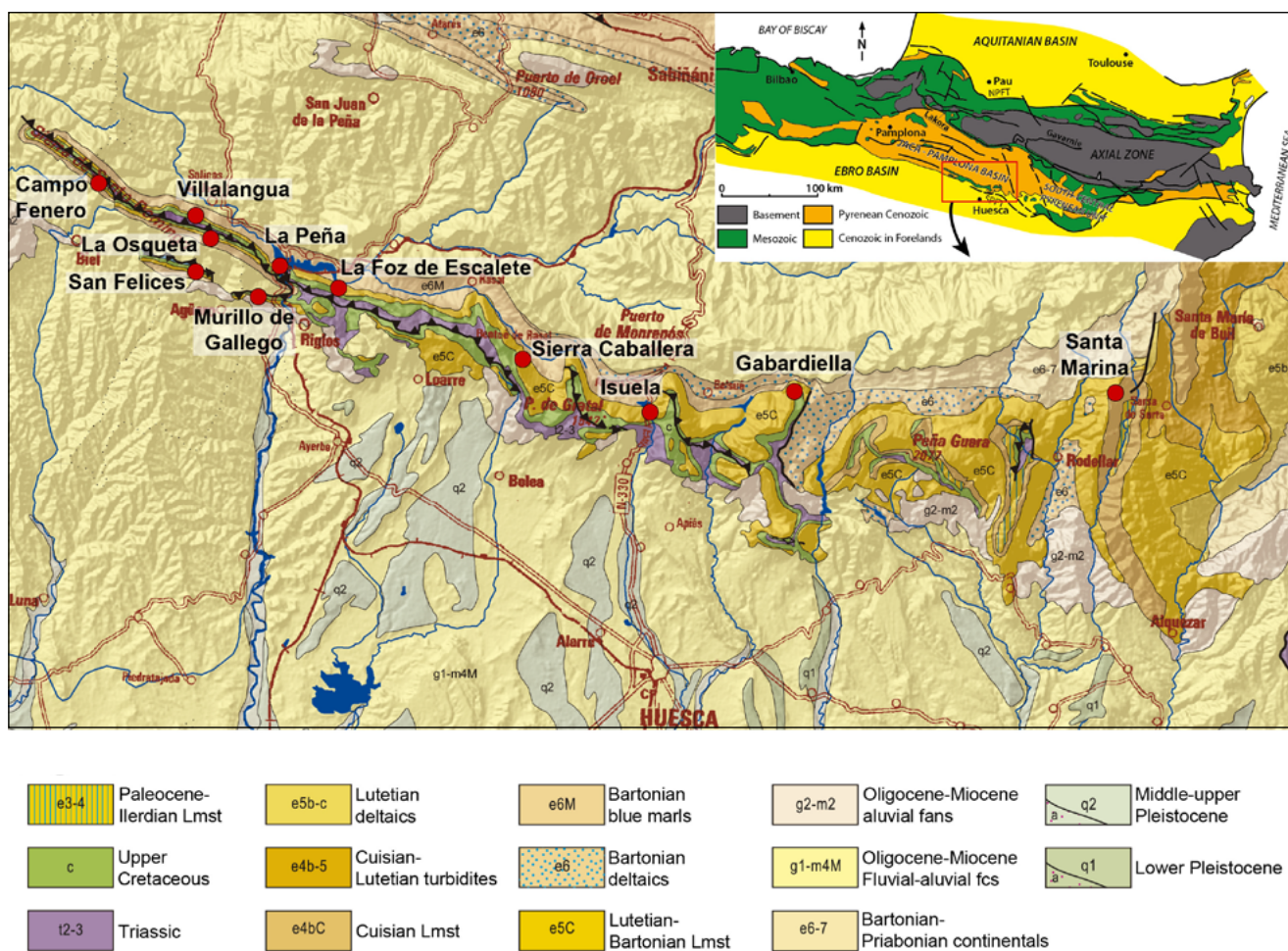


FIGURE 1. Simplified geological map of the study area in the Pyrenean Sierras Exteriores, with location of the sections described in the text.

section is considered the reference section of the Guara Fm. and of all its members:

- **Lower Guara Mb.** This unit has been recognized in the Santa Marina (Fig. 2), Gabardiella (Fig. 3), Isuela (Fig. 4) and Sierra Caballera sections (Fig. 5). The thickness of this unit ranges from 200m in the eastern part of the study area (Gabardiella section) to 100m in the Sierra Caballera section, its westernmost outcrop. In the Isuela reference section, the Lower Guara Mb. consists of an alternation of bioclastic limestones (mainly composed of porcellaneous larger foraminifera) and marls, with some characteristic levels of conglomerates. This unit was deposited in transitional to shallow marine subtidal environments (Rodríguez-Pintó et al., 2012a; Samsó et al., 1992; Silva-Casal, 2017).

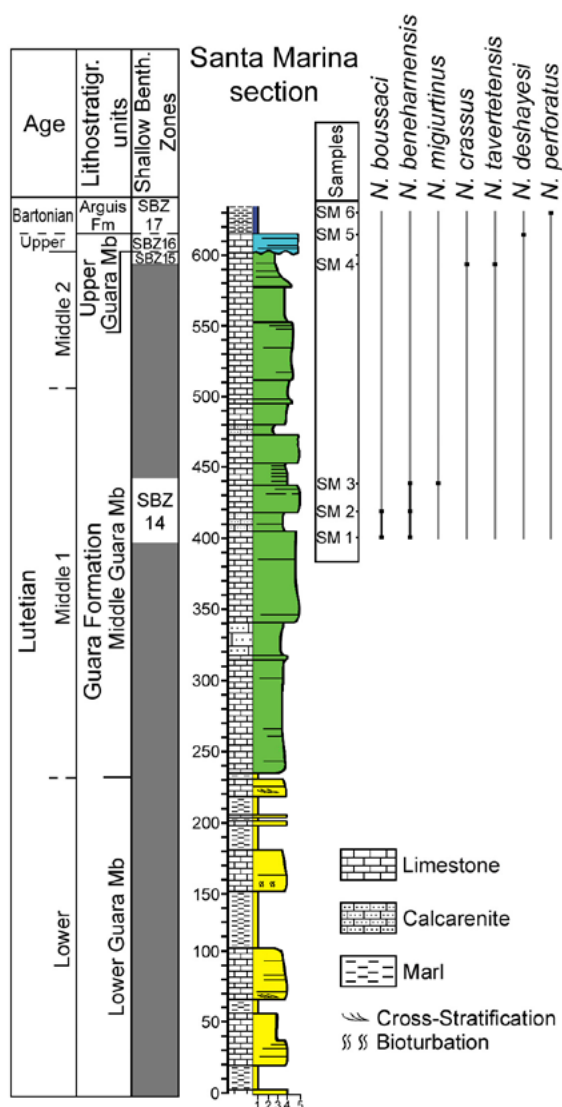


FIGURE 2. Stratigraphic succession (modified from Rodríguez-Pintó et al., 2012b) and distribution of larger foraminifera in the Santa Marina section.

- **Middle Guara Mb.** This unit crops out in the Santa Marina, Gabardiella, Isuela, Sierra Caballera, la Foz de Escalete, La Peña, Murillo de Gállego and Villalangua sections (Figs. 2-9). According to Samsó et al. (1992) and Rodríguez-Pintó et al. (2012a), the basal contact of this unit is transgressive. This member is mainly composed of porcellaneous foraminiferal facies, with abundant *Alveolina* and *Orbitolites*, and trematophore miliolids (*Idalina*, *Pseudolacazina*, among others), deposited in shallow subtidal environments (Silva-Casal, 2017, Silva-Casal et al., 2019). Cross stratification, including large-scale cross-bedding, is common. Despite the overall facies homogeneity of this unit, it changes to the west to more restricted environments, with the occurrence of lagoonal marls and some siliciclastic levels, whereas to the east *Nummulites*-rich beds can be observed. This lateral change of facies from distal-to-proximal, i.e. east to west, could explain the reduction in thickness from 550m in the Gabardiella section to only 20m in the Villalangua section.

- **Upper Guara Mb.** This unit is present throughout the study area, with the only exception of the Campo Fenero section. The lower boundary of this unit is an erosive surface (Santa Marina section, Fig. 2), which grades to a correlative conformity. This unit is characterized by a facies association of acervulinid and porcellaneous foraminiferal facies and *Nummulites*-bank facies, which were deposited in inner ramp vegetated environments and middle ramp environments respectively (Silva-Casal, 2017, Silva-Casal et al., 2019). In general, this unit shows a greater abundance of *Nummulites*-bank facies in the eastern outcrops, and more restricted facies to the west where acervulinid and alveolinid-rich facies predominate. In the study area, the maximum thickness (90m) is found between La Foz de Escalete section (Fig. 6) and the Isuela section (Fig. 4), and the minimum thickness (30m) in La Osqueta section (Silva-Casal et al., 2019). The top of the Guara Fm. has been interpreted as a drowning unconformity (Millán et al., 1994; Silva-Casal, 2017; Silva-Casal et al., 2019). Above this boundary, the Upper Guara Mb. is overlain by the Arguis Fm. (Puigdefàbregas, 1975).

The **Arguis Fm.** records a major change in the sedimentation in the Jaca-Pamplona basin. The dominant carbonate ramp sedimentation was replaced by a marly sedimentation, in a deeper, outer ramp environment with higher siliciclastic input. The Arguis Fm. is mainly composed of blue marls interbedded with limestones and marly limestones (Millán et al., 1994; Morsilli et al., 2012). The classic Arguis section spans from chron C18r to C16r, just below the diachronic deltaic Belsué-Atarés Fm., as deduced by paleomagnetic studies (Hogan and Burbank, 1996; Kodama et al., 2010; Pueyo et al., 2002; Rodríguez-Pintó et al., 2019). However, in the westernmost sector of the Sierras Exteriores, the marls of the lowermost part of the

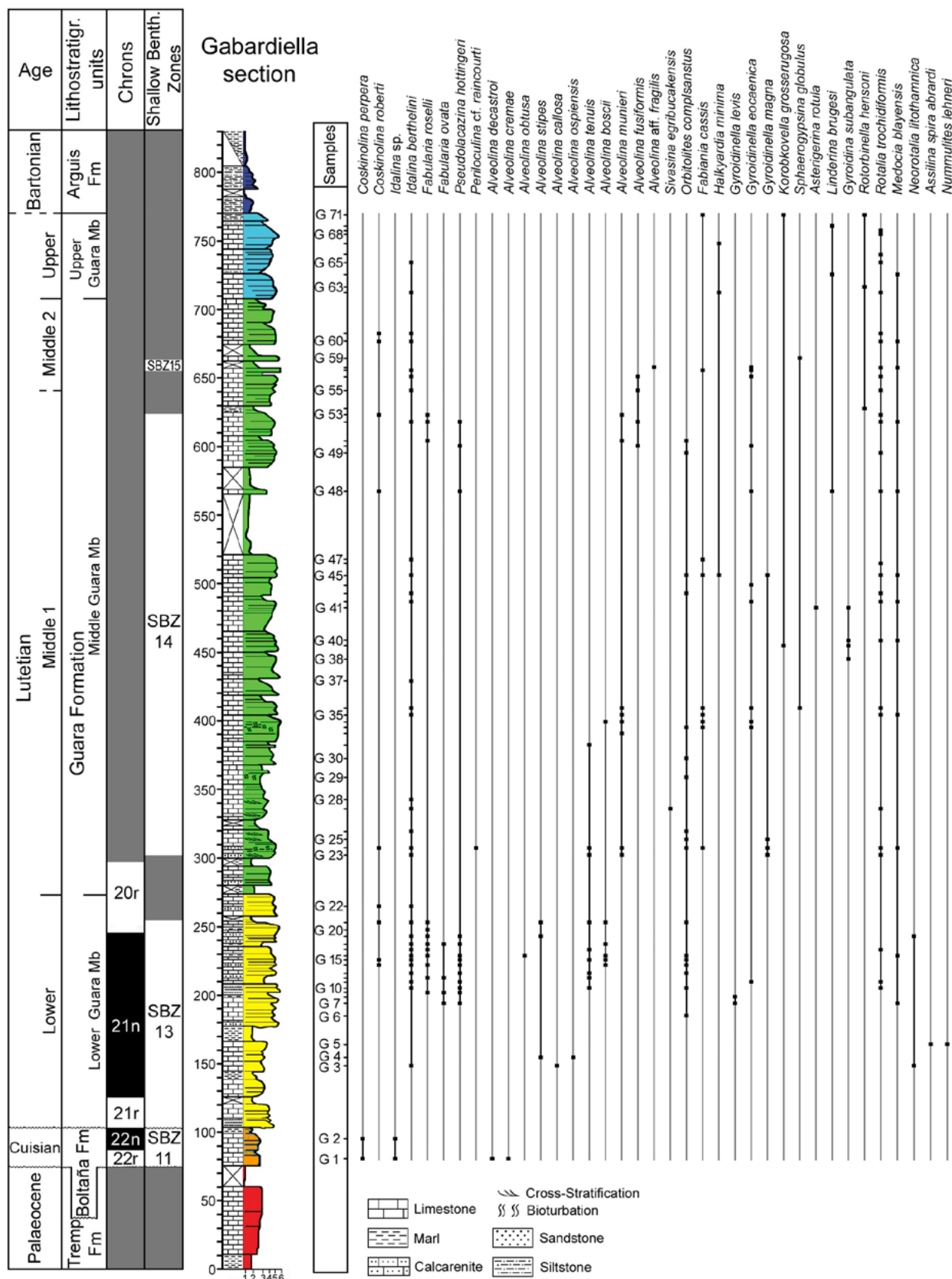
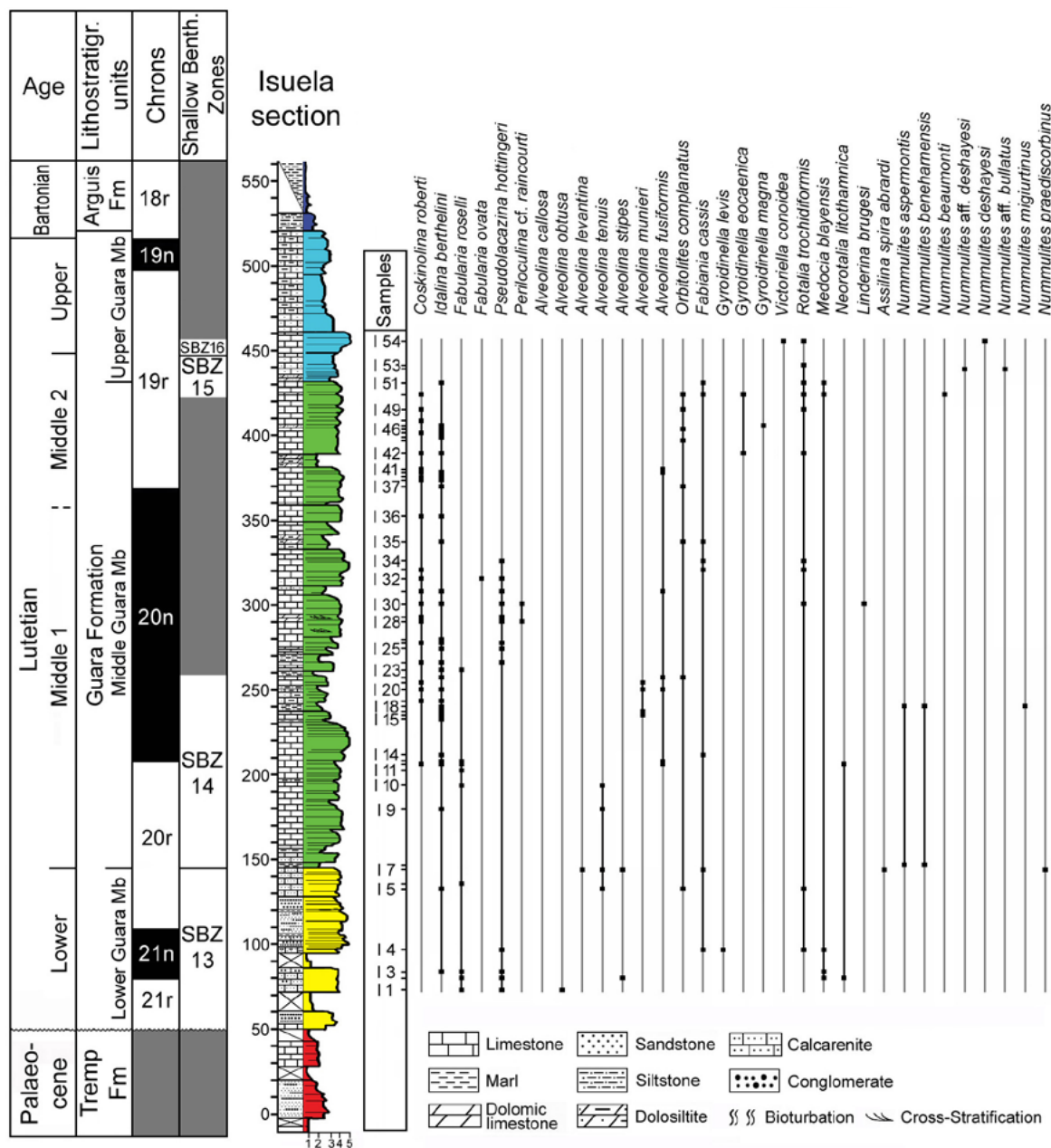


FIGURE 3. Stratigraphic succession and distribution of larger foraminifera in the Gabardiella section (modified from Rodríguez-Pintó et al., 2012a). Magnetostratigraphic data after Rodríguez-Pintó et al. (2017).

Arguis Fm. grade laterally to a limestone dominated succession, included in the Santo Domingo Limestone Mb. (Silva-Casal, 2017).

- The **Santo Domingo Mb.** (Silva-Casal, 2017; Silva-Casal et al., 2019) was formally defined by its lithological differences with the underlying Guara Fm. and its lateral transition to the marls of the lower part of the Arguis Fm. The base of the Santo Domingo Mb. is defined by an erosive surface, related to the drowning unconformity that defines the top of the Upper Guara Mb.

In this study the Santo Domingo Mb. has been logged in the Murillo de Gállego, San Felices, La Osqueta, and Campo Fenero sections (Figs. 8; 10; 11; 12). This unit is characterized by a conspicuous glauconitic level at its base, which is considered a regional datum and allows lithostratigraphic correlation between sections (Silva-Casal, 2017, Silva-Casal et al., 2019). The Santo Domingo Mb. is also characterized by a shallow carbonate ramp facies association of outer and middle ramp facies with predominance of bryozoans, orthophragminids (*Discocyclus*, *Asterocyclina*) and red algae, and



**FIGURE 4.** Stratigraphic succession and distribution of larger foraminifera in the Isuela section (modified from Rodríguez-Pintó et al., 2012a). Magnetostratigraphic data after Rodríguez-Pintó et al. (2012a) and Rodríguez-Pintó et al. (2019).

acervulinids and echinoids-rich inner ramp facies. *Nummulites* and *Alveolina*-rich facies are absent in this unit, but dispersed specimens of these species do occur.

**MATERIALS AND METHODS**

This work is based on 11 stratigraphic sections (Fig. 1) systematically and evenly sampled from the base to the top for biostratigraphic purposes. This sampling resulted in the description of 359 samples. The samples were studied in thin sections and polished slabs, except those collected to extract loose, separate specimens of nummulitids and alveolinids. These samples were disaggregated in a water, oxygen peroxide and Na<sub>2</sub>CO<sub>3</sub> solution and then sieved through mesh apertures of 1.0, 0.5 and 0.2mm. The material studied is housed in three different repositories (Appendix I). The samples from the Isuela and Gabardiella sections (also named Arguis and Lúsera) are housed in the repository of the Instituto Geológico Minero de España (IGME). Some samples are included in the Serra-Kiel collection, provisionally housed in the Department

of Earth and Ocean Dynamics, University of Barcelona (UB), and will be definitively deposited in the Museu de Ciències Naturals de Barcelona. Finally, the rest of the samples, including the new species (MPZ 2019/1681-1683 and MPZ 2020/483-554, Appendix I), are housed in the Natural Science Museum of the University of Zaragoza (Canudo, 2018).

**STRATIGRAPHY**

The biostratigraphic information obtained in this work is partly based on the revision of published material, i.e. the Isuela and Gabardiella sections (Rodríguez-Pintó et al., 2012a) and Santa Marina section (Rodríguez-Pintó et al., 2012b). The rest of the information comes from 8 new sections located at the western area of the Sierras Exteriores (Fig. 1):

**Santa Marina section**

The Santa Marina section (Rodríguez-Pintó et al., 2012b) (Fig. 2) was measured in the Cañada Zerrada

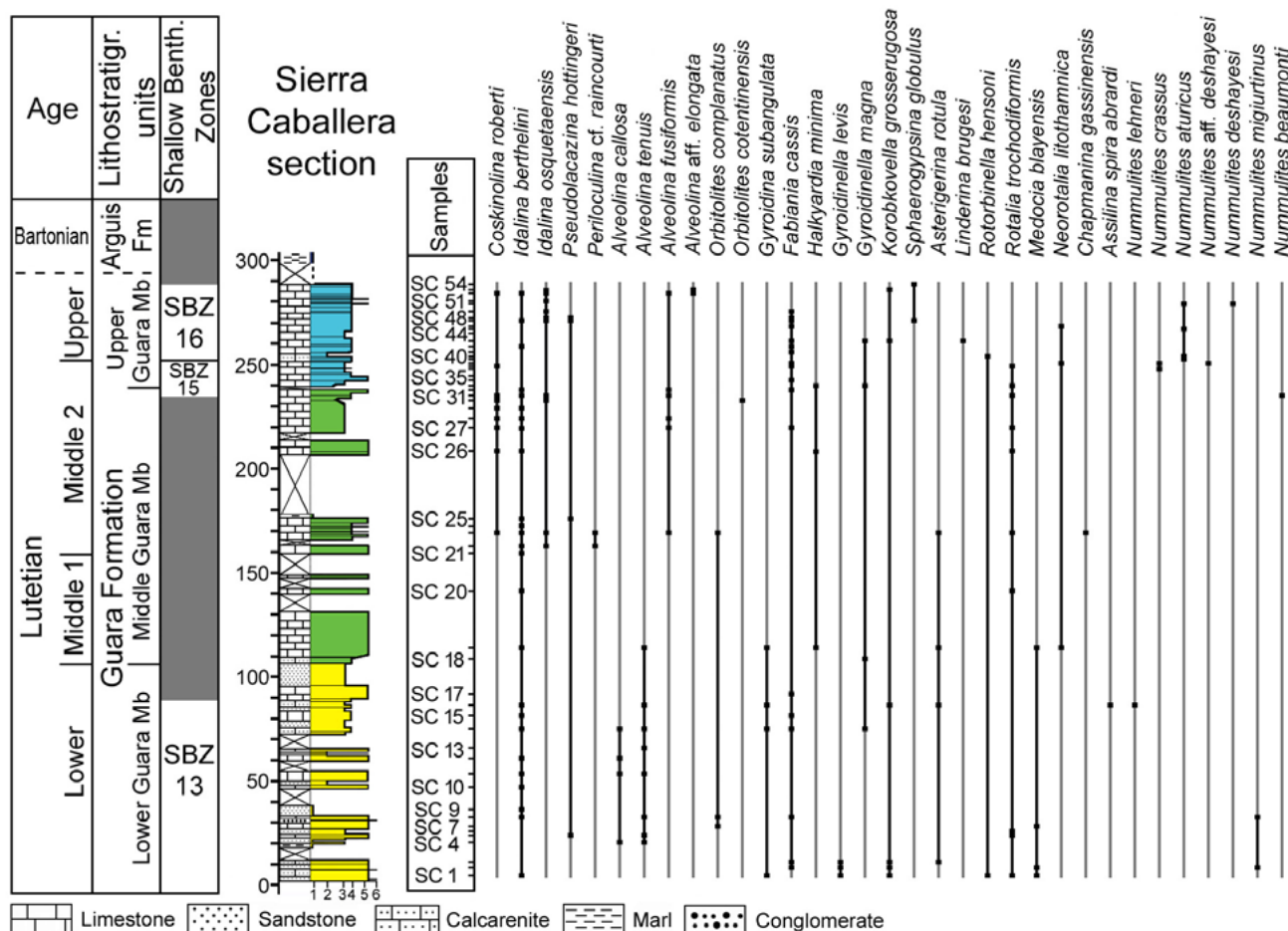


**FIGURE 5.** Stratigraphic succession and distribution of larger foraminifera in the Sierra Caballera section.

gorge to the west of Santa Marina hermitage. Coordinates UTM (ETRS89): Base 30T 744240 4689823, Top 743638 4689986. The section was tentatively dated by magnetostratigraphy (Rodríguez-Pintó et al., 2012b). Unfortunately, the occurrence of a widespread reverse remagnetization component in the most part of the profile (Rodríguez-Pintó et al., 2013b) precluded achieving a reliable dating and the magnetostratigraphic data is not been considered here.

The base of the section consist of marine sandy limestones of the Boltaña Fm., Cuisian in age. The overlying rocks are represented by the following stratigraphic units:

- **Lower Guara Mb.**, represented by a 230m thick alternation of marls and limestones, locally with cross stratification and bioturbation.

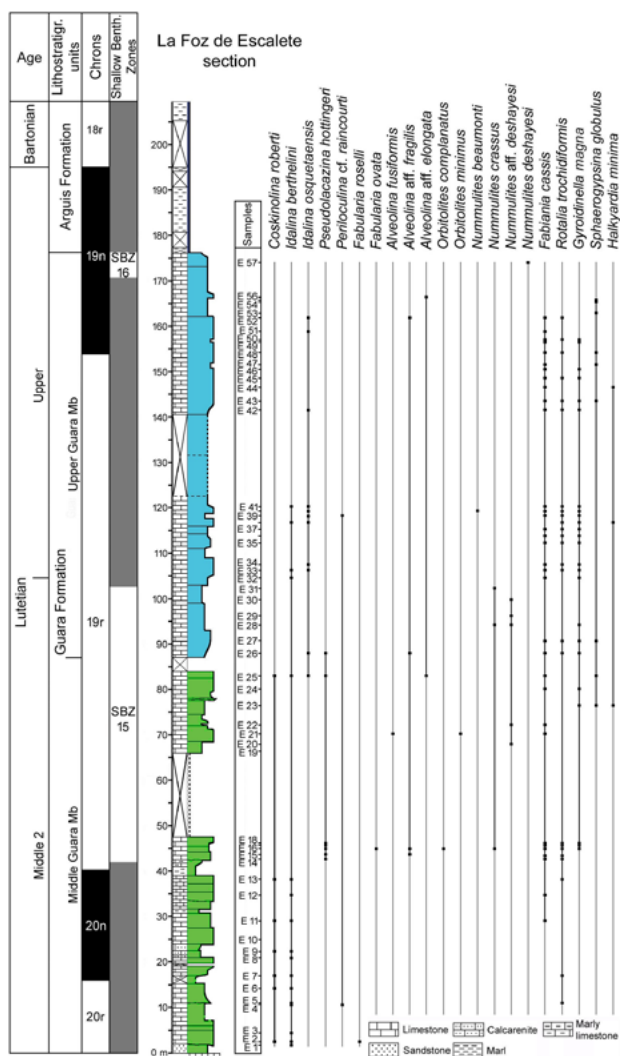


FIGURE 6. Stratigraphic succession and distribution of larger foraminifera in the La Foz de Escalete section. Magnetostratigraphic data after Silva-Casal et al. (2019).

- **Middle Guara Mb.**, represented by 370m of limestones. The occurrence of *Nummulites boussaci* and *Nummulites beneharnensis* in the middle part of this unit characterizes SBZ 14 (middle Lutetian 1). The occurrence of *Nummulites crassus* and *Nummulites tavertetensis* in the upper part characterizes SBZ 15 (middle Lutetian 2).

- **Upper Guara Mb.**, bounded at the base by and unconformity and represented by 15-20m of limestones. The occurrence of *Nummulites deshayesi* characterizes SBZ 16 (late Lutetian).

- **Arguis marls Fm.**, represented by marlstones with *Nummulites perforatus* which characterizes SBZ 17 (Bartonian).

### Gabardiella section

The Gabardiella section (Rodríguez-Pintó et al., 2012a, 2017; Samsó et al. 1994) (Fig. 3) was measured in the eastern flank of the Gabardiella anticline, along the road between the localities of Lusera and Nocito. Coordinates UTM (ETRS89): Base 30T 722132 4688600, Top 30T 721281 4688255).

The lowermost part of the section is composed of 75m of red marls and lacustrine limestones of continental facies of the Tresp Fm. The overlying rocks consist of the following stratigraphic units:

- **Boltaca Fm.**, consists of 30m of limestones and marls. The presence of *Coskinolina cf. perpera*, *Alveolina decastroii* and *Alveolina cremae* characterizes SBZ 11 (middle Cuisian). The Chron C22 was identified in this unit (Fig. 3) (Rodríguez-Pintó et al., 2017).

- **Lower Guara Mb.**, consists of a 170m thick succession of sandstones at the base, followed by an alternation of limestones, siltstones and marls. The presence of *Alveolina obtusa*, *Alveolina stipes*, *Alveolina callosa*, *Alveolina ospiensis*, *Assilina spira abrardi* and *Nummulites lehneri* characterizes SBZ 13 (early Lutetian). This unit includes Chron C21 and the lower part of Chron C20r (Rodríguez-Pintó et al., 2017).

- **Middle Guara Mb.**, is represented by 435m of limestones with frequent cross-bedding and bioturbation. The occurrence of *Alveolina munieri* characterizes SBZ 14 (middle Lutetian 1). The presence of *A. aff. fragilis* in the upper part of this unit, together with the correlation with Isuela section, suggests SBZ 15 (middle Lutetian 2). The lower part of this unit correlates to Chron C20r (Rodríguez-Pintó et al., 2017).

- **Upper Guara Mb.**, a 60m thick succession of limestones with some levels of siltstones. Despite the absence of larger foraminifera biomarkers, the correlation with the nearby Isuela section (Fig. 4) suggests SBZ 16 (late Lutetian).

**Isuela section**

The Isuela section (Fig. 4) is exposed along the old road between the localities of Nueno and Arguis, in the Isuela river gorge, on the western flank of the Pico del Águila anticline. Coordinates UTM (ETRS89): Base: 30T 712081 4685921, Top: 30T 712125 4686840).

The base of the section consists of a 50m thick succession of sandstones, conglomerates and lacustrine limestones of the Tremp Fm.

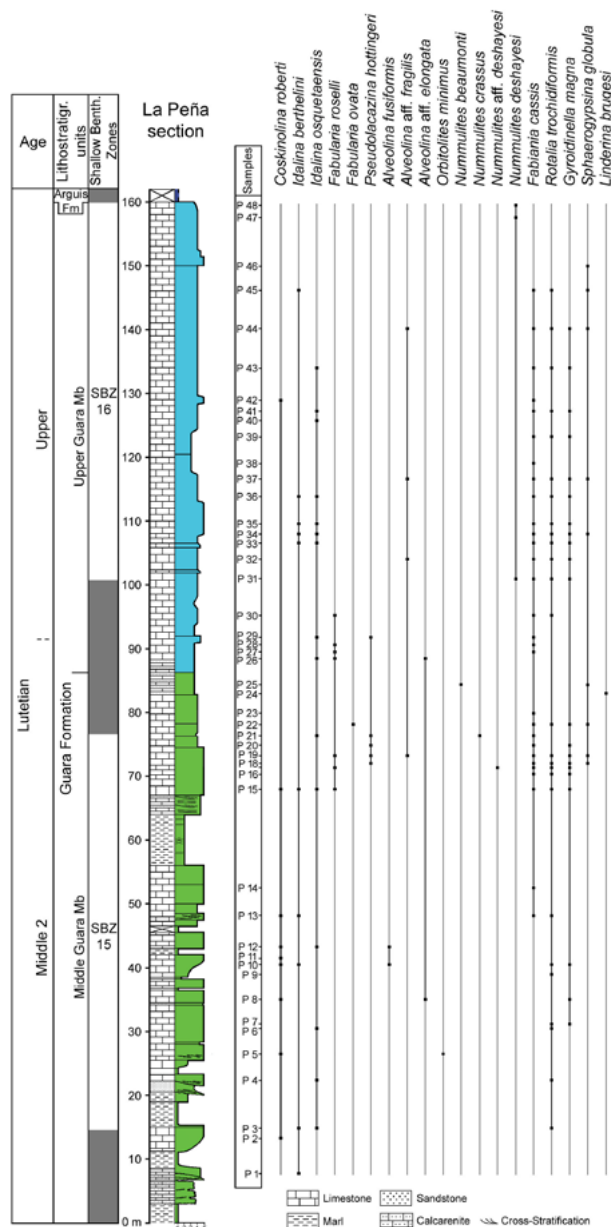


**FIGURE 7.** Stratigraphic succession and distribution of larger foraminifera in the La Peña section.

The overlying rocks are represented by the following stratigraphic units:

- **Lower Guara Mb.**, composed of 95m of sandstones, conglomerates and limestones. The presence of *Alveolina obtusa*, *A. stipes* and *Assilina spira abrardi* characterizes SBZ 13 (early Lutetian). Chron C21 is identified in the lower part of the unit, whereas its upper part correlates to chron C20r (Rodríguez-Pintó et al., 2012a).

- **Middle Guara Mb.** 285m thick unit mainly composed of limestones and thin intervals of marls, siltstones, marly limestones, dolomites and dolosiltites. The presence of *Alveolina munieri*, *Nummulites aspermontis*, *N. beneharnensis* and *N. praediscorbinus* characterized SBZ 14 (middle Lutetian 1). The presence of *N. beaumonti* in the uppermost part of this unit indicates SBZ 15 (middle Lutetian 2). This unit spans the time interval from the latter part of Chron C20r to the early C19r (Rodríguez-Pintó et al., 2012a).

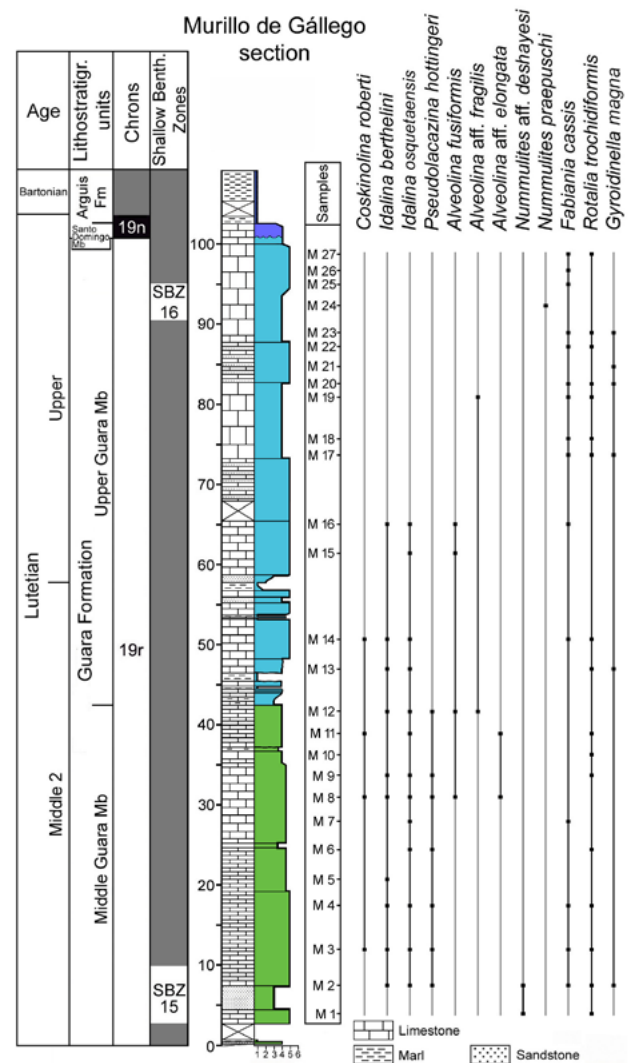


**FIGURE 8.** Stratigraphic succession and distribution of larger foraminifera in the Murillo de Gállego section. Magnetostratigraphic data after Silva-Casal et al. (2019).

- **Upper Guara Mb.** is represented by an 88m thick alternation of limestones and marly limestones. The presence of *N. aff. deshayesi* and *N. aff. bullatus* in the lower part of this unit indicates SBZ 15 (middle Lutetian 2), and *N. deshayesi* in the middle part indicates SBZ 16 (late Lutetian). Chron C19n and the base of C18r were identified in the upper part of this unit (Rodríguez-Pintó et al., 2012a, 2019).

**Sierra Caballera section**

Located in the Sierra Caballera, close to Bentué de Rasal village, the Sierra Caballera composite section is made of two subsections. The lower part was measured along an unpaved road to the south of the Foz de Portiella gorge, and the upper subsection in the gorge. Coordinates UTM (ETRS89): lower subsection Base: 30T 702363 4688711, Top: 30T 702504 4688780; upper subsection Base: 30T 702482 4689969, Top: 30T 702658 4690168.

In this section the following stratigraphic units are observed (Fig. 5):

- **Lower Guara Mb.**, composed of 108m of marls, sandstones and limestones. The presence of *Alveolina*

*callosa*, *Assilina spira* abrardi and *Nummulites lehneri* characterizes SBZ 13 (early Lutetian).

- **Middle Guara Mb.** is a 127m thick unit mainly composed of limestones, but thick intervals are covered. The presence of *N. beaumonti* in the upper part of this unit indicates SBZ 15 (middle Lutetian 2). SBZ 14 (middle Lutetian 1) biostratigraphic markers were not found.

- **Upper Guara Mb.** is a unit is mainly composed of limestones, with a minimum thickness of 55m, as its upper part could not be measured because the boundary with the Arguis Fm. is covered. . The presence of *N. crassus* and *N. aff. deshayesi* in the lower part of this unit indicates SBZ 15 (middle Lutetian 2) and the presence of *N. aturicus* and *N. deshayesi* in the middle and upper part indicates SBZ 16 (late Lutetian).

**La Foz de Escalate section**

Located along the Foz de Escalate gorge (Silva-Casal, 2017), near La Peña Estación village. Coordinates UTM (30T): Base 30T 689436 4693642, Top 30T 689543 4693952).

The following stratigraphic units have been recognized (Fig. 6):

- **Middle Guara Mb.**, 84m thick succession composed of sandstones at the base, followed by limestones with thin intervals of marls, sandstones, marly limestones and limestones. The presence of *N. crassus* and *N. aff. deshayesi* indicates SBZ 15 (middle Lutetian 2). Chron C20 and the lower part of C19r were identified in this unit (Silva-Casal, 2017).

- **Upper Guara Mb.** is composed here of 178m thick limestones. The presence of *N. crassus* and *N. aff. deshayesi* in the lower part of this unit indicates SBZ 15 (middle Lutetian 2), and *N. deshayesi* in upper part indicates SBZ 16 (late Lutetian). Chron C19r was identified in the lower part and C19n in the upper part (Silva-Casal, 2017).

- **Arguis Fm.** is represented in this section by a 1000m thick marly succession including intervals of marly limestones and sandstones (Millán et al., 1994). The lowermost Arguis Fm. consists of an alternation of marls and siltstones. The upper part of Chron C19n and its boundary with Chron C18r were identified in this unit (Silva-Casal, 2017; Silva-Casal et al., 2019).

**La Peña section**

Located along the road A-132 next to La Peña dam, in the proximity of Santa María de la Peña village (Silva-Casal, 2017). Coordinates UTM (ETRS89): Base 30T 685952 4694793, Top 30T 686323 4694917.

This section is composed of the following stratigraphic units (Fig. 7):

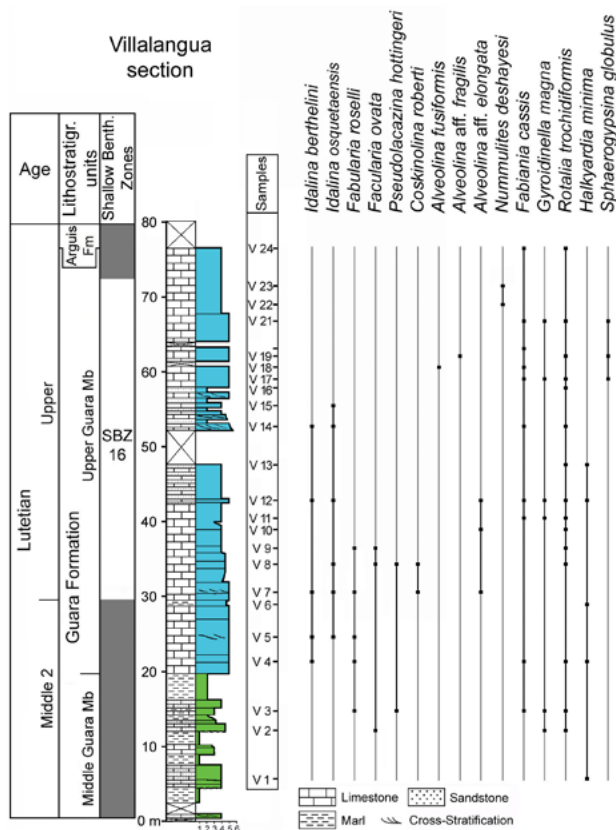


FIGURE 9. Stratigraphic succession and distribution of larger foraminifera in the Villalangua section.

- **Middle Guara Mb.**, 87m thick, composed of marls and limestones with cross stratification. The presence of *N. crassus* and *N. aff. deshayesi* indicates SBZ 15 (middle Lutetian 2).

- **Upper Guara Mb.**, composed of 73m of massive limestones. The presence of *N. deshayesi* indicates SBZ 16 (late Lutetian).

### Murillo de Gállego section

Located in the north-west of the Murillo de Gállego village (Silva-Casal, 2017). Coordinates UTM (ETRS89): Base 30T 685553 4692400, Top 30T 685490 4692302).

In this section the following stratigraphic units have been observed (Fig. 8):

- **Middle Guara Mb.** a 43m thick unit composed of limestones with thin marly intervals. The presence of *N. aff. deshayesi* at the base of this unit indicates SBZ 15 (middle Lutetian 2). Chron C19r extends throughout this unit (Silva-Casal, 2017; Silva-Casal *et al.*, 2019).

- **Upper Guara Mb.** formed of a 59m thick alternation of massive limestones with some intervals of laminated limestones. The presence of *N. praepuschi* in the upper part of this unit indicates SBZ 16 (late Lutetian). This unit belongs to the upper part of Chron C19r (Silva-Casal, 2017; Silva-Casal *et al.*, 2019). The contact surface with the overlying Santo Domingo Mb. is an unconformity.

- **Arguis Fm.**, constituted by 1.5m of glauconitic limestones of the Santo Domingo Mb. at the base, passing upwards into the typical blue marls of the Arguis Fm. Chron C19n was identified at the base of the Santo Domingo Mb. (Silva-Casal, 2017; Silva-Casal *et al.*, 2019).

### Villalangua section

This section is exposed along an unpaved road between the locality of Villalangua and the abandoned village of Salinas Viejo. The top of the section is complemented with data from the nearby Salinas gorge (Silva-Casal, 2017) Coordinates UTM (ETRS89) are: Base 30T 679218 4697917, Top 30T 679236 4697975. Salinas gorge: 30T 680115 4697682.

This section includes the following stratigraphic units (Fig. 9):

- **Middle Guara Mb.**, 20m thick succession of marls and limestones. Despite the absence of larger foraminifera biostratigraphic markers, lithological correlation with nearby sections allows the attribution of this unit to SBZ 15 (middle Lutetian 2).

- **Upper Guara Mb.**, composed of 57m of cross stratified limestones, laminated limestones and massive limestones. The presence of *N. deshayesi* at the top of this unit indicates SBZ 16 (late Lutetian).

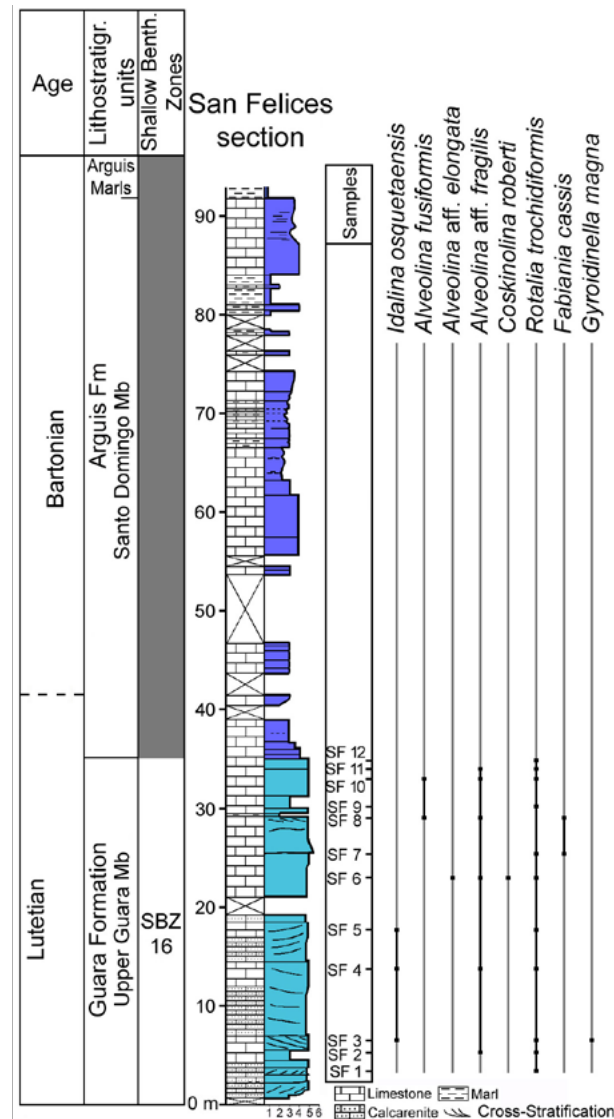


FIGURE 10. Stratigraphic succession and distribution of larger foraminifera in the San Felices section.

### San Felices section

Located at the Barranco del Villano gorge, to the north-east of San Felices (Agüero) village (Silva-Casal, 2017). The section is divided into two subsections. The upper subsection is located on an unpaved road, whereas the lower part of the section is located at the bottom of the Barranco del Villano gorge with coordinates UTM (ETRS89): Lower subsection Base 30T 679479 4694017, Top 30T 679540 4693925; Upper subsection Base 30T 679450 4693974, Top 30T 679434 4693927).

In this section the following stratigraphic units can be observed (Fig. 10):

- **Upper Guara Mb.**, 35m thick, consists of cross stratified limestones. Despite the absence of larger

foraminifera biostratigraphic markers, stratigraphic correlation with other sections allows the attribution of this unit to SBZ 16 (late Lutetian).

- **Santo Domingo Mb.** 57m thick, is composed of marly limestones with some marly intervals. Despite the absence of larger foraminifera biostratigraphic markers, the correlation to other nearby sections shows that this unit is early Bartonian in age (SBZ 17).

### La Osqueta section

Located on an unpaved road in proximity to La Osqueta pass and complemented (from meters 50 to 60) with data from the La Osqueta pass itself (Silva-Casal, 2017) Coordinates UTM (ETRS89) are: Base 30T 680560 4696568, Top 30T 680310 4696553. La Osqueta pass: 30T 679589 4696809.

The base of the section is composed of 20m of lacustrine limestones and red lutites of the Tresp Fm.

The overlying Eocene rocks are represented by the following stratigraphic units (Fig. 11):

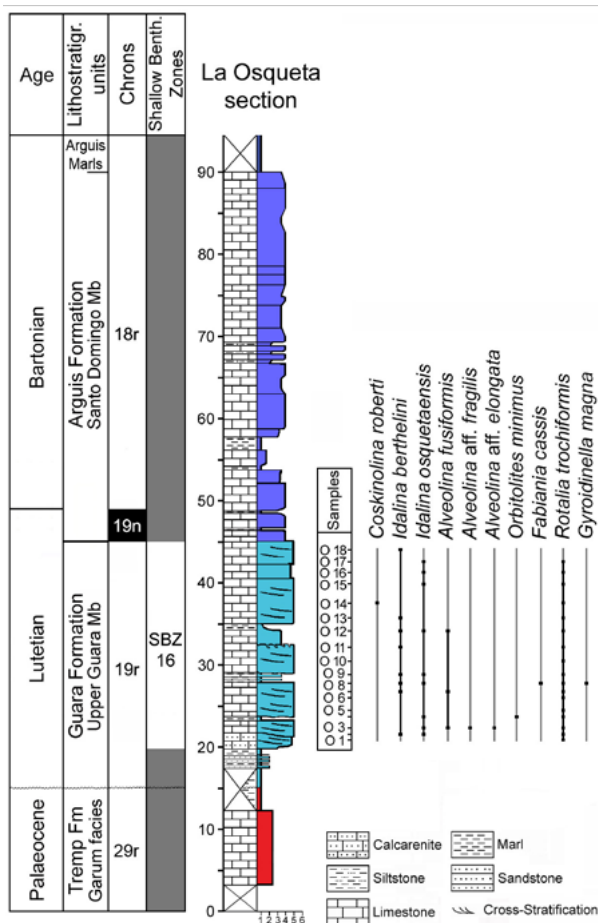


**FIGURE 11.** Stratigraphic succession and distribution of larger foraminifera in the La Osqueta section. Magnetostratigraphic data after Silva-Casal *et al.* (2019).

- **Upper Guara Mb.**, 25m thick, is composed of limestones. Despite the absence of larger foraminifera biostratigraphic markers, the stratigraphic correlation with other sections allowed to assign this unit to SBZ 16 (late Lutetian). Chron C19r was found in this unit (Silva-Casal, 2017).

- **Santo Domingo Mb.** is represented by 45m of marly limestones and marls. Despite the absence of biostratigraphic markers of larger foraminifera the stratigraphic correlation with other sections indicates that the upper part of this unit belongs to the SBZ 17 (early Bartonian). In this unit the chrons C19n and C18r have been identified (Silva-Casal, 2017; Silva-Casal *et al.*, 2019).

### Campo Fenero section

This section is located in the Sierra de Santo Domingo range, west to the source of the Arba de Biel river (Silva-Casal, 2017). This section is located along a path from a mountain hut leading to the Campo Fenero with coordinates UTM (ETRS89): Base: 30T 672841 4699265, Top: 30T 672689 4699288. The base of the section is composed of 5m of sandstones and red lutites of the Tresp Fm.

The overlying succession (Fig. 12) is represented by the Santo Domingo Mb., mainly constituted of cross stratified limestones interspersed with marls and sandstones. The presence of *Nummulites biarritzensis* and *N. beaumonti* in the middle part of this unit indicates SBZ 17 (Bartonian).

### SYSTEMATIC PALEONTOLOGY (FORAMINIFERA) by J. Serra-Kiel et R. Silva-Casal

Note: The biostratigraphic study is based on the zonation of Drobne (1977), Hottinger (1960, 1974), Hottinger and Drobne (1988), Schaub (1981) and Serra-Kiel *et al.* (1998).

**Phylum:** Foraminifera EICHWALD, 1830

**Class:** Tubothalamea PAWLOWSKI, OHOLZMANN, JAROSLAW AND TYSZKA, 2013

**Order:** Miliolida DELAGE AND HÉROUARD, 1896

**Superfamily:** Milioloidea EHRENBERG, 1839

**Family:** Hauerinidae SCHWAGER, 1876

**Subfamily:** Miliolinellinae VELLA, 1957

**GENUS** *Idalina* SCHLUMBERGER AND MUNIER-CHALMAS, 1884

**Type species:** *Idalina antiqua* SCHLUMBERGER AND MUNIER-CHALMAS, 1884

*Idalina* sp.

Figs. 13A-E; 14A-C

**Material.** This species has been identified in the Gabardiella section (Fig. 3).

**Description.** Test porcellaneous with miliolid growth. Dimorphism marked. The microspheric forms display a spherical morphology, the major length for 5 whorls is 1.85mm. The nepionic stage is formed by a small proloculus 0.60µm in diameter followed by one quinqueloculine whorl. The ephebic stage shows a bilocular growth. The basal layer is thin and locally slightly undulate. The megalospheric forms show an elliptical outline in sections perpendicular to the coiling axis. The nepionic stage is formed with a proloculus 120µm in diameter followed by one quinqueloculine stage. The ephebic stage shows a bilocular arrangement of the chambers. The maximum length in axial section is 1.4mm. The basal layer is thin.

**Remarks.** No formal species have been described within genus *Idalina* in the Cuisian yet. However, Drobné (1988) documented two forms assigned to *Idalina* sp. in the Cuisian of Dalmatia (p. 653, figs. 6.5 and 6.6, *op. cit.*). They differ from the specimens studied in the thickness of the basal layer and the size of the test. The scarcity of available material did not allow us to describe this species as a new species.

**Age.** This species is associated with *Alveolina cremae* and *A. decastroi* (samples G 1 and G 2; Fig. 3), indicating middle Cuisian (*A. dainellii* Zone) (Hottinger, 1960) or SBZ 11 (Serra-Kiel et al., 1998).

#### *Idalina berthelini* SCHLUMBERGER, 1905

Figs. 13F-V; 14D-Q

1905 *Idalina berthelini* n. sp. Schlumberger, p. 120-122; text-figs. 7-9; pl. 2 figs. 33, 33a

1962 *Idalina* cf. *berthelini*. Escandell and Colom, p. 119; fig. 18

1975 *Idalina berthelini*. Colom, p. 226; fig. 81, without scale

2012a *Idalina berthelini* Schlumberger, 1905. Rodríguez-Pintó et al., on-line Supplementary Material, pl. 9, figs. 1-8

2013a *Idalina berthelini* Schlumberger, 1905. Rodríguez-Pintó et al., figs. 8-10.

**Material.** This species has been identified in the following sections: Gabardiella, Isuela, Sierra Caballera, La Foz de Escalete, La Peña, Murillo de Gállego, Villalangua and La Osqueta (Figs. 2; 3; 5-9; 11).

**Description.** The megalospheric forms show an ovoid-sub-spherical morphology. The proloculus is spherical with a diameter between 150-220µm followed by a flexostyle (Fig. 13F; H, I, U). The nepionic stage is formed of two chambers in triloculine arrangement (Fig. 13L) or of one first biloculine

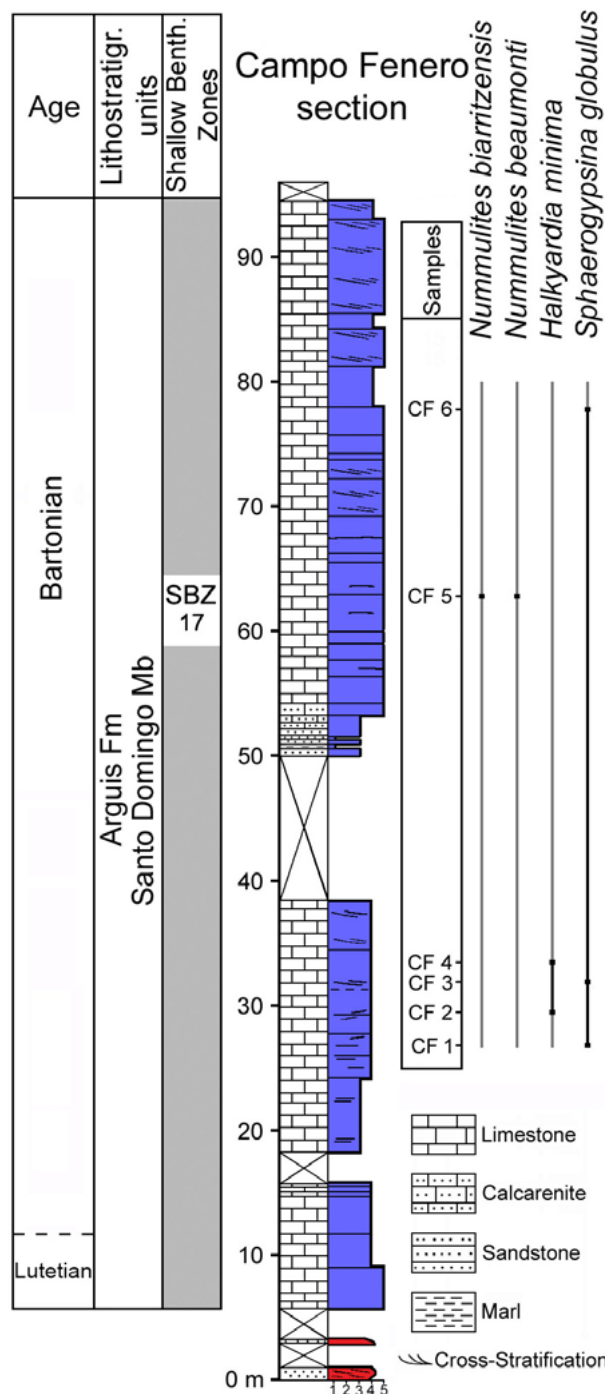


FIGURE 12. Stratigraphic succession and distribution of larger foraminifera in the Campo Fenero section.

growth stage followed by one triloculine growth stage (Fig. 13F). The neanic stage displays a biloculine arrangement of the chambers in the remaining whorls (Fig. 13F; H, I, J, K, L, S). The dimensions of the test vary between 1.7-2mm in axial section and 1.6-2mm in the longitudinal section. The microspheric forms show a subspherical morphology. Dimorphism is little marked. The initial growth is formed of 2-3 cycles pluriloculine in arrangement, showing then 1-2

cycles with quinqueloculine arrangement, followed by one triloculine cycle. The remaining whorls follow the biloculine mode (Fig. 13N-P). The diameter of axial section varies between 1.8-2.3mm for 4-5 biloculine chambers. In both generations the basal layer is slightly undulate and does not exceed half of the height of the chamber. The trematophore is supported by strong pillars (Fig. 13Q, R).

**Remarks.** The megalospheric forms of the studied material display the nepionic stage either in biloculine,

triloculine or quinqueloculine arrangement in its first chambers. This polymorphism was pointed out by Schlumberger (1905), who described the nepionic stage of the megalospheric forms with the two first chambers either in biloculine (Fig. 7 left, *op. cit.*) or quinqueloculine mode (Fig. 7 centre and right, *op. cit.*).

**Age.** The biostratigraphic range of *Idalina berthelini* extends from early Lutetian (SBZ 13) to late Lutetian (SBZ 16). The inclusion of *Idalina berthelini* in SBZ 13



**FIGURE 13.** SA-E) *Idalina* sp. 1, longitudinal section, microspheric form. B: axial section. C: axial section, megalospheric form. D, E: oblique sections. Specimens A, C, E: sample G 1 and B, D: sample G 2. F-V) *Idalina berthelini*. F: centered axial section, megalospheric form. G: longitudinal section. H-J: oblique centered axial sections, megalospheric forms. K, L: centered axial sections, megalospheric forms. M: almost centered longitudinal section, microspheric form. N: centered axial section, microspheric form. O, P: slightly uncentered axial section, microspheric form. Q, R: peripheral longitudinal sections. S: centered axial section, megalospheric form. T: uncentered longitudinal section. U: oblique centered axial section, megalospheric form. V: uncentered longitudinal section. Specimens F: sample G 28; G, I: sample I 45; H: sample I 47; J: sample I 42; K: sample I 38; L: sample G 60; M: sample I 22; N: sample G 13; O: sample I 44; P: sample G 35; Q: sample I 39; R: sample I 37; S: sample G 36; T: sample I 40; U: sample G 27 and V: sample I 17. Abbreviations: fl: flexostyle; pr: proloculus; bl: basal layer; th: trematophore.



**FIGURE 14.** Differences between the size of the shell and the thickness of the basal layer between *Idalina* sp. (middle Cuisian), and the Lutetian forms *Idalina berthelini* and *Idalina osquetaensis*. A-C) *Idalina* sp. A: drawing from Figure 13A. B: drawing from Figure 13B. C: drawing from Figure 13C. D-Q) *Idalina berthelini*. D: drawing from Figure 13G. E: drawing from Figure 13U. F: drawing from Figure 13S. G: drawing from Figure 13J. Specimen H: sample I 38. I: sample I 9. J: drawing from Figure 13L. K: drawing from Figure 13N. L: drawing from Figure 13M. M: drawing from Figure 13H. N: drawing from Figure 13F. O: specimen from sample O 12. P-A') *Idalina osquetaensis* n. sp. P: drawing from Figure 15A. Q: drawing from Figure 15D. R: drawing from Figure 15E. S: drawing from Figure 15F. T: drawing from Figure 15I. U: drawing from Figure 15G. V: drawing from Figure 15B. W: specimen from sample O 5. X: specimen from sample O 9. Y: drawing from Figure 15J. Z: drawing from Figure 15H. A': drawing from Figure 15C.

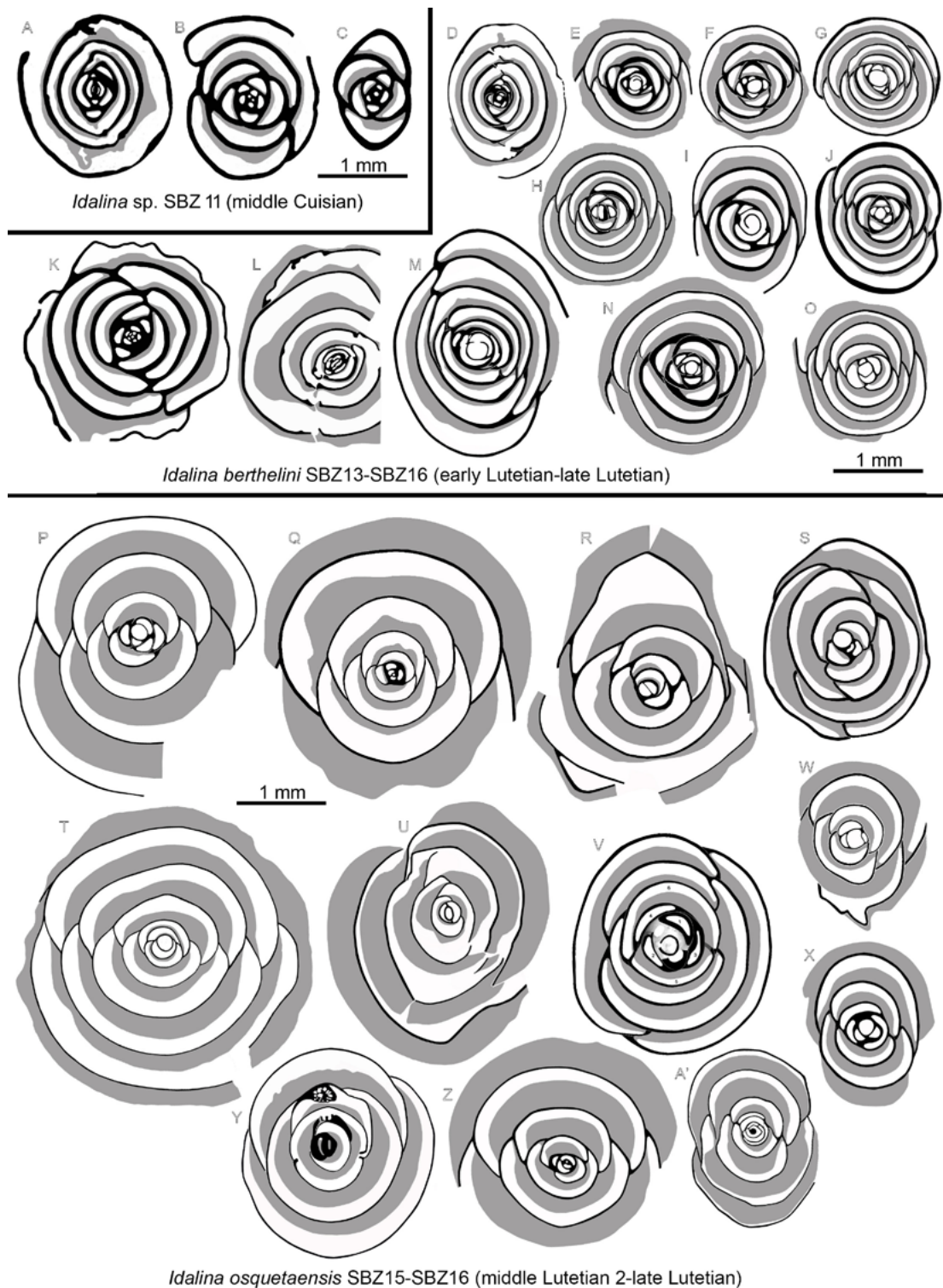


**FIGURE 15.** A-S) *Idalina osquetaensis* n. sp. A (Holotype, MPZ 2019/1681): centered axial section, megalospheric form; note the quinqueloculine nepionic stage, the size of the shell and the thickness of the basal layer. B: slightly oblique axial sections. C, D: uncentered axial sections, megalospheric forms. E (Paratype, MPZ 2019/1683): uncentered axial section, megalospheric form; note the thickness of the basal layer. F (Paratype, MPZ 2019/1682): slightly oblique axial section. G: slightly oblique longitudinal section, microspheric form. H: axial section, microspheric form. I: centered axial section, megalospheric form. J: subaxial section; note the trematophore. K: axial sections, microspheric form. L: uncentered axial sections, megalospheric form. M, N: uncentered axial sections, possible microspheric forms. O: axial sections, microspheric forms. P, Q: uncentered axial sections, possible microspheric forms. R: centered axial section, megalospheric form. S: uncentered axial section, possible microspheric form. Specimens A, E, F: sample O 3; B: sample P 21; C: sample V 9; D: sample O 2; G: sample E 33; H, K: sample M 16; J: sample V 15; L: sample O 17; I, O: sample SC 52; M: sample P 33; P: sample M 8; Q: sample V 14; R: sample V 7 and S: sample M 15. Abbreviations: bl: basal layer; th: trematophore.

is based on its association with *Alveolina stipes* (samples G 19, G 21 and I 2; Figs. 3; 4), *A. obtusa* (sample I 1; Fig. 4), and *A. callosa* (samples SC 11, SC 12 and SC 14; Fig. 5), which indicates the *A. stipes* Zone, (early Lutetian), or with *Assilina spira abrardi* (sample I 7 and SC 16; Figs. 4; 5) and *Nummulites lehneri* (sample SC 16; Fig. 5), indicating the *N. laevigatus-N. obesus* Zone (early Lutetian). The SBZ14 is characterized by the association with *A. munieri* (samples G 23, G 24, G 35, G 36, I 16, I 17, I 20 and I 22; Figs. 3; 4), indicating the *A. munieri* Zone, (middle Lutetian 1). The SBZ15 is characterized by the association of *I. berthelini* with *N. aff. deshayesi* (sample M 2; Fig. 8). Its occurrence in beds underlying beds that contain *N. crassus* (see Fig. 5) indicates the *N. sordensis-N. crassus* Zone (middle Lutetian 2). Finally, the SBZ16 is characterized by the presence of *I. berthelini* intercalated with samples of *N. aturicus* (sample SC 39, SC 40 and SC 45; Fig. 5), indicating the *N. aturicus* Zone (late Lutetian).

*Idalina osquetaensis* new species SERRA-KIEL ET SILVA-CASAL

Figs. 15A-S; 14P-A'

**Derivation of name.** The specific name refers to La Osqueta Pass, within the municipality of Las Peñas de Riglos (Huesca, Spain).

**Holotype.** Specimen MPZ 2019/1681 (Fig. 15A).

**Paratypes.** Specimens MPZ 2019/1683 (Fig. 15E) and MPZ 2019/1682 (Fig. 15F).

**Type Localit.** Located in La Osqueta section. Sample O 3 (coordinates UTM (ETRS89). 30T 680489 4696570).

**Type level.** Guara Fm., middle Lutetian 2-late Lutetian (SBZ 15-SBZ16).

**Material.** Sample O 3 from La Osqueta section (Fig. 11).

**Material.** This species occurs in the following sections: Sierra Caballera, La Foz de Escalete, La Peña, Murillo de Gállego, Villalangua, San Felices and La Osqueta (Figs. 5-11).

**Description.** The microspheric and megalospheric forms show an ovoid morphology in longitudinal section and a subcircular outline in sections perpendicular to the coiling axis. The maximum diameter observed in megalospheric forms in axial section is 3.5mm. The proloculus is spherical with a diameter around 180 $\mu$ m, followed by five chambers arranged in quinqueloculine mode; the remaining whorls follow the biloculine mode (Fig. 15A). The trematophore is supported by short pillars

(Fig. 15J). The basal layer is very thick, smooth and slightly undulate, exceeding half of the height of the chamber.

**Remarks.** The size of the test and the thickness of the basal layer of this species are greater than those of the species *I. berthelini* described above. The size of the test and the thickness of the basal layer increase following an evolutionary trend from *Idalina* sp. (Cuisian) to *I. berthelini* and *I. osquetaensis* (Lutetian) (Fig. 14).

**Age.** The biostratigraphic range of *Idalina osquetaensis* extends from middle Lutetian 2 (SBZ15) to late Lutetian (SBZ16). The SBZ15 is characterized by the association of this species with *Nummulites* aff. *deshayesi* (sample M 2; Fig. 8), and the SBZ16 is characterized by the alternation of samples containing *I. osquetaensis* and samples with of *N. aturicus* (samples SC 39, SC 40, SC 45 and SC 51; Fig. 5).

**Superfamily:** Alveolinoidea EHRENBERG, 1839

**Family:** Fabulariidae EHRENBERG, 1839

**GENUS** *Fabularia* DEFRANCE, 1820

Type species: *Fabularia discolites* DEFRANCE IN BRONN, 1825

***Fabularia roselli*** CAUS, 1979

Fig. 16A-O

1976 *Fabularia* sp. CAUS, p. 26; figs. 1.1, 1.2

1979 *Fabularia roselli* n. sp. CAUS, p. 31, 33; text-fig. 2; pl. 1, figs. 1-13

1988 *Fabularia roselli* Caus. Drobne, figs. 8.13-8.14

2012a *Fabularia roselli* Caus, 1979. Rodríguez-Pintó *et al.*, on-line Supplementary Material, pl. 7, figs. 1-5; pl. 8, figs. 1-12

2013a *Fabularia roselli* Caus, 1979. Rodríguez-Pintó *et al.*, figs. 4-6

**Material.** This species occurs in the Gabardiella, Isuela, La Foz de Escalete, La Peña and Villalangua sections (see Figs. 3; 4; 6; 7; 9).

**Description.** The megalospheric forms show an ovoid morphology and a subcircular outline in axial section. The proloculus is spherical with a diameter between 195-260 $\mu$ m, followed by a flexostyle (Fig. 16F, N). The neanic stage is formed of chambers in biloculine arrangement (Fig. 16G-H, L-O). The axial length measured for 4-5 biloculine chambers varies between 1.5mm and 1.9mm. The basal layer is thick and can reach the same height as the chamberlets (Fig. 16F, G, L-O). The basal layer exhibits the anastomosed passages in irregular distribution (Fig. 16J). The apertural system in polar location is formed of a trematophore with apertures in cribrate distribution and supported by pillars (Fig. 16I, K). The septula reach the ceiling of the chamber subdivided into almost regular chamberlets (Fig. 16F-G, L-O). The microspheric forms show an ovoid-sub spherical

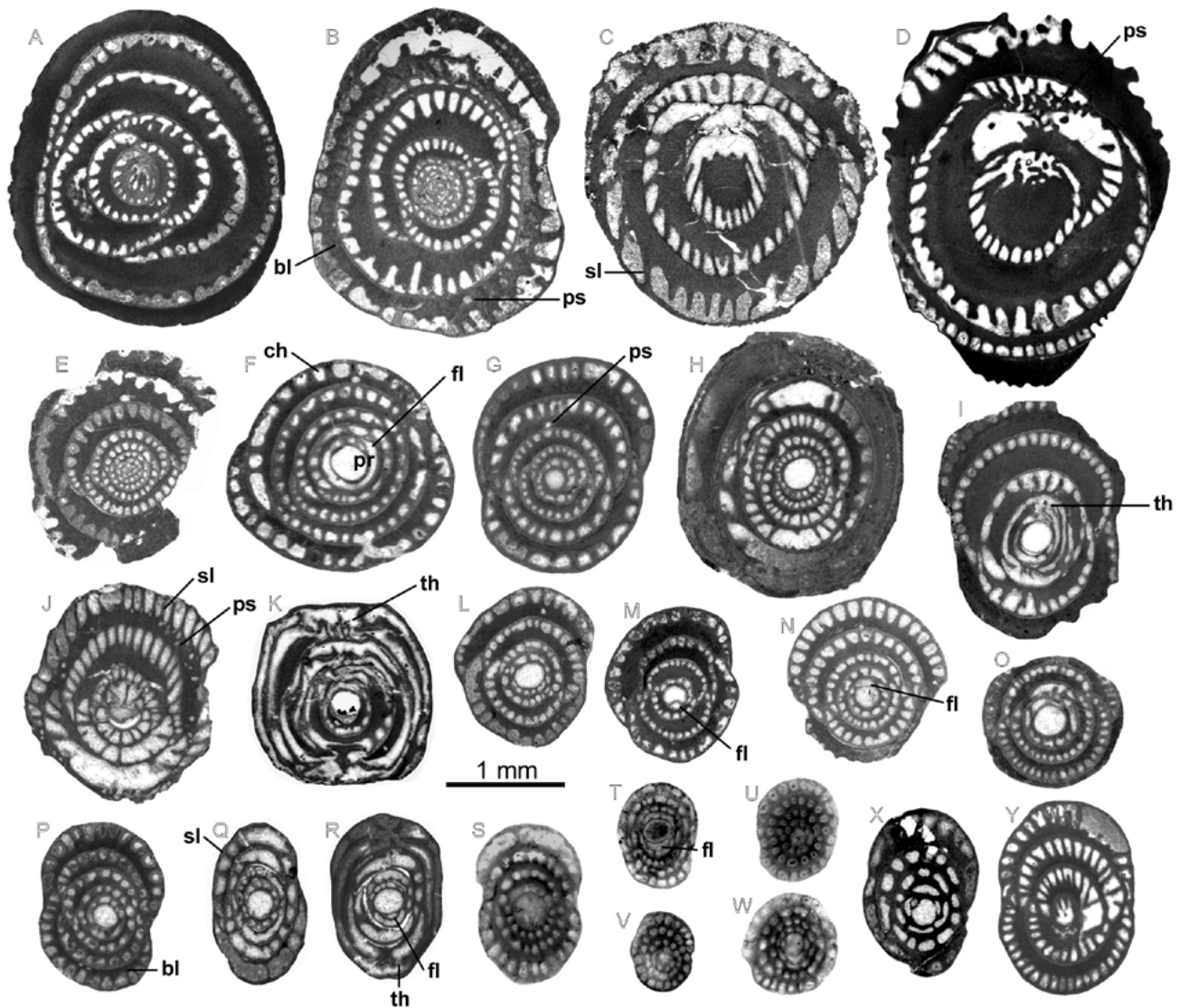


**FIGURE 16.** A-O) *Fabularia roseli*. A: uncentered axial section, microspheric form. B: centered axial section, microspheric form. C, D: oblique sections, microspheric forms; note the passage in the basal layer. E: centered axial sections, microspheric form. F-H: centered axial sections, megalospheric forms; note the flexostyle. I: centered slightly oblique axial section; note the trematophore. J: uncentered slightly oblique axial section; note the passages in the basal layer. K: centered longitudinal section; note the pillars and forams in the trematophore. L-O: centered axial sections, megalospheric forms; note the flexostyle in N. Specimens A, D, I, K, L, M: sample G 21; B: sample G 20; C: sample I 1; F, N: sample G 18; E: sample G 12; G: sample G 16; H, O: sample G 19 and J: from sample I 2. P-Y) *Fabularia ovata*. P: centered axial section. Q-R: slightly oblique axial sections; note the flexostyle and trematophore in R. S-T: centered axial sections. U-W: uncentered axial sections. X: slightly oblique axial sections. Y: subaxial section. Specimen P from sample G 18; Q, R, Y: sample G 9; S, U, W: sample V 9; T: sample E 16; V: sample P 22 and X: sample I 32. Abbreviations: bl: basal layer; th: trematophore; ch: chamberlet; ps: passage; pr: proloculus; fl: flexostyle; sl: septulum.

morphology. The axial section shows a subcircular outline slightly depressed at the junction of the chambers (Fig. 16A, B). The nepionic stage is formed of 2-3 quinqueloculine chambers with quinqueloculine arrangement, followed by the neanic stage composed of chambers in biloculine arrangement (Fig. 16B, O). The maximum diameter in axial section is around 2.75mm. The basal layer increases in thickness from the first to second biloculine chamber and can reach 3 or 4 times the height of the chamberlets and shows sporadically passages as in the megalospheric forms (Fig. 16B, D).

**Age.** The biostratigraphic range of *Fabularia roseli* extends from early Lutetian (SBZ13) to middle Lutetian 2 (SBZ15). The SBZ13 is characterized by the association with *Alveolina obtusa* (sample G 16; Fig. 3), *A. stipes* (samples G 19, G 21 and I 2; Figs. 3; 4), *A. tenuis* (sample I 7; Fig. 4) and *Assilina spira abrardi* (sample I 7; Fig. 4), indicating early Lutetian (*Alveolina stipes* and *Assilina spira abrardi* zones). The SBZ14 is characterized by the association of this species with *Nummulites aspermontis*, *N. beneharnensis* (sample I 8; Fig. 4), indicating middle Lutetian 1 (*N. gratus*-*N. beneharnensis* Zone). Finally, the

SBZ15 is characterized by the association of this species with *N. aff. deshayesi* (sample P 17; Fig. 7), indicating middle Lutetian 2 (N. sordensis-N. crassus Zone).

***Fabularia ovata*** DE ROISSY, 1805

Fig. 16P-Y

1964 *Fabularia discolithes* (Defrance). Hottinger *et al.*, p. 642, 644; pl. 6, figs. 2a, 2b

1988 *Fabularia ovata* (de Roissy). Drobne, figs. 9.10-9.11

**Material.** This species occurs in the Gabardiella, La Foz de Escalete, La Peña and Villalangua sections (Figs. 3; 6; 7; 9).

**Description.** The megalospheric forms show an ovoid morphology. The outline in axial section is elliptical to slightly depressed at the junction of the chambers (Fig. 16P, S-U). The embryonic apparatus is formed of a spherical proloculus with a diameter between 180-300 $\mu$ m, followed by a flexostyle and chambers in biloculine arrangement (Fig. 16R). For 8 biloculine chambers, in axial section, the maximum elliptical diameter varies between 0.90mm and 1.30mm and the minimum between 675 $\mu$ m and 950 $\mu$ m. The trematophore is supported by a short pillar (Fig. 16R). The basal layer is thin and the septula form chamberlets with a regular distribution (Fig. 16R, S). The chamberlets show a rectangular outline in axial section in the internal chambers, while it changes to a subrectangular shape with rounded base and a flat ceiling in the external chambers.

**Remarks.** This species differs from *Fabularia roselli* in the smaller size of the test, in displaying axial sections with an elliptical instead of a subcircular outline and in the tighter growth pattern of the chambers.

**Age.** The biostratigraphic range of *Fabularia ovata* extends from early Lutetian (SBZ13) to middle Lutetian 2 (SBZ15). The SBZ13 is characterized by the alternation of samples with this species with samples with *A. stipes* (Fig. 3), indicating early Lutetian (A. stipes Zone). In the material studied, no characteristic species of the SBZ14 (middle Lutetian 2) were found associated with *Fabularia ovata*. Finally, the SBZ15 is characterized by the alternation of samples with this species with samples containing *N. crassus* (Fig. 6) which indicate middle Lutetian 2 (N. sordensis-N. crassus Zone).

GENUS ***Pseudolacazina*** CAUS, 1979

Type species: *Pseudolacazina hottingeri* CAUS, 1979

***Pseudolacazina hottingeri*** CAUS, 1979

Fig. 17A-R

1979 *Pseudolacazina hottingeri* n. gen. n. sp. Caus, p. 33 and 36; text-figs. 3-4; pl. 2 figs. 1-9; pl. 3 figs. 1-8

2012a *Pseudolacazina hottingeri* Caus, 1979. Rodríguez-Pintó *et al.*, on-line Supplementary Material, pl. 4, figs. 1-3; pl. 5, figs. 1-8; pl. 6, figs. 1-9

2013a *Pseudolacazina hottingeri* Caus, 1979. Rodríguez-Pintó *et al.*, figs. 1-3

**Material.** This species occurs in the Gabardiella, Isuela, Sierra Caballera, La Foz de Escalete, La Peña, Murillo and Villalangua sections (Figs. 2-9).

**Description.** The megalospheric forms show an ovoid-sub-spherical morphology. The embryonic apparatus is formed of a subspherical proloculus with a diameter between 175-340 $\mu$ m, followed by a flexostyle (Fig. 17M, P). The neanic stage is composed of chambers in biloculine arrangement. However, some specimens show a nepionic stage formed of chambers in triloculine arrangement following the flexostyle (Fig. 17J). The basal layer is thin without passages inside it. Four biloculine chambers measured in equatorial section were around 2.3mm across, whereas in axial section they measured 1.8mm. In axial section, the septula subdivided the chamber in chamberlets, some septa do not reach the ceiling of the chamber (Fig. 17D, I, M). The apertural system is a trematophore supported by pillars and apertures in cribrate distribution (Fig. 17H). The microspheric forms show a subspherical morphology and maximum diameter of 4.2mm (Fig. 17A).

**Age.** The biostratigraphic range of *Pseudolacazina hottingeri* extends from early Lutetian (SBZ13) to late Lutetian (SBZ16). The SBZ13 is characterized by the association of this species with *Alveolina obtusa* (samples G 16, I 1; Figs. 3; 4), *A. callosa* (samples SC 11 and SC 14; Fig. 5), and *A. stipes* (sample I 2; Fig. 4), indicating early Lutetian (A. stipes Zone). Samples belonging to the SBZ14 are characterized by the presence of *P. hottingeri* in beds underlying samples with *A. munieri*, *Nummulites aspermontis* and *N. beneharnensis* (Fig. 4), indicating middle Lutetian 1 (A. munieri and N. gratus-N. beneharnensis zones). The SBZ15 is characterized by the association of *P. hottingeri* with *N. crassus* (sample E 16; Fig. 6), indicating middle Lutetian 2 (N. sordensis-N. crassus Zone). Finally, the SBZ16 is characterized by the occurrence of *P. hottingeri* above samples with *N. aturicus* and *N. deshayesi* (Figs. 5; 8), indicating late Lutetian (N. aturicus Zone).

GENUS ***Periloculina*** MUNIER-CHALMAS AND SCHLUMBERGER, 1885

Type species: *Periloculina zitteli* MUNIER-CHALMAS AND SCHLUMBERGER, 1885

***Periloculina*** cf. ***raincourtii*** SCHLUMBERGER, 1905

Fig. 17S-X



**FIGURE 17.** A-R) *Pseudolacazina hottingeri*. A, B: axial sections, microspheric forms. C: oblique section, microspheric form. D-R: megalospheric forms. D: centered axial section. E: oblique section. F, G: slightly oblique axial sections. H: subaxial section; note the forams and pillars. I: slightly oblique and slightly uncentered axial section. J: oblique section. K: centered longitudinal section. L: slightly oblique axial section. M: centered axial section; note the flexostyle. N: centered longitudinal section. O: slightly oblique axial sections. P: centered longitudinal sections; note the flexostyle. Q-R: centered axial sections. Specimens A, D, E, F, K, P: sample G 18; B, M: sample G 14; C, Q: sample G 16; G: sample I 34; H: sample M 2; I, L: sample I 28; J: sample I 31; N: sample G 13; O: sample G 10 and R: sample I 30. S-X) *Periloculina cf. raincourtii*. S: oblique longitudinal section; note the forams and the pillar in the trematophore. T: uncentered axial section. U: oblique longitudinal section. V-X: uncentered axial sections; note the ribs in the basal layer. Specimens S, V: sample I 28; T: sample G 24; U: sample I 30; W: sample SC 22 and X: sample SC 23. Abbreviations: ch: chamberlet; bl: basal layer; fl: flexostyle; sl: septulum; f: foramen; pi: pillar; pr: proloculus; r: rib.

**Material.** This species occurs in the Gabardiella, Isuela and La Foz de Escalete sections (Figs. 3; 4; 6).

**Remarks.** Only oblique sections were obtained in the material studied. Nonetheless, the basal layer with coarse ribs in irregular distribution and the biloculine growth pattern of the neanic stage justify its attribution to genus *Periloculina* (Fig. 17F-X). The lack of an axial centered section is the reason why this species is left in open nomenclature.

**Age.** The biostratigraphic range of *Periloculina* cf. *raincourti* extends from middle Lutetian 1 (SBZ14) to middle Lutetian 2 (SBZ15). The SBZ14 is characterized by the association of this species with *Alveolina munieri* (sample G 24; Fig. 3), indicating middle Lutetian 1 (A. *munieri* Zone). The SBZ15 is characterized by the stratigraphic location of *P.* cf. *raincourti* above beds with *Nummulites crassus* and *N.* aff. *deshayesi* (Fig. 6), indicating middle Lutetian 2 (N. *sordensis*-N. *crassus* Zone).

**Family:** Alveolinidae EHRENBERG, 1839

GENUS *Alveolina* D'ORBIGNY, 1826

Type species: *Oryzaria boscii* DEFRANCE IN BRONN, 1825

*Alveolina ospiensis* DROBNE, 1977

Fig. 18A-D

1977 *Alveolina ospiensis* n. sp. Drobne, p. 68-69; pl. 20, figs 8 and 9

**Material.** This species is present in the Gabardiella section (Fig. 3).

**Description.** Microspheric forms not found. The megalospheric forms are of large size, subcylindrical morphology and rounded poles. The axial length ranges from 17.3mm to 23.3mm and the equatorial diameter from 2.9mm to 3.8mm for 16 whorls. The index of elongation varies from 4.6 to 6.6. The proloculus shows a circular outline in axial section and its diameter varies from 420 $\mu$ m to 700 $\mu$ m. The nepionic stage around the proloculus, formed of 4-5 whorls, produces a slight inflexion in axial section. The nepionic stage is formed of one tightly coiled whorl, followed by 10-12 elongated whorls with rounded poles in axial section. The axial elongation decreases in the last 4-5 whorls with truncated or rounded poles. At the polar zone there are abundant supplementary passages in the basal layer. In axial section the chamberlets are very small, tight, and frequent intercalary chamberlets occur in the outer whorls.

**Remarks.** As pointed out by Drobne (1977) this species is close to *A. callosa* and differs from it in its larger overall size, the larger diameter of the proloculus and the spiral more loosely coiled.

**Age.** According to Drobne in Serra-Kiel *et al.* (1998) the biostratigraphic range of this species is SBZ13-middle SBZ14. Here this species is associated with *A. callosa* (sample G 3; Fig. 3), indicating early Lutetian (A. *stipes* Zone) or SBZ13.

*Alveolina decastro* DI SCOTTO, 1966

Fig. 19A-D

1966 *Alveolina (Alveolina) decastro* n. sp. Di Scotto, p.69-70; tbl. 1, fig. 32; tbl. 2, fig. 1-6; tbl. 3, fig. 1-4; text-fig. 1 b

1977 *Alveolina (Alveolina) decastro* Di Scotto. Drobne, p. 52; Pl. 11, fig. 5-8; text-figs. 29b, 45b

2013a *Alveolina decastro* Di Scotto. 1966. Rodríguez-Pintó *et al.*, figs. 18-19

**Material.** This species is present in the Gabardiella section (Fig. 3).

**Description.** Microspheric forms not found. The megalospheric forms show an oval morphology with rounded poles. The axial length ranges from 2.0mm to 2.3mm and the equatorial diameter from 1.2mm to 1.3mm for 6 whorls. The index of elongation varies between 1.5-1.8. The proloculus is circular in axial section, with

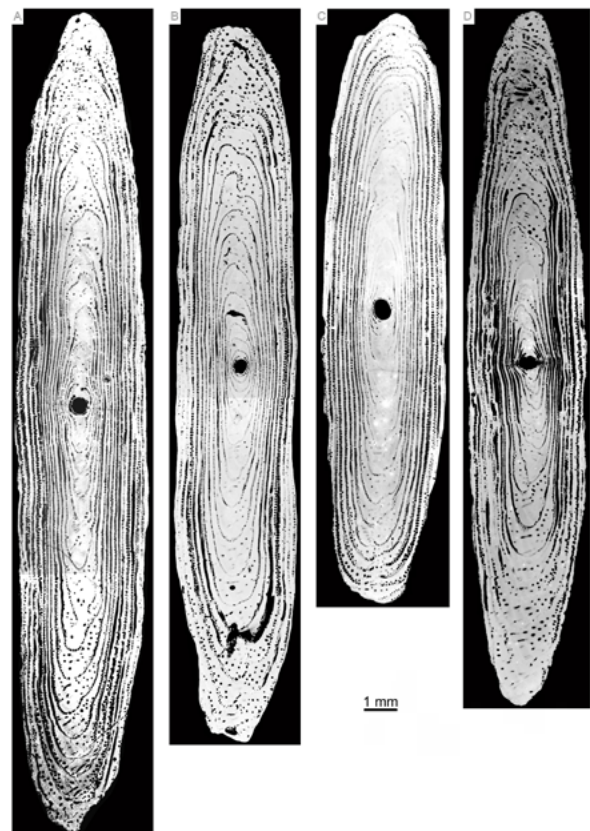
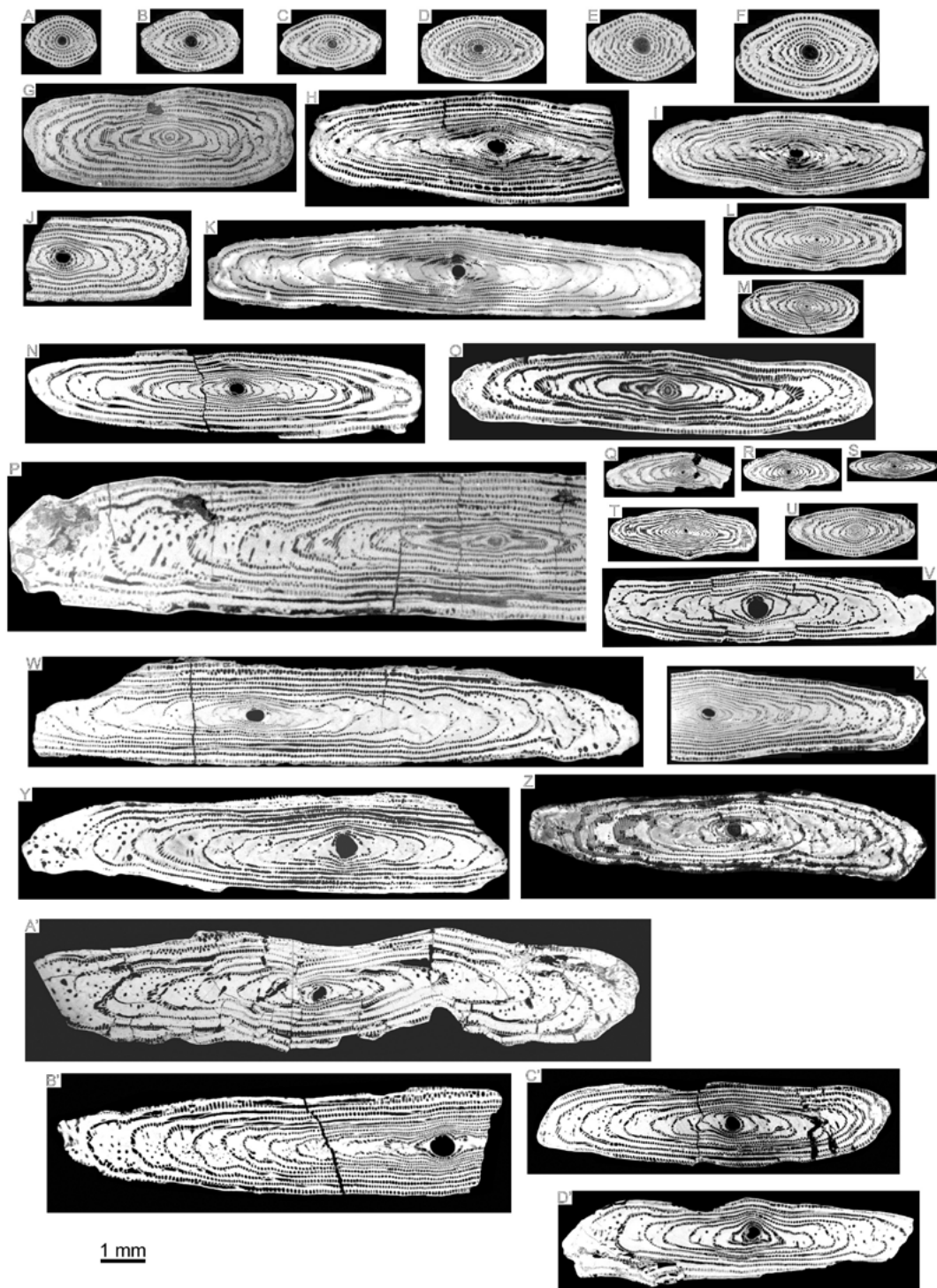


FIGURE 18. A-D) *Alveolina ospiensis*. Axial sections, megalospheric forms. All specimens from sample G 3.



**FIGURE 19.** A-D) *Alveolina decastroi* axial sections, megalospheric forms. E-F) *Alveolina cremae* axial sections, megalospheric forms. G) *Alveolina obtusa* subaxial section, megalospheric form. H-I) *Alveolina levantina* axial sections, megalospheric forms. J) *Alveolina obtusa* axial section, megalospheric form. K) *Alveolina tenuis* axial section, megalospheric form. L-M) *Alveolina boscii* oblique axial sections; megalospheric forms. N-P) *Alveolina tenuis*. N-O: axial sections, megalospheric forms. P: axial section, microspheric form. Q-U) *Alveolina boscii*. Q: centered axial section. R: oblique axial sections. S: centered axial section. T: strongly oblique axial section. U: oblique axial section. All specimens megalospheric forms. V) *Alveolina callosa* axial section, megalospheric form. W) *Alveolina stipes* axial sections, megalospheric forms. X) *Alveolina tenuis* axial section, megalospheric form. Y-Z) *Alveolina callosa* axial section, megalospheric form. A'-D') *Alveolina munieri* axial sections, megalospheric forms. A-F: sample G 1; G: sample G 16; H-I: sample I 7; J: sample G 16; K: sample I 7; L: G 15; M, Q: sample G 18; N: sample I 7; O: sample G 21; P: sample G 17; R, U: sample G 16; S: sample G 14; T: sample G 34; X: sample I 13; W: sample G 4; V, Y: sample G 3 and Z: sample SC 12; A': sample I 17; B', D': sample I 20 and C': sample I 16.

a diameter ranging between 190 $\mu$ m and 275 $\mu$ m. The nepionic stage is formed of 2-3 tightly coiled whorls followed by chambers with a moderate elongation in axial section. The chamberlets have a circular outline in the inner whorls and a subrectangular outline in the outer whorls. The equatorial spiral is tightly coiled and the basal layer is thin, except in the outer whorls where it reaches the height of the chamberlets.

**Age.** The biostratigraphic range of *A. decastroi* is middle Cuisian (SBZ11). This species occurs in the Boltaña Fm. (sample G 1; Fig. 3) associated with *A. cremae*, indicating middle Cuisian (*A. dainelli* Zone) or SBZ11.

***Alveolina cremae*** CHECCHIA-RISPOLI, 1905

Fig. 19E-F

1960 *Alveolina cremae* Checchia-Rispoli, 1905. Hottinger, p. 152-154; pl. 10, fig. 8-10; pl. 11, fig. 4-8; pl. 14, fig. 8; text-fig. 21g

1966 *Alveolina (Alveolina) cremae* Checchia-Rispoli. Di Scotto, p.71-72; tbl. 7, fig. 2-6; tbl. 8, fig. 14; tbl.9, fig. 1-6; tbl. 10, fig. 4-5; tbl. 11, fig. 5-6; tbl. 12, fig. 4-6, text-fig. 1d

1977 *Alveolina cremae* Checchia-Rispoli. Drobne, p. 55-56; pl. 12, fig. 15-17, 18-20; pl. 13, fig. 1-5; text-fig. 30 a-c

2013<sup>a</sup> *Alveolina cremae* CHECCHIA-RISPOLI. 1905. Rodríguez-Pintó *et al.*, figs. 23-14

**Material.** This species is present in the Gabardiella section (Fig. 3).

**Description.** Microspheric forms not found. The megalospheric forms show an oval to fusiform morphology with rounded poles in axial section. The axial length is 3mm and the equatorial diameter is 1.9mm for 8 whorls. The index of elongation is 1.6. The proloculus is subcircular in axial section, with a diameter of 375-410 $\mu$ m. The nepionic stage around the proloculus is formed of 3-4 tight whorls, followed by 4-5 slightly elongated whorls in axial section, and rounded poles. The chamberlets have a circular outline in the inner whorls and an oval-subrectangular outline in the outer whorls. The equatorial spiral is tightly coiled and the basal layer is thin.

**Age.** According to the data available the biostratigraphic range of *A. cremae* is middle Cuisian (SBZ11). This species occurs in the Boltaña Fm. (sample G 1; Fig. 3) associated with *A. decastroi*, indicating middle Cuisian (*A. dainelli* Zone) or SBZ11.

***Alveolina obtusa*** MONTANARI, 1964

Fig. 19G, J

1964 *Alveolina obtusa* n. sp. Montanari, p. 547-551; pl. 42, figs. 1-5, 8

1977 *Alveolina (Alveolina) obtusa* Montanari. Drobne, p. 67, pl. 19, figs. 5-8; text fig. 37

2012a *Alveolina obtusa* Montanari, 1964. Rodríguez-Pintó *et al.*, on-line Supplementary Material, pl. 10, figs. 1-6

**Material.** This species is present in the Gabardiella and Isuela sections (Figs. 3; 4).

**Description.** Microspheric forms not found. The megalospheric forms show a cylindrical morphology with truncated poles. The axial length ranges from 5.5mm to 5.7mm and the equatorial diameter from 1.9mm to 2.1mm for 9-10 whorls. The index of elongation varies between 2.7-2.9. The proloculus shows an elongated outline in axial section, and a diameter ranging between 240-370 $\mu$ m. The nepionic stage is formed of two tightly coiled whorls followed, in axial section, by two elongated whorls with pointed poles and 7-8 whorls with truncated poles. At the polar area, the basal layer shows abundant supplementary passages. The chamberlets have a circular outline in the inner whorls and a subrectangular outline in the external whorls. The basal layer is thin, except in the external whorl where it can reach the height of the chamberlets.

**Age.** The biostratigraphic range of *A. obtusa* is early Lutetian (SBZ13). The stratigraphic record of SBZ13 is characterized by the alternation of samples containing this species with samples containing *A. stipes* (Fig. 3), indicating early Lutetian (*A. stipes* Zone).

***Alveolina levantina*** HOTTINGER, 1960

Fig. 19H-I

1960 *Alveolina levantina* n. sp. Hottinger, p. 154; pl. 10, figs. 11, 13; pl. 13, figs. 10, 11; pl. 14, figs. 5, 7, text fig. 84

1974 *Alveolina levantina* Hottinger. Hottinger, p. 47; pls. 49-51

1977 *Alveolina (Alveolina) levantina* Hottinger. Drobne, p. 57; text figs. 31a, 32a, 46 a-d; pl. 14, figs. 1-6; pl. 15, figs. 1, 2

1977 *Alveolina (Alveolina) levantina* Hottinger. Drobne *et al.*, p. 74; pl. 4, fig. 5

2007 *Alveolina levantina* Hottinger. Vecchio *et al.*, p. 34-35; pl. 2, figs. 18, 19

2012a *Alveolina levantina* Hottinger, 1960. Rodríguez-Pintó *et al.*, on-line Supplementary Material, pl. 12, figs. 1-3

**Material.** This species is present in the Isuela section (Fig. 4).

**Description.** Microspheric forms not found. Megalospheric forms are fusiform, with pointed or slightly rounded poles. The axial length ranges from 5.6mm to

8.2mm and the equatorial diameter from 1.7mm to 2.0mm for 12 whorls. The index of elongation varies from 3.2 to 4. The proloculus is circular or oval in axial section and the diameter varies from 310 $\mu$ m to 580 $\mu$ m. The nepionic stage around the proloculus is formed of 1 or 2 tightly coiled whorls, followed by 9-11 whorls with axial elongation and rounded or slightly pointed poles. The chamberlets have a circular outline in the inner whorls, and are oval or subrectangular in the outer whorls. The equatorial spiral is tightly coiled and the basal layer is thin. Some specimens exhibit intercalary chamberlets and secondary passages in the basal layer at the polar zone (Fig. 19H-I).

**Age.** This species has different biostratigraphic attributions. According to Hottinger (1960) its age is probably early Lutetian. However, Hottinger (1974) and Hottinger and Drobne (1988) attributed this species to middle Cuisian-late Cuisian (see fig. 2, *op. cit.*, Hottinger and Drobne (1988)) but in the figures this species appears as a typical species of the early Lutetian (see pl. IV, *op. cit.*, Hottinger and Drobne (1988)). Finally, Serra-Kiel *et al.* (1998) constrained the age of this species from the middle part of middle Cuisian (middle part SBZ11) to late Cuisian (SBZ12). Summarizing, the biostratigraphic range of this species is from the middle part of middle Cuisian to early Lutetian (middle part SBZ11-SBZ13). In the samples studied this species is associated with *Alveolina stipes* and *Assilina spira abrardi* (sample I 7; Fig. 4), indicating early Lutetian (A. stipes Zone) or SBZ13.

***Alveolina boscii*** (DEFRANCE IN BRONN, 1825)

Fig. 19L-M, Q-U

1960 *Alveolina boscii* (DEFRANCE IN BRONN). Hottinger, p. 149; pl. 10, figs. 19-22; text figs. 78, 79

1964 *Alveolina boscii* (DEFRANCE). Hottinger *et al.*, p. 638; pl. 3

1974 *Alveolina boscii* (DEFRANCE IN BRONN). Hottinger, p. 63; pl. 87

**Material.** This species is present in the Gabardiella section (Fig. 3).

**Description.** Microspheric forms not found. Megalospheric forms are of small size, and show an oval to fusiform morphology with rounded or slightly pointed poles in axial section. The axial length ranges from 1.6mm to 2.0mm and the equatorial diameter from 0.6mm to 0.8mm for 8 whorls, with an index of elongation of 2.4-3.3. For 9 whorls the axial length varies between 2.6-3.4mm and the equatorial diameter between 0.7-1.2mm, with an index of elongation of 2.6-3.7. The diameter of the proloculus is small, 75-80 $\mu$ m. The nepionic stage is formed of 4-5 tightly coiled whorls followed by chambers with a moderate elongation in axial section. The chamberlets have a circular

outline in the inner whorls and are subrectangular in the outer whorls. The equatorial spiral is tightly coiled and the basal layer is thin.

**Age.** The biostratigraphic range of *A. boscii* extends from early Lutetian (SBZ13) to middle Lutetian 1 (SBZ14). The SBZ13 is characterized by the association of this species with *A. obtusa* and *A. stipes* (samples G 16, G 21; Fig. 3) (early Lutetian, A. stipes Zone). The SBZ14 is characterized by the stratigraphic location of *A. boscii* overlying beds with *A. munieri* (Fig. 3), indicating middle Lutetian 1 (A. munieri Zone).

***Alveolina tenuis*** HOTTINGER, 1960

Fig. 19K, N-P, X

1960 *Alveolina tenuis* n. sp. Hottinger, p. 164; pl. 16, fig. 22; pl. 18, figs. 5-9, 17; text figs. 87, 90

1965 *Alveolina tenuis* Hottinger. Dizer, p. 276; pl. 3, figs. 11-13; pl. 4, figs. 9-12; text fig. 5

1974 *Alveolina tenuis* Hottinger. Hottinger, p. 45; pl. 44, figs. 1-7

1977 *Alveolina (Alveolina) tenuis* Hottinger. Drobne, 70; pl. 21, figs. 6-8

2008 *Alveolina tenuis* Hottinger. Sirel and Acar, p. 83; pl. 75, figs. 1-4

2012a *Alveolina tenuis* Hottinger, 1960. Rodríguez-Pintó *et al.*, on-line Supplementary Material, pl. 10, figs. 12-15.

2013a *Alveolina tenuis* Hottinger, 1960. Rodríguez-Pintó *et al.*, fig. 17

**Material.** This species is present in the Gabardiella, Isuela and Sierra Caballera sections (Figs. 3; 4; 5).

**Description.** Microspheric forms show a cylindrical morphology with rounded poles. At the polar zones there are abundant and large supplementary passages in axial section. The axial length is 10.8mm and the equatorial diameter is 3.3mm for 14-15 whorls. The megalospheric forms show a subcylindrical morphology and rounded poles. The axial length ranges from 9.2mm to 10.3mm and the equatorial diameter from 1.7mm to 1.9mm for 10-11 whorls. The index of elongation varies from 4.7 to 5.4. The proloculus is circular or slightly elongated in axial section and the diameter varies from 320 $\mu$ m to 340 $\mu$ m. The nepionic stage is formed of one tightly coiled whorl, followed by 2-3 whorls with moderate axial elongation and pointed poles. The neanic stage is formed of 7-10 whorls with strong axial elongation and rounded poles. At the polar zone there are abundant supplementary passages in the basal layer. The chamberlets are small, very numerous and, in axial section, show a circular outline in the inner whorls, and an oval to subrectangular outline in the outer whorls. The equatorial spiral is tightly coiled and the basal layer is thin.

**Age.** This species was found associated with *Alveolina stipes* and *Assilina spira abrardi* (sample I 7; Fig. 4), indicating early Lutetian (A. stipes and A. spira abrardi zones) or SBZ13. *A. tenuis* occurs interbedded with samples containing *Nummulites aspermontis* and *N. beneharnensis* (Fig. 4), which indicate middle Lutetian 1 (N. gratus-N. beneharnensis Zone) or SBZ14. Thus, according to the stratigraphic location of *Alveolina tenuis* (Figs. 3-5) we confirm the biostratigraphic range proposed for this species by Drobne in Serra-Kiel et al. (1998), from the middle of SBZ13 to the middle of SBZ14.

***Alveolina callosa* HOTTINGER, 1960**

**Fig. 19V, Y-Z**

- 1960 *Alveolina callosa* n. sp. Hottinger, p. 160; pl. 14, figs. 18, 19; pl. 15, figs. 7-10; text fig. 84  
 1964 *Alveolina callosa* Hottinger. Montanari, p. 547; pl. 62, figs. 1-5, 8  
 1974 *Alveolina callosa* Hottinger. Hottinger, p. 43; pl. 39  
 1977 *Alveolina (Alveolina) callosa* Hottinger. Drobne, p. 68; pl. 20, figs. 1-5  
 2008 *Alveolina callosa* Hottinger. Sirel and Acar, p. 82; pl. 75, figs. 7-8  
 2012a *Alveolina callosa* Hottinger, 1960. Rodríguez-Pintó et al., on-line Supplementary Material, pl. 10, fig. 16; pl. 11, figs. 1-4

**Material.** This species is present in the Gabardiella and Sierra Caballera sections (Figs. 3; 5).

**Description.** Microspheric forms not found. The megalospheric forms show subcylindrical morphology and rounded poles. For 9 whorls the axial length is 7.8mm and the equatorial diameter is 1.7mm. The index of elongation is 4.5. The proloculus shows a circular outline in axial section and the diameter varies from 290µm to 310µm. The nepionic stage is formed of one tightly coiled whorl, followed by 8-9 whorls with axial elongation and pointed poles. At the polar zone there are abundant large supplementary passages in the basal layer. In axial section, the chamberlets show a circular outline in the inner whorls, and an oval to subrectangular outline in the outer whorls. The basal layer can reach the height of the chamberlets in equatorial section.

**Age.** In the material studied *A. callosa* occurs along with *A. tenuis* in beds below samples with *Nummulites lehneri* and *Assilina spira abrardi* (Fig. 5), indicating early Lutetian (N. laevigatus-N. obesus and A. spira abrardi zones) or SBZ13.

***Alveolina stipes* HOTTINGER, 1960**

**Fig. 19W**

- 1960 *Alveolina stipes* n. sp. Hottinger, p. 163; pl. 16,

- figs. 8, 9; pl. 17, figs. 5-10; pl. 18, fig. 16; text figs. 86-88  
 1964 *Alveolina stipes* Hottinger. Hottinger et al., p. 638; pl. 3  
 1974 *Alveolina stipes* Hottinger. Hottinger, p. 44-45; pl. 43. Figs. 1-6  
 1977 *Alveolina (Alveolina) stipes* Hottinger. Drobne, p. 69; pl. 21, figs. 2-4  
 1977 *Alveolina (Alveolina) stipes* Hottinger. Drobne et al., p. 77; pl. 6, figs. 1-2  
 2007 *Alveolina stipes* Hottinger. Vecchio et al., p. 35; pl. 3, figs. 1-10  
 2008 *Alveolina stipes* Hottinger. Sirel and Acar, p. 81; pl. 75, figs. 9-11  
 2012a *Alveolina stipes* Hottinger, 1960. Rodríguez-Pintó et al., on-line Supplementary Material, pl. 10, figs. 17-21

**Material.** This species is present in the Gabardiella and Isuela sections (Figs. 3; 4).

**Description.** Microspheric forms not found. The megalospheric forms show a fusiform to subcylindrical morphology, slightly inflated around the first whorls in axial section, and rounded or slightly truncated poles. For 10 whorls the axial length ranges from 12mm to 14.6mm and the equatorial diameter from 1.6mm to 2mm. The index of elongation varies from 6.0 to 8.6. The proloculus shows a circular or slightly elongated outline in axial section and a diameter of 390 µm to 500µm. The nepionic stage is formed of one tightly coiled whorl. The neanic stage is formed of whorls with axial elongation and abundant supplementary passages in the basal layer at the polar zones. The equatorial spiral is tightly coiled and the basal layer is thin. The chamberlets exhibit a circular axial section in the inner whorls whereas they are oval to subrectangular in the external whorls.

**Age.** This species was considered a biomarker of the early Lutetian (A. stipes Zone) by Hottinger (1960, 1974) and Hottinger and Drobne (1988). In the material studied, *A. stipes* occurs along with *Assilina spira abrardi* (sample I 7; Fig. 4), indicating early Lutetian (A. spira abrardi Zone) or SBZ13.

***Alveolina munieri* HOTTINGER, 1960**

**Fig. 19A'-D'**

- 1960 *Alveolina munieri* n. sp. Hottinger, p. 165; pl. 16, figs. 16-21; pl. 17, figs. 1-4; pl. 18, figs. 1-4, 18; text figs. 86-88, 91  
 1974 *Alveolina munieri* Hottinger. Hottinger, p. 45; pl. 44, figs. 1-7  
 1977 *Alveolina (Alveolina) munieri* Hottinger. Drobne, p. 69; pl. 21, fig. 5  
 2012a *Alveolina munieri* Hottinger, 1960. Rodríguez-Pintó et al., on-line Supplementary Material, pl. 10, figs. 16-20

**Material.** This species is present in the Gabardiella and Isuela sections (Figs. 3; 4).

**Description.** Megalospheric forms show a cylindrical morphology and rounded poles. For 12 whorls the axial length is 8mm and the equatorial diameter is 2.36mm. The index of elongation is 6.7. The proloculus shows a circular outline in axial section and a diameter of 300-570 $\mu$ m. The nepionic stage is formed of one tightly coiled whorl around the proloculus, followed by whorls with axial elongation. There are abundant supplementary passages located at the polar zone and intercalated chamberlets in the more external whorls. The thickness of the basal layer increases progressively from the proloculus towards the outside of the test in the equatorial section. The chamberlets exhibit a circular axial section in the inner whorls and an oval to subrectangular axial section in the external whorls.

**Age.** This species was considered a biomarker for the middle Lutetian 1 (A. munieri Zone) by Hottinger (1960, 1974) and Hottinger and Drobne (1988). In the sections studied, beds with *A. munieri* alternate with beds containing *Nummulites aspermontis* and *N. beneharnensis* (Fig. 4), which indicates middle Lutetian 1 (N. gratus-N. beneharnensis Zone) or SBZ14.

*Alveolina fusiformis* SOWERBY IN DIXON, 1850

Fig. 20A-L

1960 *Alveolina fusiformis* Sowerby in Dixon. Hottinger, p. 169-170; pl. 12 figs.5-7, pl. 14 figs. 1-4; pl. 17 fig. 17; pl. 18, fig. 11; text-figures 92, 94

1962 *Alveolina fusiformis* Sowerby. Adams, p. 48; pl. 1 figs. 1-5; pl. 2, figs. 1-12; pl. 3, figs. 1-8

1965 *Alveolina fusiformis* Sowerby. Dizer, p. 278; pl. 4, figs. 1-8, text fig. 5

1974 *Alveolina fusiformis* Sowerby in Dixon. Hottinger, p. 47, 50; pl. 52

2008 *Alveolina fusiformis* Sowerby. Sirel and Acar, p. 84; pl. 76, figs. 2-5

2012<sup>a</sup> *Alveolina fusiformis* Sowerby. Rodríguez-Pintó *et al.*, on-line Supplementary Material, pl. 12, figs. 9-12

**Material.** This species is present in the Gabardiella, Isuela, Sierra Caballera, La Foz de Escalete, La Peña, Murillo, Villalangua, San Felices and La Osqueta sections (Figs. 3-11).

**Description.** Microspheric forms not found. Megalospheric forms show a fusiform to subcylindrical morphology with frequent irregularities in the surface and rounded poles. The axial length at the 8<sup>th</sup>, 10<sup>th</sup> and 12<sup>th</sup> whorls measures 3.9-7.2mm, 5.0-7.4mm and 6.8-8.8mm respectively, and the equatorial diameter 0.77-1.22mm, 1.0-1.36mm and 1.3-1.7mm respectively. The index of

elongation varies from 4.5 to 6.8. The proloculus displays circular or elongated axial outline and a length of 220-470 $\mu$ m. The nepionic stage is formed of one tightly coiled whorl followed by chambers with axial elongation. The basal layer is thin in equatorial section, and in axial section its thickness increases gradually from the 2<sup>nd</sup> whorl to the external whorls. There are rare chamberlets intercalated in the external whorls and frequent supplementary passages at the polar area.

**Remarks.** *Alveolina fusiformis* from the “Biarritzian” of Grotte de Brassempouy and Lasserre in Aquitaine, France (Hottinger 1974: pl. 52, figs 2, 6; Fig. 20H-L) displays a much larger morphological variability than the material studied here (Fig. 20A-G).

**Age.** Dizer (1965) found this species associated with *Nummulites aturicus* JOLY AND LEYMERIE, 1848 (Karasivri, Haymana Basin, Turkey, p. 278 *op. cit.*), indicating a late Lutetian age. On the other hand, Hottinger (1960, 1974) considered *A. fusiformis* to be “Biarritzian” in age, and Sirel and Acar (2008) Bartonian, unfortunately these data was not supported by other larger foraminifera, such as *Nummulites*. In the material studied the association of *A. fusiformis* with *A. munieri* (samples I 20; see Fig. 4) indicates middle Lutetian 1 (A. munieri Zone) or SBZ14. The alternation of beds with *A. fusiformis* with beds containing *N. crassus* and *N. aff. deshayesi* (Fig. 5) indicates middle Lutetian 2 (N. sordensis-N. crassus Zone) or SBZ15. Finally, the alternation of beds with *A. fusiformis* with samples with *N. aturicus* and *N. deshayesi* (Fig. 5) indicate late Lutetian (N. herbi-N. aturicus Zone) or SBZ16. The entire dataset determines that the biostratigraphic range of *Alveolina fusiformis* spans from middle Lutetian 1 or SBZ14 to late Lutetian or SBZ16 and probably up to early Bartonian or SBZ17.

*Alveolina aff. fragilis* HOTTINGER, 1960

Fig. 20M-P

**Material.** This species is present in the La Foz de Escalete, La Peña, Murillo, Villalangua, San Felices and La Osqueta sections (Figs. 6-11).

**Description.** Microspheric forms not found. Megalospheric forms show a cylindrical morphology with rounded poles. The axial length ranges from 8mm to 10.4mm and the equatorial diameter from 1mm to 1.5mm for 9-10 whorls. The index of elongation varies between 5.3 and 7.2. The proloculus shows an elongated outline in axial section with a diameter between 400-420 $\mu$ m. The equatorial section is very tightly coiled. The basal layer is thin in equatorial section and its thickness increases in axial section.

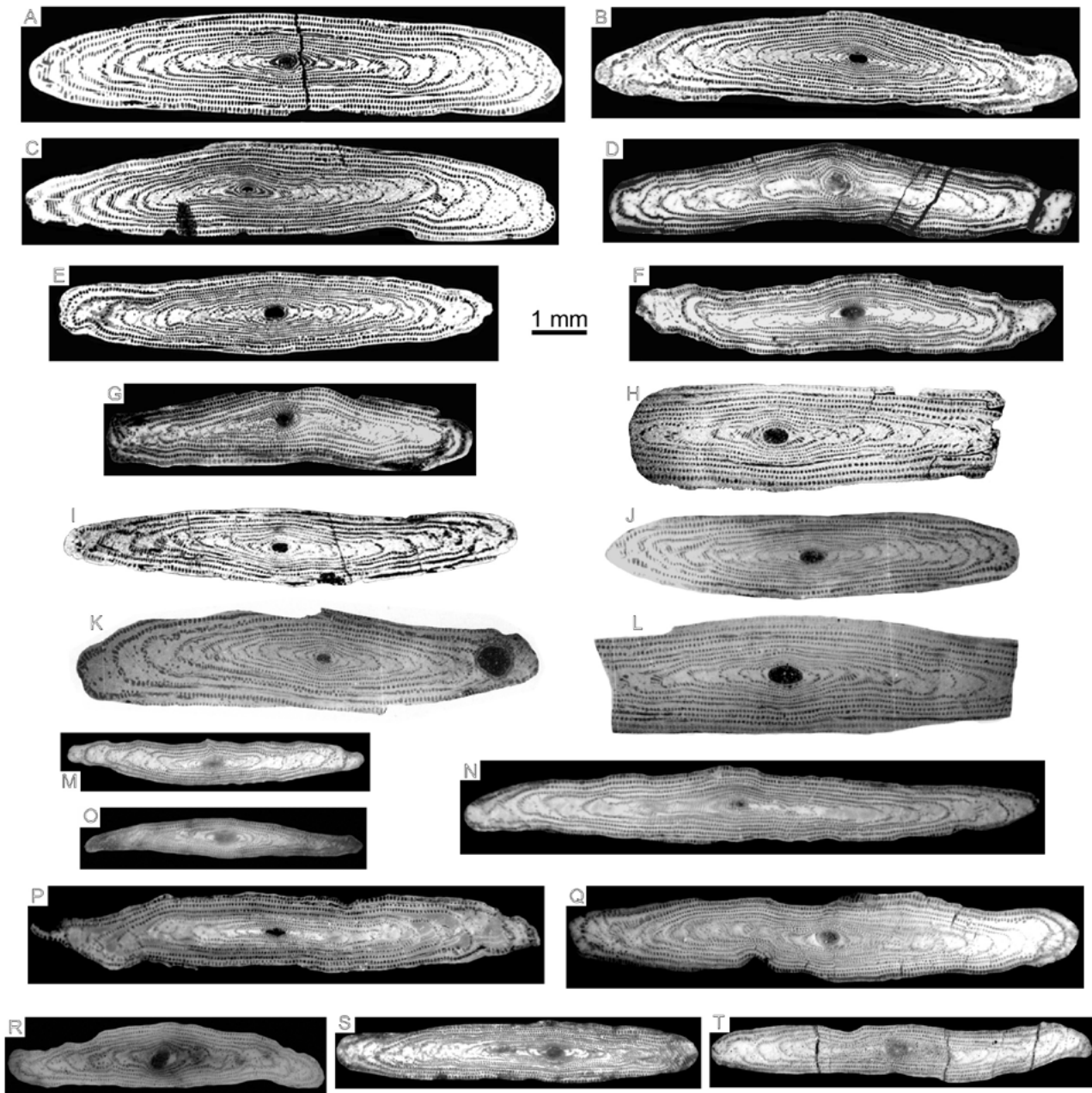


**FIGURE 20.** A-L) *Alveolina fusiformis* axial sections, megalospheric forms. Specimens A, E: sample I 20; B: sample O 7; C, F: sample I 22; D: sample O 3 and G: sample P 12. H, K, L: specimens from Lassere, Bastennes (Hottinger, 1974). I-J: specimens from Grotte de Brassempouy, Bastennes (Hottinger, 1974). M-P) *Alveolina aff. fragilis* axial sections, megalospheric forms. Specimen M: sample E 52; O: sample SF 6; N: sample P 32; P: sample E 15. Q-T) *Alveolina aff. elongata* axial sections, megalospheric forms. Specimen Q: sample SC 53; R: sample SF 6; S: sample V 10 and T: sample O 3.

**Remarks.** *A. aff. fragilis* is considered here to be ancestor of *A. fragilis* because of the smaller dimensions of the test and proloculus.

**Age.** The biostratigraphic range of *A. aff. fragilis* extends from middle Lutetian 2 (SBZ15) to late Lutetian (SBZ16). The SBZ15 is characterized by the association of this species with *N. crassus* (sample E 16; Fig. 6), indicating middle Lutetian 2 (*N. sordensis*-*N. crassus*

Zone). The SBZ16 shows *A. aff. fragilis* interbedded with beds containing *N. deshayesi* (Fig. 7).

*Alveolina aff. elongata* D'ORBIGNY IN DESHAYES, 1828  
Fig. 20Q-T

**Material.** This species is present in the Sierra Caballera, La Foz de Escalete, La Peña, Murillo, Villalangua, San Felices and La Osqueta sections (Figs. 5-11).

**Description.** Microspheric forms not found. The megalospheric forms show an elongated fusiform morphology, rough in the external whorls, and pointed poles. The axial length ranges from 6.2mm to 10.8mm and the equatorial diameter from 0.9mm to 1.6mm for 8-10 whorls. The index of elongation varies between 5.6 and 6.9. The proloculus shows a circular or slightly oval outline in axial section with a diameter of 350-410 $\mu$ m. The nepionic stage is formed of one tightly coiled whorl followed by chambers with axial elongation and truncated poles. At the polar area, the basal layer shows abundant supplementary passages. The test is tightly coiled in equatorial section. The thickness of the basal layer is irregular, except in the equatorial section, where it reaches the height of chamberlets.

**Remarks.** This species is considered here to be the ancestral chrono-species of *A. elongata* because of its smaller size. *A. aff. elongata* differs from *A. aff. fragilis* in the outline of the proloculus, which is circular to slightly elongate in the former and elongated in the latter. Moreover, *A. aff. elongata* shows a rougher surface and more supplementary passages at the polar zone.

**Age.** The biostratigraphic range of *A. aff. elongata* extends from middle Lutetian 2 (SBZ15) to late Lutetian (SBZ16). The stratigraphic record of SBZ15 is characterized by the alternation of *A. aff. elongata* beds with beds containing *N. crassus* (Figs. 6; 7), which indicates middle Lutetian 2 (N. sordensis-N. crassus Zone). The stratigraphic record of SBZ16 is characterized by the occurrence of *A. aff. elongata* beds overlying beds with *N. aturicus* and *N. deshayesi* (Fig. 5), indicating late Lutetian (N. herbi-N. aturicus Zone).

**Family:** Peneroplidae SCHULTZE, 1854

GENUS *Spirolina* LAMARCK, 1804

Type species: *Spirolina cylindracea* LAMARCK, 1804

*Spirolina austriaca* D'ORBIGNY, 1846

Fig. 21A-B

1963 *Spirolina austriaca* D'Orbigny. Hottinger, p. 966; pl. 3, figs. 1-2; text-figs. 2 m, r

**Material.** This species is present in the Gabardiella and Isuela sections (Figs. 3; 4).

**Remarks.** Small shell, with a maximum length of 0.9mm. The first 17-18 chambers display a planispiral arrangement, followed by an uniserial pattern. The uniserial length for 5 chambers is 0.4-0.6mm. Proloculus small, 20 $\mu$ m in diameter.

**Age.** This species has not biostratigraphical significance. It is found in the Guara Formation, where it is

abundant in facies attributed to seagrass environments rich in porcellanous foraminifera (Silva-Casal, 2017).

GENUS *Sivasina* SIREL AND ÖZGEN-ERDEM, 2013

Type species: *Sivasina egribucakensis* SIREL AND ÖZGEN-ERDEM, 2013

*Sivasina egribucakensis* SIREL AND ÖZGEN-ERDEM, 2013

Fig. 21C

1963 *Peneroplis cf. elegans* D'Orbigny. Hottinger, p. 969; pl. 5, figs. 3-5

1963 *Peneroplis cf. farensis* Henson. Hottinger, p. 969; pl. 5, figs. 6, 7; Fig. 2a, b

1963 *Peneroplis aff. honestus* Tood and Post. Hottinger, p. 969; pl. 5, fig. 9

2013 *Sivasina egribucakensis* n. gen. n. sp. Sirel *et al.*, p. 96, 99; pl.46, figs. 1-14; pl. 5, figs. 1-10; pl. 6, figs. 1-6; Figs. 6G, H

2016 *Sivasina egribucakensis*. Sirel and Özgen-Erdem, Serra-Kiel *et al.*, p. 24; figs. 19.22-19.30

**Material.** This species is present in the Gabardiella section (sample G 27, Fig. 3). One specimen.

**Description.** The specimen shows a nepionic stage formed of chambers in planispiral-involute arrangement with the apertures located at the base of the chambers. The neanic stage displays uncoiled growth and dendritic aperture. The septa are inclined and slightly arcuate.

**Age.** Sirel *et al.* (2013) and Serra-Kiel *et al.* (2016) located this species in Rupelian (Oligocene) rocks from Slovenia and Socotra Island (Yemen) respectively. Here, *S. egribucakensis* occurs between samples with *Alveolina munieri*, indicating middle Lutetian 1 (A. munieri Zone) or SBZ14. Thus, its biostratigraphical range extends from middle Lutetian 1 or SBZ14 to Rupelian.

GENUS *Penarchaias* HOTTINGER, 2007

Type species: *Peneroplis glynnjonesi* HENSON, 1950

*Penarchaias* sp.

Fig. 21D-G

**Material.** This species is present in the Gabardiella section (Fig. 3).

**Description.** The test of the megalospheric forms is planispiral-involute, with an equatorial diameter of about 0.9-1.0mm for 5 whorls with 50 chambers. The nepionic stage is formed of a spherical proloculus with a diameter of ca. 130 $\mu$ m and a flexostyle. The chambers with inclined septula present low ridges at the base (Fig. 21D, F).

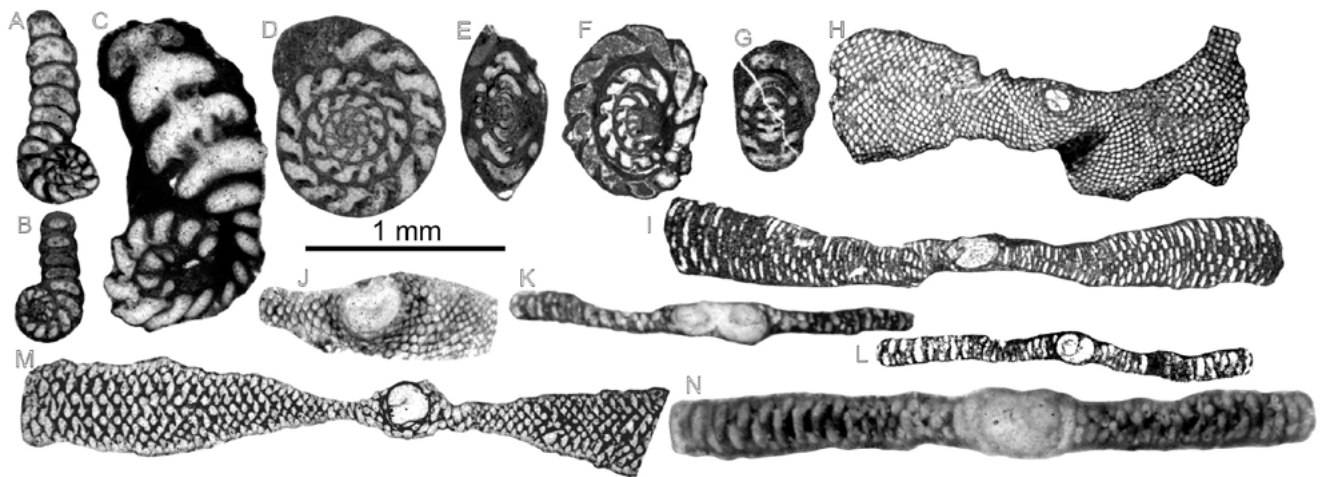


**FIGURE 21.** A-B) *Spirolina austriaca*. A-B: centered longitudinal sections. Specimen A: sample I 23; B: sample G 50. C) *Sivasina egribucakensis* longitudinal section, specimen from sample G 27. D-G) *Penarchaias* sp. D: centered equatorial section. E-F: oblique sections. G: subaxial section. Specimen D: sample G 28, E: sample G 37; F: sample G 42 and G: sample G 43. H-I) *Orbitolites complanatus*. H: equatorial section. I: oblique axial sections. Specimen H: sample G 25; I: sample I 50. J-K) *Orbitolites minimus*. J: equatorial section. K: axial section. Specimen J: sample P 5 and K: sample E 21. L-M) *Orbitolites complanatus*. L: axial section. M: oblique axial section. Specimen M: sample G 30 and L: sample SC 23. N) *Orbitolites contentinensis* axial section, specimen from sample SC 30.

**Remarks.** The specimens studied are smaller than the specimens identified as *P. glynnjonesi* (type species) by Hottinger (2007) and Serra-Kiel *et al.* (2016).

**Age.** According to Hottinger (2007) and Serra-Kiel *et al.* (2016) this genus extends from Bartonian to Rupelian (Oligocene). Here, this genus was found between samples containing *Alveolina munieri*, indicating middle Lutetian 1 (A. munieri Zone) or SBZ14. Thus, the biostratigraphical range of this genus extends from middle Lutetian 1 or SBZ14 to Rupelian.

**Family:** Soritidae EHRENBERG, 1839

**Subfamily:** Soritinae EHRENBERG, 1839

**GENUS** *Orbitolites* LAMARCK, 1801

Type species: *Orbitolites complanatus* LAMARCK, 1801

***Orbitolites minimus*** HENSON, 1950

Fig. 21J-K

1950 *Orbitolites complanata* Lamarck var. *minima* var. nov. Henson, p. 58; pl. 3, fig.1

2007 *Orbitolites minimus* Henson 1950. Hottinger, p. 10; pl. 15, figs. 6 and 9

**Material.** This species is present in the following sections: La Foz de Escalete, La Peña and La Osqueta (Figs. 6; 7; 11).

**Description.** Small test of discoidal, flattened morphology and annular-cyclic growth. The diameter of the shell for 17-19 annuli is around 3mm. Embryonic apparatus large, with a maximum diameter of 475 $\mu$ m, measured in

axial section, and 200 $\mu$ m in height. Juvenarium (nepionic stage) formed of 2-3 annuli. In axial section, this species shows an endoskeleton simpler than the endoskeleton of other species of this genus.

**Age.** This species is from a sample located between samples containing *Nummulites crassus* and *N. aff. deshayesi* (Fig. 6), which indicates middle Lutetian 2 (N. sordensis-N. crassus Zone) or SBZ15. Thus, the biostratigraphic range of this species is SBZ15, extending into SBZ16, if its less precise occurrence in late Lutetian (sample O 4; Fig. 11) is considered.

***Orbitolites complanatus*** LAMARCK, 1801

Fig. 21H-I, L-M

1961 *Orbitolites complanatus* n. sp. Lehmann, p. 618-622; Pl, 1, figs. 1-4; pl. 2, figs. 1-3; Text-figs. 18-20

1972 *Orbitolites complanatus* Lamarck, 1801. Vanová, p. 77; pl. 18, fig. 1

1978 *Orbitolites complanatus* Lamarck. Le Calvez and Blondeau, pl. 3, fig. 1

2012a *Orbitolites complanatus* Lamarck, 1801. Rodríguez-Pintó *et al.*, on-line Supplementary Material, pl. 13, figs. 13

**Material.** This species is present in the Gabardiella, Isuela and Sierra Caballera sections (Figs. 3-5).

**Description.** Test of discoidal, flattened morphology and annular-cyclic growth. Endoskeleton composed of septulum subdividing the annular chambers and stolons in crosswise-oblique disposition. The axial section of the embryonic apparatus is 190 $\mu$ m in diameter and

150µm in height. Juvenarium (nepionic stage) formed of 3-5 annuli.

**Age.** This species occurs between beds that contain *Alveolina stipes* and *A. obtusa* (Fig. 3), indicating early Lutetian (A. stipes Zone) or SBZ13. The association of *O. complanatus* with *A. munieri* (samples G 24 and G 51; Fig. 3) indicates middle Lutetian 1 (A. munieri Zone) or SBZ14, whereas its association with *Nummulites beaumonti* (sample I 50; Fig. 4) indicates middle Lutetian 2 or SBZ15. Summarizing, according to the material studied the biostratigraphic range of this species extends from early Lutetian (SBZ13) to middle Lutetian 2 (SBZ15).

***Orbitolites cotentinensis*** LEHMANN, 1961

Fig. 21N

1961 *Orbitolites cotentinensis* n. sp. Lehmann, p. 627-630; pl. 8, figs. 1-6; fig. 24, 25 and 26

**Material.** This species is present in the Sierra Caballera section (Fig. 5).

**Description.** Test of discoidal, flattened morphology with a cyclic growth of annuli. Endoskeleton composed of septulum subdividing the annular chambers and stolons in crosswise-oblique disposition. The embryonic apparatus in axial section is 600µm in diameter and 350µm in height. Juvenarium (nepionic stage) formed of 4-5 annuli.

**Remarks.** This species differs from *Orbitolites reicheli* LEHMANN, 1961 and *Orbitolites armoricensis* LEHMANN, 1961 in the larger diameter of the proloculus

**Age.** Hottinger in Lehmann (1961) associated this species with *Alveolina elongata* which indicate early Bartonian or SBZ17 (Serra-Kiel *et al.*, 1998). Here this species occurs in SBZ15 (sample SC 30; Fig. 5) which extends its biostratigraphic range from middle Lutetian 2 (SBZ15) to early Bartonian (SBZ17).

**Class:** Globothalamea PAWLOWSKI *et al.*, 2013

**Order:** "Textulariida" (DELAGE AND HÉROUARD, 1896)  
partim

**Superfamily:** Coscinophragmatacea THALMANN, 1951

**Family:** Haddoniidae Chapman, 1898

GENUS *Haddonia* CHAPMANN, 1898

Type species: *Haddonia torresiensis* CHAPMANN, 1898

***Haddonia heissigi*** HAGN, 1968

Fig. 22A-C

1968 *Haddonia heissigi* n. sp. Hagn, p. 11-16; pl. 1, figs. 1, 3, 4; pl. 2, figs. 1-3; pl. 3, figs. 1-2, text figs. 3-7

1978 *Haddonia heissigi*. Matteucci, fig. 9.c; p. 397-398; fig. 11 a-f

1980 *Haddonia heissigi*. Benjamini, pl. 4, fig. 10

1993 *Haddonia heissigi*. Schmidt and Jäger, pl. 1-4-4

**Material.** This species is present in the Gabardiella and Isuela sections (Figs. 3; 4).

**Description.** The test shows an irregular morphology and protuberances on its external surface. The wall is composed of two layers. The inner layer has large pores aligned perpendicular to the surface. The external layer is composed of coarse agglutinated particles. Nepionic stage formed of a spherical proloculus about 95µm across, followed by chambers in planispiral arrangement. Apertures are located at the base of the chambers, with a small ridge in the base.

**Remarks.** This species has been interpreted to be living attached to the substrate, and was probably abundant in seagrass and reef environments of the inner shelf (Hagn, 1968).

**Age.** According to Hagn (1968) and Matteucci (1978) the biostratigraphic range of this species extends from Lutetian to Priabonian. Here, beds containing this species are interbedded with beds containing *Alveolina stipes* which indicates early Lutetian or SBZ13 (sample G 6; Fig. 3). In the Isuela section (sample I 37; Fig. 4) this species occurs in an imprecise interval between SBZ14 and SBZ15. Thus, its biostratigraphic range is Lutetian-Priabonian.

**Superfamily:** Ataxophragmioidea SCHWAGER, 1877

**Family:** Coskinolinidae MOULLADE, 1965

GENUS *Coskinolina* STACHE, 1875

Type species: *Coskinolina liburnica* STACHE, 1875

***Coskinolina cf. peperera*** HOTTINGER AND DROBNE, 1980

Fig. 22D-E

**Material.** This species is present in the Boltaña Fm.

**Description.** Test with high-conical morphology. The wall is thick; the poor state of preservation of the specimens did not allow to observe the pseudo-keriothecal texture.

**Remarks.** The scarce material available and the absence of centered longitudinal sections did not allow its specific determination.

**Age.** In the material studied this species is associated with *Alveolina decastroi* and *A. cremae* (sample G1, see Fig. 3), indicating middle Cuisian (A. dainelli Zone) or SBZ11.

***Coskinolina roberti*** SCHLUMBERGER, 1905

Fig. 22F-T



**FIGURE 22.** A-C) *Haddonina heissigi*. A: spherical proloculus. B-C: perpendicular to coiling axis sections. Specimens A, B: sample I 37 and C: sample G 6. D-E) *Coskinolina cf. perpera*. D: uncentered longitudinal section. E: oblique section. Specimens D: sample G 2 and E: sample G 1. F-T) *Coskinolina roberti*. F: longitudinal section, G-M: oblique longitudinal sections, note the foramen distribution in I. N-P: longitudinal sections. Q: basal section. Note the foramen distribution in Q. R-S: oblique longitudinal sections, note the pillar in S. T: longitudinal sections. Specimen F: sample I 28; G, H: sample I 31; I: sample I 24; J: sample I 33; K, R: sample I 50; L: sample I 41; M: sample I 38; N: sample I 48; O, T: sample I 42; P, S: sample I 45 and Q: sample P 10. Abbreviations: f: foramen; pi: pillar.

1980 *Coskinolina (Coskinolina) roberti* (SCHLUMBERGER, 1905). Hottinger and Drobne, p. 228-229; pl. 9, figs. 1-16

2012a *Coskinolina roberti* (SCHLUMBERGER, 1905). Rodríguez-Pintó *et al.*, on-line Supplementary Material, pl. 3, figs. 1-14

**Material.** This species is frequent in the following sections: Gabardiella, Isuela, Sierra Caballera, La Foz de Escalate, La Peña and Murillo de Gállego (Figs. 3-8).

**Description.** The megalospheric forms show a high-conical morphology. The wall is thick and the texture pseudo-keriothecal. The nepionic stage is formed of protoconch and deuteroconch in eccentric location, followed by 7-10 chambers with high-trochospiral arrangement (Fig. 22F). The neanic stage is formed of 5-7 chambers in uniserial arrangement (Fig. 22N-O). The endoskeleton is formed of pillars beginning in the 3<sup>rd</sup>-4<sup>th</sup> nepionic chamber. At the apex of the cone the diameter ranges 330-375µm, with a maximum diameter of 1.5-2.0mm. The axial length is 2.0-2.3mm and the axial plane cuts 4-5 pillars. The pillars are discontinuous from one chamber to the next (Fig. 22J). The chamber sutures are slightly depressed. The apertural face is slightly convex, and the apertures show a cribrate distribution (Fig. 22I, Q).

**Age.** The biostratigraphic range of *Coskinolina roberti* extends from early Lutetian (SBZ13) to late Lutetian (SBZ16). The SBZ13 is characterized by its association with *Alveolina stipes* (sample G 21; Fig. 3), indicating early Lutetian (A. stipes Zone). The SBZ14 is characterized by the association of *C. roberti* with *A. munieri* (samples G 24, I 16, I 17, I 20 and I 21; Figs. 3; 4), indicating middle Lutetian 1 (A. munieri Zone). In the sections studied, the SBZ15 is characterized by the alternation of samples with *Coskinolina roberti* with samples with *Nummulites crassus* (Fig. 5; 7). The SBZ16 is characterized by the stratigraphic location of *C. roberti* in samples overlying samples with *N. aturicus* and *N. deshayesi* (Fig. 5).

**Order:** Rotaliida (DELAGE AND HÉROUARD, 1896)

**Superfamily:** Chilostomellacea BRADY, 1881

**Family:** Gavelinellidae HOFKER, 1956

**Gavelinellidae** indet.

Fig. 23A-F

1972 *Gyroidina subangulosa* (Plummer, 1926), Samuel *et al.*, pl. 37, fig. 1-6

**Material.** This species is present in the Gabardiella section (Fig. 3).

**Description.** The test is bilamellar with coarse pores and low-trochospiral growth. The dorsal side is convex and

smooth; the ventral side is slightly convex and displays an umbo with beads (Fig. 23C). The lamination is composed of a thicker and perforate outer layer and a thin inner layer. Between both layers there is a marked dark median layer. The proloculus is spherical with a diameter of 80-100µm (Fig. 23A, E). The equatorial diameter is 0.77mm with 21 chambers and the longitudinal diameter is 0.52mm.

**Age.** This species is located in samples interbedded with *Alveolina munier* (samples G 38, G 39 and G 40 (Fig. 3), indicating middle Lutetian 2 or SBZ14.

**Superfamily:** Planorbuloidea schwager, 1877

**Family:** Cymbaloporidae CUSHMAN, 1927

**Subfamily:** Fabianinae DELOFFRE AND HAMAOU, 1973  
**GENUS** *Fabiania* SILVESTRI, 1924

Type species: *Patella (Cymbolia) cassis* OPPENHEIM, 1896

***Fabiania cassis*** (OPPENHEIM, 1896)

Fig. 23G-J

1973 *Fabiania cassis* (Oppenheim). Deloffre and Hamaoui, pl. 6, figs. 1-7; pl. 7, fig. 1-3 and 5; pl. 8, fig. 1-6pl. 9, fig. 1-3, 5-7; pl. 10, fig. 1-9

**Material.** This species is frequent in the following sections: Gabardiella, Isuela, Sierra Caballera, La Foz de Escalate, La Peña, Murillo, Villalangua and La Osqueta (Figs. 3-9; 11).

**Description.** Test of high-conical morphology. Nepionic stage composed of proloculus and two chambers in low-trochospiral arrangement. Neanic stage formed of chambers in high-trochospiral arrangement. The diameter of the proloculus varies between 145µm and 160µm. The lateral wall shows coarse pores and an exoskeleton formed of folds of the inner layer (Fig. 23I). The peripheral sections show a pseudo-polygonal network formed of folds of the inner layer over the outer lamella of the chamber lateral wall (Fig. 23I). Apertures in interiomarginal location (Fig. 23G). The septum backwards to umbiliculus overlaps the previous septum forming a massive accumulation of folia.

**Age.** The biostratigraphic range of *Fabiania cassis* extends from early Lutetian (SBZ13) to late Lutetian (SBZ16). The stratigraphic record of SBZ13 is characterized by its association with *Alveolina stipes* (sample I 7; Fig. 4), indicating early Lutetian (A. stipes Zone). SBZ14 is characterized by the association of *F. cassis* with *A. munieri* (samples G 24, G 34, G 35 and G 36; Fig. 3), and SBZ15 is characterized by its association with *Nummulites crassus* (samples SC 38 and P 21; Figs. 5; 7), indicating middle Lutetian 2 (N. sordensis-N. crassus Zone). Finally, SBZ16 is characterized by the occurrence of *F. cassis* overlying samples with *N. aturicus*

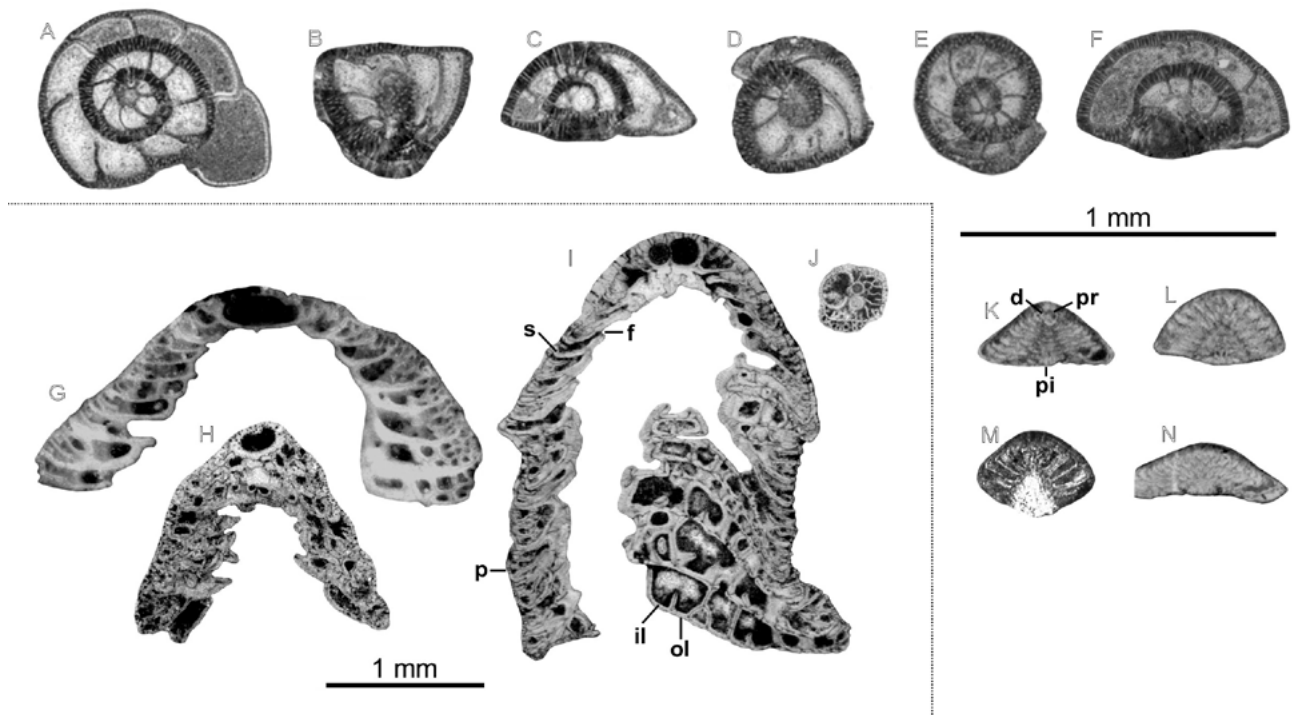


**FIGURE 23.** A-F) *Gavelinellidae* indet. A: centered perpendicular to coiling axis section. B: uncentered longitudinal section. C: centered longitudinal section. D: uncentered perpendicular to coiling axis section. E: centered perpendicular to coiling axis sections. F: oblique section. Specimens A, C, D: sample G 40; B, F: sample G 39 and E: sample G 38. G-J) *Fabiania cassis*. G, H: longitudinal centered sections. I: slightly longitudinal section. J: Nepionic stage. Specimen G: sample E 41; H: sample I 33; I: sample G 33 and J: sample G 36. K-N) *Halkyardia minima*. K: centered longitudinal section. L: oblique sections. M: uncentered longitudinal section. N: oblique sections. Specimen K: sample G 67; L: sample G 62; M: sample SC 19 and N: sample G 48. Abbreviations: pr: proloculus; s: septum; p: pore; f: foramen; d: deuterocoench; il: inner layer; ol: outer layer; pi: pile.

and *N. deshayesi* (Fig. 5), indicating late Lutetian (N. herbi-N. aturicus Zone).

**Subfamily:** Halkyardiinae KUDO, 1931

GENUS *Halkyardia* HERON-ALLEN AND EARLAND IN HALKYARD, 1918

Type species: *Cymbalopora radiata* VON HAGENOW var. *minima* LIEBUS, 1911

***Halkyardia minima*** (LIEBUS, 1911)

Fig. 23K-N

1969 *Halkyardia minima* (Liebus). Cimerman, p. 298-300; pl. 58, figs. 1-6

1973 *Halkyardia minima* (Liebus). Deloffre and Hamaoui. pl. 2, figs. 1-7.

1975 *Halkyardia minima* (Liebus). Colom, p. 239; pl. 27, fig. 1; figs. 85.1-4

1994 *Halkyardia minima* (Liebus, 1911). Pignatti, pl. 8, figs.4-5

2000 *Halkyardia cf. minima* (Liebus). Sirel, pl. 3; figs. 15-16

2001 *Halkyardia minima* (Liebus) 1911. Romero, p. 180-181; pl. 7, figs. 1-11

2003 *Halkyardia minima* (Liebus). Sirel, pl. 8, figs. 16 and 20

2012a

*Halkyardia minima* (Liebus).

Rodríguez-Pintó *et al.*, on-line Supplementary Material, pl. 13, figs. 13

**Material.** This species is present in the Gabardiella, La Foz de Escalate, Villalangua and Campo Fenero sections (Figs. 3; 6; 9; 12).

**Description.** Shell of small size and conical morphology. Cone diameter varies between 0.45-0.55mm and the cone height is around 0.2mm. The dorsal side is convex and the ventral side flat or slightly convex. Embryonic apparatus composed of protoconch and deuterocoench (Fig. 23K) followed by chambers distributed in cycles. The umbilical area shows horizontal lamellae and thin pillars (Fig. 23L).

**Age.** Cimerman (1969) and Romero (2001) found this species in Bartonian and Priabonian rocks of Slovenia and Spain (Igalada Basin). Here this species is present in samples intercalated with *Alveolina munieri*, indicating middle Lutetian 1 or SBZ14. It also occurs in samples intercalated with *Nummulites aff. deshayesi* and *N. crassus* (Fig. 6), indicating middle Lutetian 2 or SBZ15. The stratigraphic location and biostratigraphic context suggest that this species belongs to SBZ16 (Figs. 3; 9), with a

biostratigraphic range extending from middle Lutetian 1 (SBZ14) to late Eocene (Priabonian).

**Family:** Victoriellinae CHAPMAN AND CRESPIN, 1930  
**GENUS** *Gyroidinella* LE CALVEZ, 1949  
 Type species: *Gyroidinella magna* LE CALVEZ, 1949

*Gyroidinella levis* (GRIMSDALE, 1952)

Fig. 24A-C

1952 *Eorupertia incrassata* (Uhlig). Grimsdale, p. 239; pl. 20, figs. 15-21

1971 *Eorupertia cristata laevis* (Grimsdale). Boulanger and Poignant, pl. 3, figs. 5-6

2014 *Gyroidinella levis* (Grimsdale, 1952). Hottinger, p. 187, pl. 9.10, figs. 1-13.

**Material.** This species is present in the Gabardiella, Isuela and Sierra Caballera sections (Figs. 3-5).

**Description.** Trochospiral test with flattened umbilical side and concave dorsal side. Smooth dorsal side with marked pores. Length in axial section is around 1.5mm, and length in section perpendicular to the coiling axis is 1.4mm for 12-14 chambers. Small proloculus with a diameter of ca. 120µm (Fig. 24C).

**Age.** According to Hottinger (2014) the biostratigraphic range of this species is from SBZ10 (Cuisian) to SBZ13 (early Lutetian). In the Gabardiella and Isuela sections this species was found intercalated with samples containing *Alveolina stipes* (Figs. 3; 4) which indicates early Lutetian (A. stipes Zone) or SBZ13.

*Gyroidinella eocaenica* (SACAL AND DEBOURLE, 1957)

Fig. 24D-F

2000 *Gyroidinella eocaenica* (Sagal and Debourle, 1957). Sztrákos, p. 40; pl. 2, fig. 11.

2014 *Gyroidinella eocaenica* (Sagal and Debourle, 1957). Hottinger, p. 190, pl. 9.11, figs. 1-16.

**Material.** This species is present in the Gabardiella and Isuela sections (Figs. 3; 4).

**Description.** Test with trochospiral growth. Thick lateral wall with coarse pores. Flat or slightly convex ventral side and concave dorsal side. In axial section, the diameter for three whorls is ca. 2mm and the length of the section perpendicular to the coiling axis is about 1.7mm for 10 chambers. Septum inclined backwards in dorsal side (Fig. 24D). The diameter of the proloculus is ca. 150µm (Fig. 24E). Foramen located in interiomarginal position.

**Age.** According to Hottinger (2014) the biostratigraphic range of this species is SBZ13 (early Lutetian). Here, the biostratigraphic range of this species is SBZ13-SBZ14.

Its stratigraphic location intercalated with samples with *Alveolina stipes* (Figs. 3; 4) indicates early Lutetian (A. stipes Zone) or SBZ13. The SBZ14 is characterized by the association of *G. eocaenica* with *A. munieri* (sample G 36; Fig. 3), indicating middle Lutetian 1 (A. munieri Zone). Thus, the biostratigraphic range of this species extends from SBZ13 (early Lutetian) to SBZ14 (middle Lutetian 1).

*Gyroidinella magna* LE CALVEZ, 1949

Fig. 24G-M

2014 *Gyroidinella magna* (Sagal and Le Calvez, 1949). Hottinger, pl. 9.10, fig. 17.

**Material.** This species is present in the Gabardiella, Isuela, Sierra Caballera, La Peña, La Foz de Escalete, Murillo de Gállego, Villalangua, San Felices, La Osqueta sections (Figs. 3-11).

**Description.** Shell with trochospiral growth. Flat umbilical side and conical dorsal side. Slightly depressed sutures in subequatorial section (Fig. 24H, L). In axial section, the diameter for three whorls is around 2.3mm and the length of the section perpendicular to the coiling axis is around 2.4mm for 18-20 chambers. Proloculus about 190µm in diameter.

**Age.** According to Hottinger (2014) the biostratigraphic range of this species is SBZ13 (early Lutetian). Here, this species was found in Lutetian rocks. In the SBZ13 it is associated with *Alveolina callosa* (sample SC 14; Fig. 5), and in SBZ14 it is associated with *A. munieri* (samples G 23 and G 24; Fig. 3), indicating middle Lutetian 1 (A. munieri Zone). Samples with this species are intercalated with *Nummulites crassus* and *N. aff. deshayesi* (Fig. 5), indicating middle Lutetian 2 (N. sordensis-N. crassus Zone) or SBZ15. Finally, samples with this species are intercalated with *N. aturicus* and *N. deshayesi* (Figs. 5; 7), indicating late Lutetian (N. herbi-N. aturicus Zone) or SBZ16. Thus, the biostratigraphic range of this species extends from SBZ13 (early Lutetian) to SBZ16 (late Lutetian).

**GENUS** *Korobkovella* HAGN AND OHMERT, 1971

Type species: *Truncatulina grosserugosa* GÜMBEL, 1870

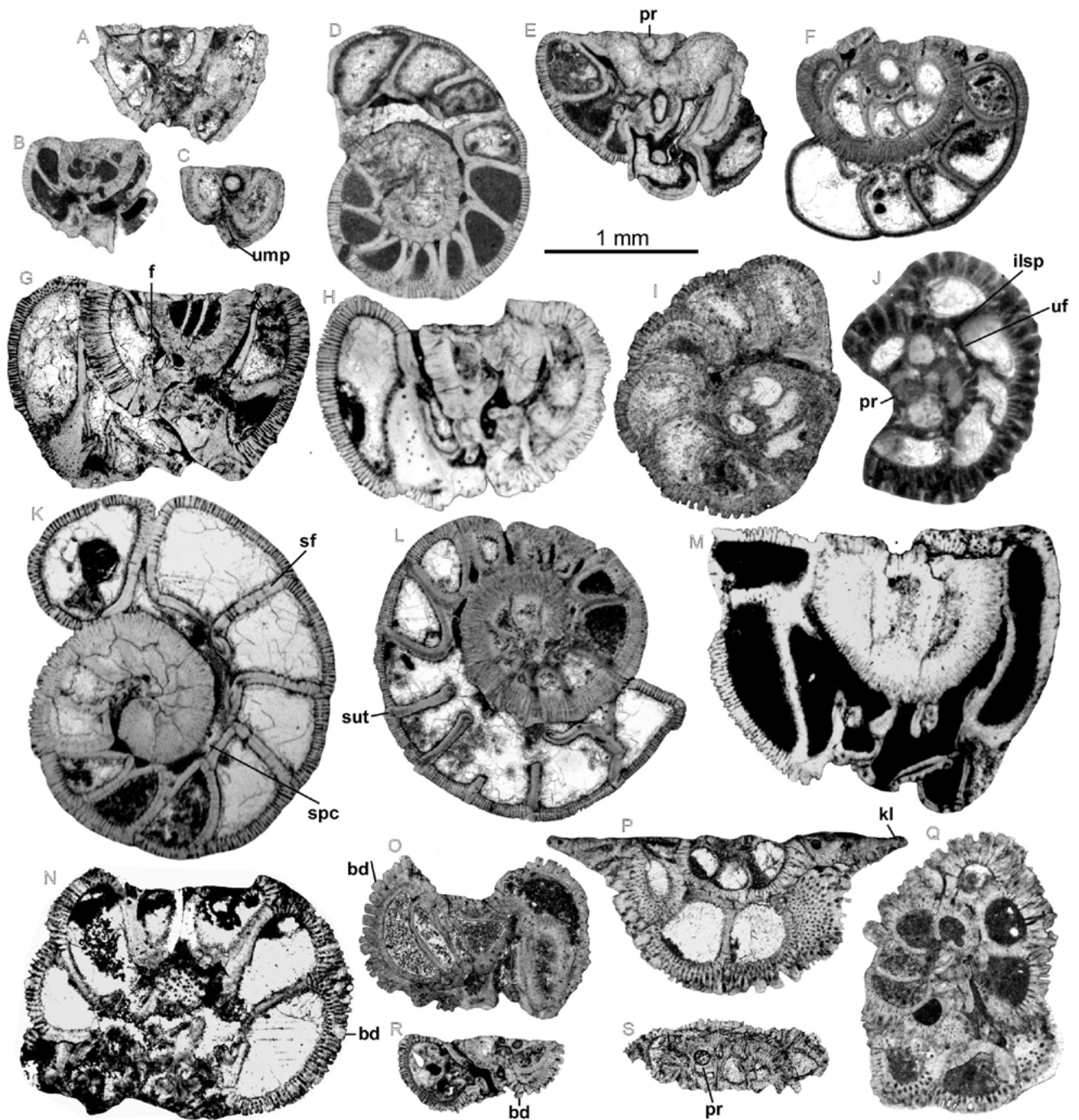
*Korobkovella grosserugosa* (GÜMBEL, 1870)

Fig. 24N-P, R-S

1987 *Korobkovella grosserugosa*. Loeblich, Jr and Tappan, p. 595-596; pl. 658, figs. 1-9, p. 180-181; pl. 9, figs. 1, 3-6

2001 *Korobkovella cf. grosserugosa*. Romero, p. 180-181; pl. 9, figs. 1, 3-6

**Material.** This species is present in the Gabardiella and Sierra Caballera sections (Figs. 3; 5).



**FIGURE 24.** A-C) *Gyroidinella levis*. A-C: centered axial sections. Specimen A: sample SC 1; B: sample G 7 and C: sample I 4. D-F) *Gyroidinella eocaenica*. D: uncentered perpendicular to coiling to axis section. E: subaxial section. F: oblique section. Specimens D, E: sample G 36 and F: sample G 33. G-M) *Gyroidinella magna*. G-H: subaxial sections. I-J: centered perpendicular to coiling to axis sections. K-L: uncentered perpendicular to coiling to axis sections. M: subaxial sections. Specimen G: sample G 45; H, K: sample G 23; I: sample G 58; J: sample V 8; L: sample G 26 and M: sample G 24. N-P) *Korobkovella grosserugosa*. N-O: oblique subaxial sections. P: subaxial section, note the keel. Specimen N: sample SC 53; O: sample G 71; P: sample SC 53. Q) *Victoriella conoidea* longitudinal section, specimen from sample I 54. R-S) *Korobkovella grosserugosa*. R: oblique subaxial sections. S: oblique section, note the proloculus. R: sample G 39 and S: sample SC 53. Abbreviations: pr: proloculus; f: foramen; bd: bead; spc: spiral canal; sf: septal flat; sut: suture; ilsp: intra-septal interloccular space; uf: umbilical flat; ump: umbilical pile; kl: keel.

**Description.** Test low-trochospiral with a flat or convex dorsal side and a slightly convex umbilical side. Thick lateral wall with coarse pores and marked beads (Fig. 24S). Septum inclined backwards in dorsal side. The dorsal side shows a keel without pores (Fig. 24P).

**Age.** Romero (2001) found this species in Bartonian rocks from the Igualada Basin (Spain). In the material studied this species is located in samples intercalated with *Alveolina munieri* (A. munieri Zone), indicating middle Lutetian 1 or SBZ14 (Fig. 3). Samples with *K. grosserugosa* are intercalated with *Nummulites aturicus* (Figs. 5), indicating late Lutetian (N. herbi-N. aturicus Zone) or SBZ16. Thus, the biostratigraphic range of this species extends from SBZ14 (middle Lutetian) to SBZ17 (early Bartonian).

GENUS *Victoriella* CHAPMAN AND CRESPIN, 1930

Type species: *Victoriella conoidea* RUTTEN, 1914

*Victoriella conoidea* (RUTTEN, 1914)

Fig. 24Q

1987 *Victoriella conoidea*. Loeblich and Tappan, p. 596; pl. 657, figs. 11-13

1993 *Victoriella conoidea* (Rutten). Robinson and Wright, p. 307, 309; figs. 16.5-6

2007 *Victoriella conoidea* (Rutten, 1914). Serra-Kiel *et al.*, p. 369; pl. 2, figs. 8 and 9

**Material.** This species occurs in the Isuela section (Fig. 4).

**Description.** Test with low-trochospiral growth. The first whorls show a conical morphology and are followed by whorls with enlarged morphology. The sutures between chambers are depressed. Thick wall with marked pores and beads (Fig. 24Q). The length in longitudinal section is 1.85mm and in sections perpendicular to the coiling axis is 1.3mm.

**Age.** According to Robinson and Wright (1993) and Serra-Kiel *et al.* (2007) the biostratigraphic range of this species is late Eocene to Oligocene. Here, this species was found associated with *Nummulites deshayesi* (sample I 54; Fig. 4), indicating late Lutetian (N. herbi-N. aturicus Zone) or SBZ16. Consequently, its biostratigraphic range extends from late Lutetian to Oligocene.

**Superfamily:** Acervulinoidea SCHULTZE, 1854

**Family:** Acervulinidae SCHULTZE, 1854

GENUS *Solenomeris* DOUVILLE, 1924

Type species: *Solenomeris ogormani* DOUVILLE, 1924

*Solenomeris* cf. *ogormani* DOUVILLE, 1924

Fig. 25A-C

2003 *Solenomeris ogormani* Douvillé, 1924. Bassi, p. 339-341; figs. 1 and 2

**Material.** This species is present in the Gabardiella, Isuela, Sierra Caballera, La Foz de Escalete, La Peña, Murillo, Villalangua and La Osqueta sections (Figs. 3-9; 11).

**Remarks.** This species was formerly considered to be a red algae. Later, Perrin (1987, 1994) and Bassi (2003) showed that its morphostructure was rather the morphostructure of an acervulinid foraminifera. As pointed out by the later author “each layer of the test consists of an expanse chamber subdivided into small, chamberlets connected by tubular passages”. Unfortunately, the embryonic apparatus could not be observed, leading to a less well-defined taxonomic attribution.

**Age.** This species has been interpreted to be living attached to the substrate, especially in seagrass and reef environments of the inner shelf (Silva-Casal, 2017; Tomás *et al.*, 2016). It has not biostratigraphic significance since it ranges from early Paleogene (Plaziat and Perrin, 1992; Perrin, 1994) to late Lutetian.

GENUS *Gypsina* CARTER, 1877

Type species: *Polytrema planum* CARTER, 1877

“*Gypsina*” *moussaviani* BRUGNATTI AND UNGARO, 1987  
Fig. 25D-G

1987 “*Gypsina*” *moussaviani* n. sp. Brugnatti and Ungaro, p. 9-12; pl. 5, figs. 1-4

**Material.** This species is frequent in the Gabardiella, Isuela, Sierra Caballera, La Foz de Escalete, La Peña, Murillo, Villalangua and La Osqueta sections (Figs. 3-9; 11).

**Remarks.** Brugnatti and Ungaro (1987) described this species following morphological and structural criteria. In axial section the chambers show an arcuate outline with stolons located at the base of the chambers (Fig. 24E-F). According to these authors the concave morphology of the shell indicates an epiphytic habitat and suggests attachment to the substrate. This species was probably abundant in seagrass and reef environments of the inner shelf (Silva-Casal, 2017; Tomassetti *et al.*, 2016). Its biostratigraphic significance is moderate since it occurs throughout the Lutetian.

GENUS *Sphaerogypsina* GALLOWAY, 1933

Type species: *Ceripora globulus* REUSS, 1848

*Sphaerogypsina globulus* REUSS, 1848

Fig. 25H-I

1971 *Sphaerogypsina globula* (Reuss, 1848). Ferrer, p. 57; pl. 7, fig. 17

1975 *Sphaerogypsina globula* (Reuss). Colom, p. 241; pl. 28, fig. 1

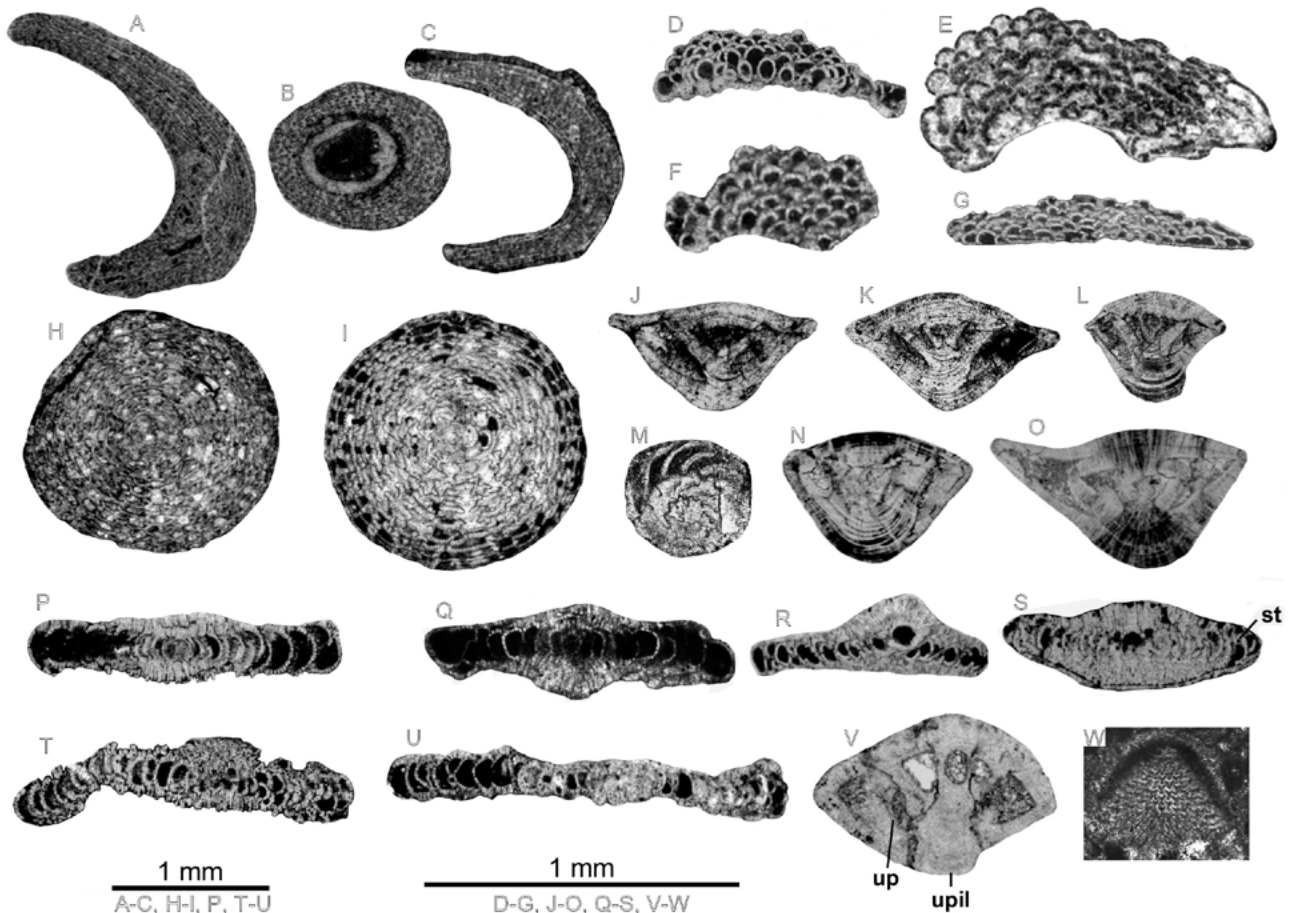


**FIGURE 25.** A-C) *Solenomeris* cf. *ogormani*. Specimen A: sample G 50; B: sample I 33 and C: sample V 10. D-G) “*Gypsina*” *moussaviani*. Specimen D: sample G 38; E: sample I 47; F: sample G 50 and G: sample G 30. H-I) *Sphaerogypsina globulus*. Specimen H: sample P 25 and I: sample G 59. J-O) *Asterigerina rotula*. J-L: uncentered axial sections. M: uncentered equatorial section. N-O: uncentered axial sections. Specimens J, K: sample SC 19; L: sample SC 1; M: sample SC 16 and N-O: from sample G 41. P) *Planolinderina?* axial section; note the embryonic apparatus with two chambers. Specimen from sample G 69. Q-S) *Linderina* cf. *brugesi*. Q: axial section. R: oblique section showing the orbitoidal growth. S: subaxial section showing the involute lamellar pattern. Q: sample SC 40; R: sample G 48 and S: sample G 64. T-U) *Planolinderina?* Subaxial sections.; T: sample G 62 and U: sample I 38. V) *Rotorbinella hensoni* axial section. specimen from sample G 71. W) *Chapmanina gassinensis* sublongitudinal section, specimen from sample SC 23. Abbreviations: st: stolon; up: umbilical plate; upil: umbilical pile.

1979 *Sphaerogypsina globula* (Reuss). Drobne *et al.*, p. 185; pl. 4, figs. 3

1994 *Sphaerogypsina globulus* (Reuss, 1848). Pignatti, pl. 3, fig. 6-7

2000 *Sphaerogypsina globula* (Reuss). Sirel, pl. 3, fig. 17

2001 *Sphaerogypsina globula* (Reuss, 1847). Romero, p. 184; pl. 12, figs. 1-4

2012a *Sphaerogypsina globula* (Reuss). Rodríguez-Pintó *et al.*, on-line Supplementary Material, pl. 13, figs. 13

**Material.** This species occurs in the Gabardiella, Sierra Caballera, La Foz de Escalete, La Peña and Villalangua and Campo Fenero sections (Figs. 3; 5-8; 12).

**Remarks.** Test spherical. Chambers distributed in the sphere and subdivided in chamberlets with chessboard

pattern (*sensu* Hottinger, 2006). The ceilings of the chamberlets are flat or slightly concave (Fig. 25I) and its wall shows coarse pores. The apertures are located at the base of the lateral wall and connect the chamberlets of adjacent chambers.

**Age.** Romero (2001) identified this species in Bartonian rocks from the Igualada Basin (Spain) and Pignatti (1994) in Priabonian rocks from the Maiella (Italy), pointing its limited biostratigraphic significance. In the material studied this species is associated with *Alveolina munieri* (sample G 36; Fig. 3), indicating middle Lutetian 1 (A. *munieri* Zone) or SBZ14. Besides, it occurs between samples that contain *Nummulites crassus* and *N. aff. deshayesi* (Fig. 6), indicating middle Lutetian 2 (N. *sordensis*-N. *crassus* Zone) or SBZ15, and between samples with *N. aturicus* and *N. deshayesi* (Figs. 5; 7) which indicates late Lutetian or SBZ 16. Finally, this species is also found in beds overlying

deposits containing *N. biarritzensis* and *N. beaumonti* (sample CF 6; Fig. 12), indicating early Bartonian or SBZ17. Summarizing, its biostratigraphic range is middle Lutetian 1 (SBZ14) to Oligocene.

**Superfamily:** Asterigerinacea D'ORBIGNY, 1839

**Family:** Asterigerinidae D'ORBIGNY, 1839

GENUS *Asterigerina* D'ORBIGNY, 1839

Type species: *Asterigerina carinata* D'ORBIGNY, 1839

*Asterigerina rotula* (KAUFMAN, 1867)

Fig. 25J-O

1979 *Asterigerina rotula* (Kaufman). Drobne *et al.*, p. 185; pl. 4, figs. 5

2001 *Asterigerina rotula* (Kaufman, 1867). Romero, p. 185; pl. 13, figs. 1-6

**Material.** This species is present in the Gabardiella and Sierra Caballera sections (Figs. 3; 5).

**Description.** Test hyaline, with asymmetrical biconvex outline in axial section. The umbilical side shows a marked umbo (Figs. 25J, K, N; 24O). The septula are falciform, inclined backwards in subequatorial section (Fig. 25M). The periphery is carinate.

**Age.** Drobne *et al.* (1979) found this species in the Oligocene of Slovenia and Romero (2001) identified it in the Bartonian in the Igualeada Basin (Spain). Here, it is associated with *Assilina spira abrardi* and *Nummulites leheneri* (samples SC 16; Figs. 3; 5), indicating early Lutetian or SBZ13. Its occurrence in sample G 41 (Fig. 3) between samples with *Alveolina munieri* (*A. munieri* Zone) indicates middle Lutetian 1 or SBZ14. Thus, the biostratigraphic range of this species extends from early Lutetian to Oligocene.

**Superfamily:** Orbitoideoidea SCHWAGER, 1876

**Family:** Linderinidae LOEBLICH AND TAPPAN, 1986

GENUS *Linderina* SCHLUMBERGER, 1893

Type species: *Linderina brugesi* SCHLUMBERGER, 1893

*Linderina brugesi* SCHLUMBERGER, 1893

Fig. 25Q-S

1999 *Linderina brugesi* Schlumberger. Ferràndez-Cañadell and Serra-Kiel, figs. 2.4 and 2.5

**Material.** This species is present in the Gabardiella, Sierra Caballera and La Peña sections (Figs. 3; 5; 7).

**Remarks.** Shell of lenticular morphology and involute arrangement of lamellae. Chambers with annular-cyclic growth of orbitoidal type. Lateral thickness of the test formed by the superposition of the successive involute outer lamellae of the different chambers. Stolon in crosswise oblique distribution, alternately in axial rows (Fig. 25S).

The axial length is around 1mm and the thickness is ca. 0.300mm.

**Age.** The presence of this species in SBZ14 is justified by its intercalation with beds containing *Alveolina munieri* (Fig. 3), indicating middle Lutetian 1 (*A. munieri* Zone). The belonging of *L. brugesi* to SBZ15 is justified by its stratigraphic location between samples with the association *Nummulites crassus* - *N. aff. deshayesi* and samples with *N. deshayesi* (sample P 24; Fig. 7). Finally, *L. brugesi* is associated with *N. aturicus* (sample SC 40; Fig. 5), indicating late Lutetian (*N. herbi-N. aturicus* Zone) or SBZ16. In sum, its biostratigraphic range is SBZ14 to SBZ16.

**Superfamily:** Planorbulinacea schwager, 1877

**Family:** Planorbulinidae schwager, 1877

GENUS *Planolinderina* FREUDENTHAL, 1969

Type species: *Planolinderina escornebovensis* FREUDENTHAL, 1969

*Planolinderina?* FREUDENTHAL, 1969

Fig. 25P-U

2001 *Planolinderina?* sp. Romero, p. 175-177, pl. 12, fig.7; pl. 14, figs. 1-6; pl. 15, figs. 1-6, 6

**Material.** This species is present in the Gabardiella and Isuela sections (Figs. 3; 4).

**Remarks.** Three axial sections showing a discoidal, practically flat, morphology, convex at the polar zone because of the involute lamellae of early chambers. Later the chambers show an evolute growth pattern. The walls of the chambers show coarse pores. The embryonic apparatus seems formed of two chambers (Fig. 25P). The lack of centered equatorial sections in the material studied hinders a more precise taxonomic attribution.

**Age.** Romero (2001) identified this taxon in the Bartonian from Igualeada Basin (Spain). In the sections studied this genus has an imprecise biostratigraphic range between SBZ14 and SBZ15 (sample I 38; Fig. 4). In the Gabardiella section this species occurs in samples G 62 and G 69 (Fig. 3) belonging to late Lutetian or SBZ 16. Thus, its complete biostratigraphic range extends from middle Lutetian 2 (SBZ15) to Bartonian.

**Superfamily:** Rotalioidea ehrenberg, 1839

**Family:** Rotaliidae EHRENBERG, 1839

**Subfamily:** Rotaliinae EHRENBERG, 1839

GENUS *Rotorbinella* BANDY, 1944

Type species: *Rotorbinella colliculus* BANDY, 1944

*Rotorbinella hensoni* (SMOUT, 1954)

Fig. 25V

1954 *Rotalia hensoni* n. sp. Smout, p. 45; pl. 15, fig. 8

2001 *Rotorbinella* sp. Romero, p. 174-175; pl. 16, figs. 1-5, 7-9

2006 *Rotorbinella* sp. Hottinger, p. 86; pl. 2, figs. 11-16

2014 *Rotorbinella hensoni* (SMOUT, 1954). Hottinger, p. 24; Figs. 3.2, 3.3A-F; pl. 3.2, figs. 1-13

**Material.** This species is present in the Gabardiella section (Fig. 3).

**Description.** Test of small size with bilamellar-perforate wall, low-trochospiral growth and rounded periphery. Ventral and dorsal sides highly convex. The umbo is pronounced with a massive plug. The diameter of the proloculus is around 100µm. The diameter of the test with 2 whorls is around 0.75mm and the length in section perpendicular to the coiling to axis is 0.50mm.

**Age.** The specimens identified here as *Rotorbinella hensoni* show the same size of the test and structural elements as *R. hensoni* described and illustrated by Hottinger (2014) in the Paleocene (SBZ2-SBZ3) and *Rotorbinella* sp. by Romero (2001) in the Bartonian-Priabonian from the Igualada Basin (Spain). In the section studied, this species occurs in the middle Lutetian 2 or SBZ 15 (samples G 54; Fig.3) and in the upper Lutetian or SBZ 16 (samples G 64 and G 71; Fig. 3). Thus, its biostratigraphic range extends from the Palaeocene to the Bartonian-Priabonian.

#### GENUS *Rotalia* LAMARCK, 1804

Type species: *Rotalites trochidiformis* LAMARCK, 1804

#### *Rotalia trochidiformis* (LAMARCK, 1804)

##### Fig. 26A-G

1954 *Rotalia trochidiformis* (LAMARCK). Smout, p. 43, pl. 1, figs. 1-6.

1963 *Rotalia trochidiformis* (LAMARCK). Reiss, p. 91, pl. 4, fig. 11; pl. 5, figs. 3, 18.

1980 *Rotalia trochidiformis* LAMARCK. Müller-Merz, p. 34, text-figs. 16-17, pl. 2, figs. 1-4; pl. 9, figs. 1-4; pl. 15, fig. 3.

2014 *Rotalia trochidiformis* (LAMARCK, 1804). Hottinger, p. 35; pl. 3.4, figs. 1-4.

**Material.** This species is frequent in the following sections: Gabardiella, Isuela, Sierra Caballera, La Foz de Escalate, La Peña, Murillo and La Osqueta (Figs. 3-8; 11).

**Description.** Test with trochospiral growth and lenticular-subconical morphology. The dorsal side is smooth, and the ventral side is flattened or slightly convex. The ventral side shows the umbilical piles distributed from the umbo to the periphery of the shell. The length in longitudinal section is 0.9-1.8mm and in section perpendicular to the coiling axis is 0.8-1.0mm for 4-5 whorls. The diameter of the proloculus is around 120µm.

**Age.** According to Hottinger (2014) the biostratigraphic range of this species is Lutetian (SBZ13-SBZ16). In the material studied the SBZ13 is characterized by the intercalation of beds with this species (Figs. 3; 4; 5) and samples with *Alveolina obtusa*, *A. callosa* and *A. stipes* (*A. stipes* Zone) and samples with *Assilina spira abrardi* and *Nummulites lehneri* (*A. spira abrardi* and *N. laevigatus*-*N. obesus* Zones) indicating early Lutetian. The record of the SBZ14 is characterized by the intercalation of *R. trochidiformis* with beds bearing *N. aspermontis* and *N. beneharnensis* (Fig. 4), which indicates middle Lutetian 1 (*N. gratus*-*N. beneharnensis* Zone). The SBZ 15 is characterized by the association of *R. trochidiformis* with *N. crassus* and *N. aff. deshayesi* (samples E 16, P 17, M 1 and M 2; Figs. 6; 7; 8), indicating middle Lutetian 2 (*N. sordensis*-*N. crassus* Zone). Finally, the SBZ16 is characterized by its association with *N. deshayesi* (samples I 54 and P 31; Figs. 4; 7), indicating late Lutetian (*N. herbi*-*N. aturicus* Zone).

#### GENUS *Medocia* PARVATI, 1971

Type species. *Medocia blayensis* PARVATI, 1971

#### *Medocia blayensis* PARVATI, 1971

##### Fig. 26H-O

1978 *Medocia blayensis* Parvati. Le Calvez and Blondeau, p. 28; pl. 1, figs. 1-2

2007 *Medocia blayensis* Parvati, 1971. Hottinger, p. 15; Pl. 12, figs. 1-9; pl.13, figs. 1-10

2014 *Medocia blayensis* Parvati, 1971. Hottinger, p. 35-37; figs. 3.8A-I and 3.9A-F

2016 *Medocia blayensis* Parvati, 1971. Serra-Kiel *et al.*, p. 60-62; fig. 44

**Material.** This species is present in the Gabardiella, Isuela and Sierra Caballera sections (Figs. 3-5).

**Description.** Test with trochospiral growth and lenticular-subconical morphology. The dorsal side is smooth. The ventral side is convex-flattened and shows an umbo composed of tight piles. The wall is perforated by fine and well-marked pores. The funnels in longitudinal section are continuous (Fig. 26I). The diameter of the proloculus is around 120µm (Fig. 26K).

**Age.** According Hottinger (2007, 2014) and Serra-Kiel *et al.* (2016) the biostratigraphic range of this species is early?-middle Lutetian to Priabonian (SBZ13? -SBZ20). In the samples studied this species is associated with *Alveolina stipes* (sample I 2; Fig. 4), which are between samples of *A. callosa* (Fig. 5), indicating early Lutetian (*A. stipes* Zone) or SBZ13. On the other hand, the association of *M. blayensis* with *A. munieri* (samples G 24 and G 35; Fig. 3) indicates middle Lutetian 1 (*A. munieri* Zone) or SBZ14. Finally, the presence of this species in SBZ15 is justified by

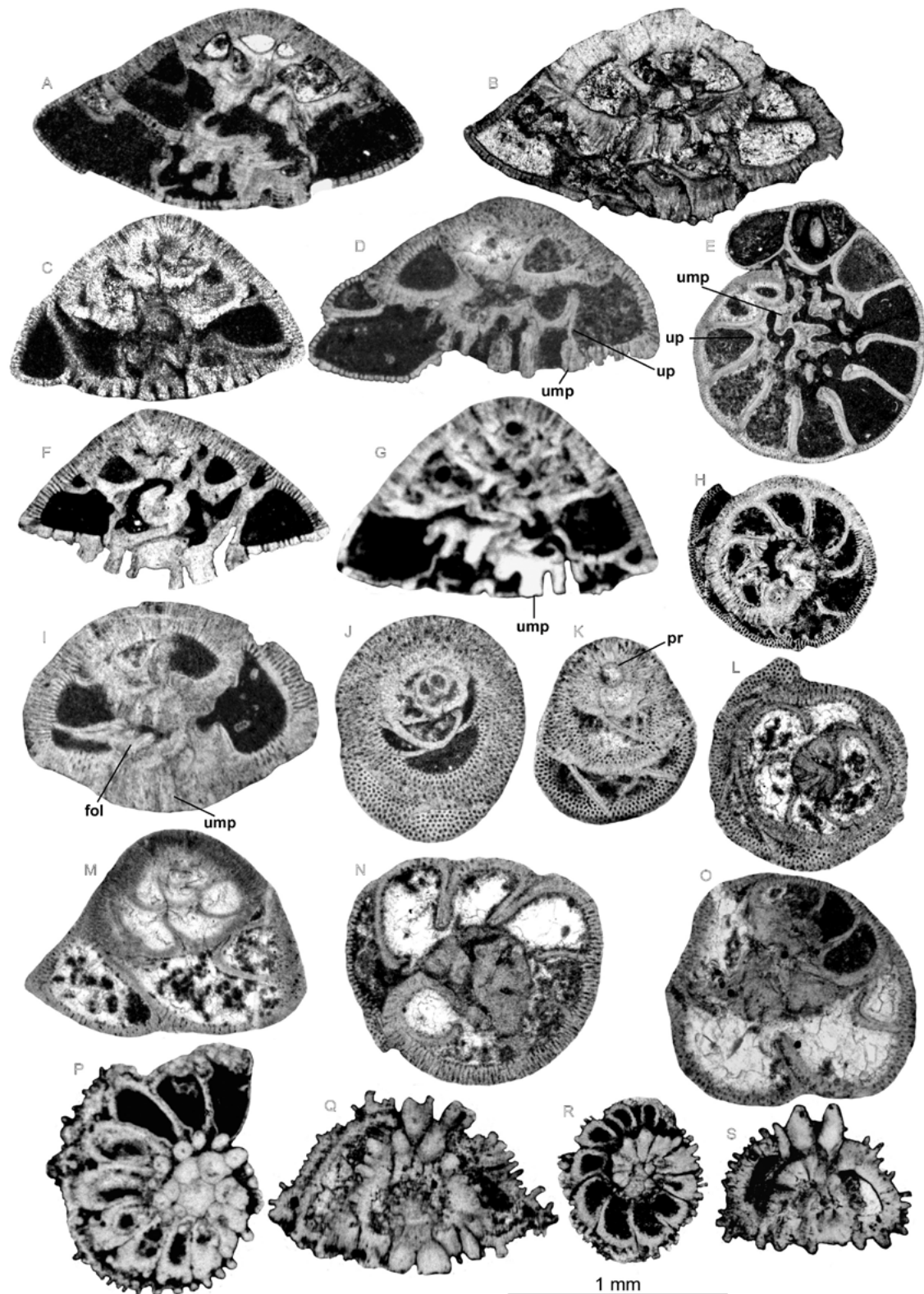


**FIGURE 26.** A-G) *Rotalia trochidiformis*. A: uncentered axial section. B: centered axial sections. C-D: uncentered axial sections. E: section perpendicular to coiling axis. F-G: centered axial sections. Specimen A: sample I 4; B: sample SC 1; C: sample SC 32; D: sample I 51; E: sample G 48; F: sample I 54 and G: sample G 23. H-O) *Medocia blayensis*. H: section perpendicular to coiling axis. I: oblique axial section. J, K: oblique peripheral sections. L: sections perpendicular to coiling axis. M: oblique section. N, O: oblique sections perpendicular to coiling axis. Specimen H: sample G 58; I: sample G 60; J-L, N, O: sample I 50 and M: sample G 16. P-S) *Neorotalia lithoamnica*. P, R: oblique sections perpendicular to coiling axial. Q, S: oblique axial sections. Specimen P: sample I 12; Q: sample G 3; R: sample I 2 and S: sample G 19. Abbreviations: pr: proloculus; up: umbilical plate; ump: umbilical pile; fol: folia.

its biostratigraphic context (Figs. 3; 4). Summarizing, the biostratigraphic range of this species is early Lutetian to Priabonian (SBZ13-SBZ20).

**Family:** Chapmaninidae THALMANN, 1938

GENUS *Chapmanina* SILVESTRI, 1905

Type species: *Chapmanina gassinensis* SILVESTRI, 1905

*Chapmanina gassinensis* SILVESTRI, 1905 Fig. 25W

1973 *Chapmanina gassinensis* (Silvestri). Deloffre and Hamaoui, pl. 11, fig. 8.

1975 *Chapmanina gassinensis* (Silvestri). Colom, p. 239, pl. 27, fig. 2; text-figs. 85.5-7

1979 *Chapmanina gassinensis* (Silvestri). Drobne *et al.*, pl. 3, figs. 7 and 8

1994 *Chapmanina gassinensis* (Silvestri 1905). Pignatti, pl. 3, fig. 8

2000 *Chapmanina gassinensis* (Silvestri). Sirel, pl. 3, fig. 14

2001 *Chapmanina gassinensis* Silvestri 1905. Romero, p. 192-193; pl. 18, figs. 1-7; pl. 19, figs. 1-9

2003 *Chapmanina gassinensis* (Silvestri, 1931). Sirel, p. 305; pl. 8, fig. 17

**Material.** This species is present in the Sierra Caballera section (Fig. 5).

**Remarks.** Only a non centered longitudinal section was available. Test of conical morphology. The neanic stage displays a uniserial arrangement of the chambers which are connected by crosswise stolons.

**Age.** According to Romero (2001) and Sirel (2003) the biostratigraphic range of this species is Bartonian-Priabonian (SBZ17-SBZ20). This species belongs to sample SC 23 (Fig 5) which occurs below beds with *Nummulites crassus* (N. sordensis-N. crassus Zone), indicating middle Lutetian 2 or SBZ15. Thus, the biostratigraphic range of this species extends from middle Lutetian 2 (SBZ15) to Priabonian (SBZ20).

**Taxa Excluded from the Family ROTALIIDAE by Hottinger (2014)**

GENUS *Neorotalia* BERMÚDEZ, 1952

Type species: *Rotalia mexicanai* NUTTALL, 1928

*Neorotalia lithamnica* (UHLIG, 1886)

Fig. 26P-S

2014 *Neorotalia lithamnica* (Uhligh, 1886). Hottinger, pl. 8.2

**Material.** This species is present in the Gabardiella and Isuela sections (Figs. 3; 4).

**Description.** Test with trochospiral growth and lenticular morphology. The dorsal and ventral sides show large plugs

and piles distributed from the polar and umbilical zones to the periphery. The length for 15 chambers, measured in a section perpendicularly to the coiling axis, is 1.2mm.

**Age.** According to Hottinger (2014) the biostratigraphic range of this species is SBZ13-SBZ14 (early-middle Lutetian 1). In the material studied this species is associated with *Alveolina callosa*, *A. ospiensis* and *A. stipes* (samples G 3 and G 19; Fig 3), indicating early Lutetian (A. stipes Zone) or SBZ13. The presence of *N. lithamnica* in SBZ14 is justified by its occurrence between samples with *Nummulites aspermontis* and *N. beneharnensis* (Fig. 4), indicating middle Lutetian 1.

**Family:** Nummulitidae DE BLAINVILLE, 1825

**Subfamily:** Nummulitinae DE BLAINVILLE, 1825

GENUS *Assilina* D'ORBIGNY, 1839

Type species: *Assilina depressa* D'ORBIGNY, 1850

*Assilina spira abrardi* SCHAUB, 1981

Fig. 27A-L

1963 *Assilina spira* (De Roissy). Schaub, p. 294, fig. 5

1966 *Assilina spira*. Schaub, fig. 1

1981 *Assilina spira abrardi* n. ssp.. Schaub, p. 202; fig. 114; pl. 78, figs. 6, 11-20; pl. 79, figs. 1-16; pl. 80, figs. 1-13; tbl. 16, fig. i

2012a *Assilina spira abrardi* Schaub, 1981. Rodríguez-Pintó *et al.*, on-line Supplementary Material, pl. 1, figs. 1-3, pl. 2, figs. 30-31

**Material.** This species is present in the Gabardiella, Isuela and Sierra Caballera sections (Figs. 3-5).

**Description.** Micro- and megalospheric forms with planispiral and evolute growth, showing a lenticular flattened morphology and rounded periphery. Diameter is 18.5mm for 11 whorls. In both generations the ornamentation is formed of spiral and septal ridges and granules at the polar zones and over the septal ridges in the inner whorls. Slightly irregular spiral growth. Marginal cord thin, varying in thickness from 1/4 the chamber's height in the external whorls to 1/5 in the inner whorls. Chambers higher than long. The septa are straight and slightly curved backwards at the top of the chambers. The septa distribution is regular in the inner whorls and irregular in the outer ones. The diameter of the megalospheric forms is around 8.2-8.5mm for 5 whorls. The proloculus of the megalospheric forms is 420-680µm in diameter. Further measurements of the equatorial section of megalospheric forms in Table 1.

**Age.** This species is associated with *Alveolina stipes* (sample I 7; Fig. 4) and with *Nummulites lehneri* (samples G 4 and SC 16; Figs. 3; 5), indicating early Lutetian (A. stipes and N. laevigatus-N. obesus zones) or SBZ13.

GENUS *Nummulites* LAMARCK, 1801Type species: *Camerina laevigata* BRUGUIÈRE, 1792*Nummulites lehneri* SCHAUB, 1981

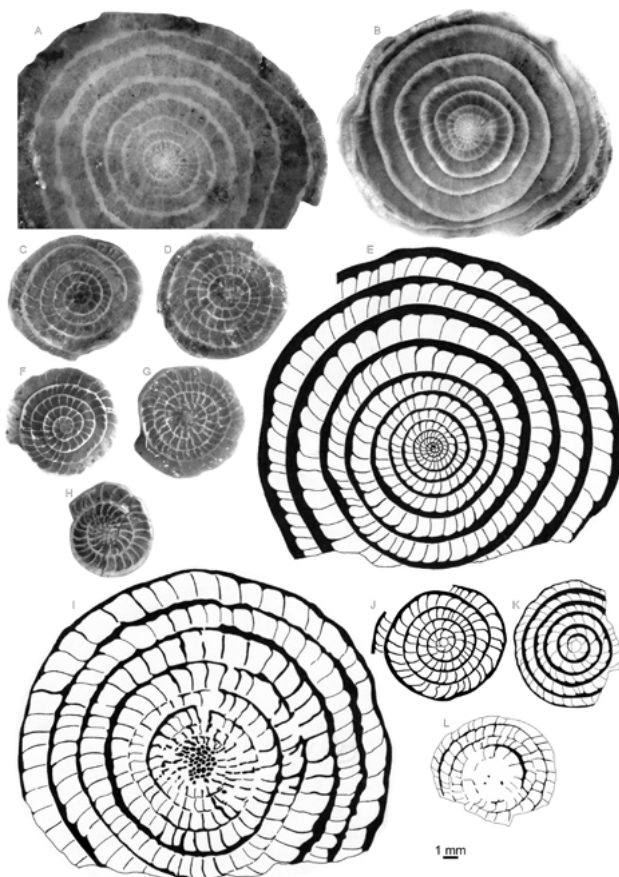
Fig. 28A-L

1981 *Nummulites lehneri* n. sp. Schaub, p. 97; fig. 81; pl. 11, figs. 13-27; tbl. 4, fig. a2012a *Nummulites lehneri* Schaub, 1981. Rodríguez-Pintó *et al.*, on-line Supplementary Material, pl. 1, figs. 10-15; pl. 2, figs. 1-5**Material.** This species is present in the Gabardiella and Sierra Caballera sections (Figs. 3; 5).**Description.** The microspheric forms show a lenticular morphology and an acute periphery. Diameter 5.7-6.2mm for 10 whorls, 10.7mm for 16 whorls with a thickness of 4.5mm. Spiral growth regular and divided in three zones, the first zone formed of 4-5 tightly coiled whorls, thesecond zone formed of 5-6 looser whorls and the third zone is poorly developed and formed only of 1-2 tight whorls. Chambers are isometric except in the external whorls, where they are slightly longer than high. Ornamentation composed of sinuous filaments bearing granules. Marginal cord thin. Septa inclined. The megalospheric forms show a lenticular morphology. The diameter of the test is 3.5-4.0mm and the thickness of the test is 2.5mm for 4-5 whorls. Ornamentation similar to the one in the microspheric forms. Chambers with rhomboidal outline mainly longer than high. Septa inclined, some slightly curved backwards at the top. Proloculus is 380-440 $\mu$ m in diameter. The equatorial section in megalospheric forms shows the values listed in Table 2.**Age.** This species is associated with *Assilina spira abrardi* (samples G 4 and SC 16; Figs. 3; 5), indicating early Lutetian (*A. spira abrardi* and *N. laevigatus*-*N. obesus* zones) or SBZ13.*Nummulites aspermontis* SCHAUB, 1981

Fig. 28M-U

1981 *Nummulites aspermontis* n. sp. 1981. Schaub, p. 104, fig. 85; pl. 13, figs. 24, 26-37; tbl. 4, fig. n2012a *Nummulites aspermontis* Schaub, 1981. Rodríguez-Pintó *et al.*, on-line Supplementary Material, pl. 1, figs. 4-6; pl. 2, figs. 6-10**Material.** This species is present in the Isuela section (Fig. 4).**Description.** Microspheric forms of middle size, lenticular morphology and acute periphery. Diameter around 10.2mm for 14-15 whorls. Ornamentation formed of meandriform filaments and granules on and between the filaments. Spiral growth divided in three zones, the first zone comprising 4-5 tightly coiled whorls, the second zone comprising 9-10 looser and regular whorls, and the third zone comprising 1-3 tight whorls. Marginal cord thick, approximately 1/2 of the height of the chambers. Megalospheric forms with a morphology and an ornamentation similar to that of the B-forms. Spiral growth is regular with diameters of 3.4-4.0mm for 4 whorls and 4.0-4.3mm for 5 whorls. The thickness of the marginal cord is 1/2-1/3 of the chamber height. Proloculus is 400-680 $\mu$ m in diameter. The equatorial section in megalospheric forms shows the values in Table 3.

In both generations the septa are inclined and curved. In the external whorls of the microspheric forms particular septa may be undulate. The chambers are rhomboidal in morphology, isometric in the inner whorls, longer than high in the other whorls.

**Remarks.** *N. aspermontis* shows the marginal cord thicker, the distribution of chambers more regular, the

**FIGURE 27.** A-L) *Assilina spira abrardi*. A: external view, microspheric form. B: equatorial section, microspheric form. C-D: equatorial sections, megalospheric forms. E: drawings on photography, equatorial section, microspheric form. F: equatorial sections, megalospheric forms. G-H: external view, megalospheric forms. I-L: drawings on photography. I: external view, microspheric form. J-K: equatorial sections, megalospheric forms. L: external view, megalospheric form. All specimens from sample G 5.



**FIGURE 28.** A-L) *Nummulites lehneri*. A: equatorial section, microspheric form. B: external view, microspheric form. C-K: equatorial sections, megalospheric forms. L: external view, megalospheric form. All specimens from sample G 5. M-U) *Nummulites aspermontis*. M: equatorial section, microspheric form. N-S: equatorial sections, megalospheric forms. T, U: external view, megalospheric forms. All specimens from sample I 8. V-B') *Nummulites beneharnensis*. V-W: equatorial sections, megalospheric forms. X: equatorial section, microspheric form. Y-A') megalospheric forms. B': external view, megalospheric form. All specimens from sample I 18. C'-L') *Nummulites crassus*. C': equatorial section, microspheric form. D': external view, microspheric form. E'-J'): equatorial sections, megalospheric forms. K': external view and L': axial section, megalospheric form. All specimens from sample SM 4. M'-Q') *Nummulites taverletensis*. M': equatorial section, microspheric form. N'-P'): equatorial sections, megalospheric forms. Q': external view, megalospheric form. All specimens from sample SM 4. R'-X') *Nummulites aturicus*. R'-S'): equatorial section, megalospheric forms. T': equatorial section, microspheric form. U'-V'): equatorial section, megalospheric forms. W', X': external views, megalospheric forms. Specimens R'-T', W: sample SC 39 and U', V', X': sample SC 50.

septum inclined and curved backwards at the top and the granules less dense on the surface than *N. beneharnensis*.

**Age.** This species is found associated with *N. beneharnensis* (sample I 8; Fig. 4), indicating middle Lutetian 1 (N. gratus-N. beneharnensis Zone) or SBZ14.

***Nummulites beneharnensis*** DE LA HARPE, 1926

Fig. 28V-B'

1981 *Nummulites beneharnensis* De La Harpe, 1926. Schaub, p.86; fig. 76; pl. 12, figs. 33-44; pl. 13, figs. 1-22, 25; tbl. 2 fig. k

2012a *Nummulites beneharnensis* De La Harpe, 1926 Rodríguez-Pintó *et al.*, on-line Supplementary Material, pl. 1, figs. 7-9, pl. 2, figs. 11-15

**Material.** This species is present in the Santa Marina and Isuela sections (Figs. 2; 4).

**Description.** Microspheric forms show an inflated lenticular morphology and rounded periphery. Diameter 13.3mm, thickness 4.8mm for 20 whorls. Ornamentation formed of meandriform filaments and granules on and between the filaments. Spiral growth divided in three zones. The first zone comprising 4-5 tightly coiled whorls, the second zone comprising 9 looser and irregular whorls, and the third zone comprising 1-2 tight whorls. Megalospheric forms of inflated lenticular morphology. Diameter 4.0-4.3mm and thickness 2.2mm for 5 whorls. Ornamentation formed of sinuous filaments and granules on and between the filaments. Proloculus is 400-460 $\mu$ m in diameter. Equatorial section in megalospheric forms shows values as in Table 4.

In both generations the septa are inclined and curved, in the external whorls of the microspheric forms some septa can be undulate. Chambers are rhomboidal, isometric in the inner whorls, and longer than high in the rest of the whorls. Irregular spiral growth. Thin marginal cord, representing 1/5 and 1/3 of the height of the chambers.

**Remarks.** *N. beneharnensis* differs from *N. aspermontis* in the tighter spiral growth, thinner marginal cord and denser granules on the surface.

**Age.** This species occurs along with *N. aspermontis* (sample I 8 and I 18; Fig. 4) and *N. boussaci* (sample SM 1; Fig. 2), indicating middle Lutetian 1 (N. gratus-N. beneharnensis Zone) or SBZ14.

***Nummulites crassus*** BOUBÉE, 1831

Figs. 28C'-E

1963 *Nummulites crassus* Boubée. Schaub, p. 286-294; fig. 3

1972 *Nummulites crassus* Boubée. Blondeau, P 81, 161; pl.34, fig. 5

1981 *Nummulites crassus* Boubée, 1831. Schaub, p. 91; fig. 78; pl. 19, figs. 9-24; tbl. 3, fig. c

1984 *Nummulites crassus* Boubée. Serra-Kiel, p. 128-133; pl. 13, figs. 9-12; pl. 14, figs. 1-5; figs. 4.155-158, 4.160-162

**Material.** This species is present in the Santa Marina, Sierra Caballera, La Foz de Escalote and La Peña sections (Figs. 2; 5-7).

**Description.** Microspheric forms of middle-large size, lenticular morphology and rounded periphery. Diameter 16.8mm and thickness 5.9mm for 20 whorls. Spiral growth divided in three zones; first zone comprising 5 tight whorls, second zone comprising 12-14 looser whorls and third zone formed of 2-3 very tightly closed whorls. Megalospheric forms of lenticular morphology. Diameters 4.4-5.3mm and thickness 2.4mm for 6 whorls. For 7 whorls the diameter can reach 5.5mm and the thickness 2.7mm. Proloculus is 500-720 $\mu$ m in diameter. Equatorial section in megalospheric forms shows values as in Table 5.

In both generations chambers changes from isometric in the inner whorls to longer than high in the other whorls. Ornamentation formed of meandriform filaments and granules on and between the filaments. Spiral growth regular. Thickness of the marginal cord is 1/2 or more of the height of the chambers. Septa inclined, slightly curved backwards at the top and sinuous in the external whorls.

**Remarks.** *N. crassus* differs from *N. aturicus* and *N. deshayesi* in the thicker marginal cord and in the spiral growth being more regular.

**Age.** This species is a biomarker of the middle Lutetian 2 according to Schaub (1981). In the material studied this species is associated with *N. aff. deshayesi* (samples SC 38 and E 28; Figs. 5; 6), indicating middle Lutetian 2 (N. sordensis-N. crassus) or SBZ15.

***Nummulites tavertetensis*** REGUANT AND CLAVELL, 1967

Fig. 28M'-Q'

1967 *Nummulites tavertetensis* n. sp. Reguant and Clavell, p. 45, 46; pl. 1

1967 *Nummulites tavertetensis* Reguant and Clavell, 1967. Reguant, p. 269-270; pl. 36

1981 *Nummulites tavertetensis* Reguant and Clavell, 1967. Schaub, p. 104; pl. 22, figs. 29, 37-45; pl. 23, figs. 1-8, 10-19

1984 *Nummulites tavertetensis* Reguant and Clavell, 1967. Serra-Kiel, p. 94-100; pl. 11, figs. 1-9; figs. 4.94-97, 4.99-101.

**Material.** This species is present in the Santa Marina section (Fig. 2).

**Description.** Microspheric forms of middle-large size, inflated lenticular morphology with rounded periphery. Diameter 14.2mm for 20 whorls. Spiral divided in three zones; first zone comprising 5 tight whorls, second zone comprising 10-12 looser whorls and third zone formed of 4-5 very tightly closed whorls. Megalospheric forms of inflated lenticular morphology, with Diameter 3.8-4.2mm for 4-5 whorls. Proloculus is 520-620 $\mu$ m in diameter.

Equatorial section in megalospheric forms shows values as in [Table 6](#).

In both generations the chambers change from isometric in inner whorls to longer than high in the other whorls. Ornamentation formed of meandriform filaments and granules on and between the filaments. Spiral growth irregular. Thickness of the marginal cord is around 1/3

**TABLE 1.** Measurements of the ecuatorial section of *Assilina spira abardi*

Whorl (n°)	1	2	3	4	5
Radius (mm)	0.8-1.1	1.4-1.8	1.2-2.6	2.9-3.7	4.0-4.5
Septa (n°)	7-8	19-24	43-50	68-79	92-118

**TABLE 2.** Measurements of the ecuatorial section of *Nummulites leheneri*

Whorl (n°)	1	2	3	4	5
Radius (mm)	0.6-0.9	1.0-1.2	1.4-1.9	1.6-2.0	2.0
Septa (n°)	7-9	17-26	48-52	71-75	77

**TABLE 3.** Measurements of the ecuatorial section of *Nummulites aspermontis*

Whorl (n°)	1	2	3	4	5
Radius (mm)	0.7-0.9	1.2-1.5	1.5-1.9	1.8-2.1	2.1-2.3
Septa (n°)	6-9	16-23	33-43	55-72	85-88

**TABLE 4.** Measurements of the ecuatorial section of *Nummulites beneharnensis*

Whorl (n°)	1	2	3	4	5
Radius (mm)	0.7-0.8	1.1-1.2	1.3-1.5	1.7-1.9	1.9-2.2
Septa (n°)	6-9	19-27	39-41	57-83	84-94

**TABLE 5.** Measurements of the ecuatorial section of *Nummulites crassus*

Whorl (n°)	1	2	3	4	5	6
Radius (mm)	0.6-1.0	1.0-1.5	1.5-1.9	1.9-2.3	2.1-2.6	2.5-2.6
Septa (n°)	6-9	16-27	32-45	51-82	70-90	105-107

of the height of the chambers. Septa inclined and curved backwards at the top.

**Age.** This species occurs associated with *N. deshayesi* (sample SC 50; Fig. 5), indicating late Lutetian (N. herbi-N. aturicus Zone) or SBZ16.

*Nummulites* aff. *deshayesi* D'ARCHIAC AND HAIME, 1853  
Fig. 29A-L

2012a *Nummulites* aff. *deshayei* d'Archiac and Haime, 1853. Rodríguez-Pintó *et al.*, on-line Supplementary Material, pl. 1, figs. 16-19; pl. 2, figs. 18-21

**Material.** This species is present in the Isuela, Sierra Caballera, La Foz de Escalate, La Peña, Murillo and Villalangua sections (Figs. 4-8).

**Remarks.** This species shows similarities to *N. deshayesi* described thereafter and is considered here to be its phylogenetic predecessor. It differs from *N. deshayesi* in the smaller parameters of the test.

**Age.** This species is associated with *N. crassus* (sample SC 38; Fig. 5), indicating middle Lutetian 2 (N. sordensis-N. crassus Zone) or SBZ15.

*Nummulites deshayesi* D'ARCHIAC AND HAIME, 1853  
Fig. 29M-U

1981 *Nummulites deshayesi* D'Archiac and Haime, 1853. Schaub, p. 88; fig. 76; pl. 15, figs. 1-19; tbl. 2, fig. 1

2012a *Nummulites deshayesi* D'Archiac and Haime, 1853. Rodríguez-Pintó *et al.*, on-line Supplementary Material, pl. 1, figs. 20-23; pl. 2, figs. 26-29

**Material.** This species is present in the Santa Marina, Isuela, Sierra Caballera, La Foz de Escalate, La Peña and Villalangua sections (Figs. 2; 4-7; 9).

**Description.** Microspheric forms of large size, inflated lenticular morphology and rounded periphery. Diameter of the test 17.4mm for 32 whorls, 14.2mm for 22 whorls and 13.8mm for 17 whorls. The thickness is 1.75mm for 22 whorls. Spiral growth divided in three zones, with the first zone comprising 5-7 tight whorls, the second zone comprising 16-18 looser whorls and the third zone comprising 10 or more very tightly-closed whorls. Megalospheric forms of inflated lenticular morphology. For 6 whorls the diameter of the test is 4.62-5.20mm and the thickness 2.7-2.8mm, and for 7 whorls the diameter can reach 5.8mm. Proloculus is 550-720 $\mu$ m in diameter. Equatorial section in megalospheric forms shows values as in Table 8.

In both generations the chambers change from isometric in the inner whorls to longer than high in the other whorls.

Ornamentation formed of meandriform filaments and granules on and between the filaments. Spiral growth quite regular. Marginal cord thin. Septa inclined and curved backwards at the top.

**Remarks.** This species differs from *Nummulites* aff. *deshayesi* by having a larger size and by the higher morphological variability in the microspheric forms, from lenticular to spherical. The proloculus of the megalospheric forms is also larger in this species than in *N. aff. deshayesi*.

**Age.** This species is associated with *N. aturicus* (sample SC 50; Fig. 5), indicating late Lutetian (N. herbi-N. aturicus Zone) or SBZ16.

*Nummulites perforatus* (MONTFORT, 1808)

Fig. 29V-D'

1938 *Nummulites aturicus* Joly and Leymerie. Flandrin, p.64- 66; pl. 6, figs. 20-28

1938 *Nummulites rouaulti* D'Archiac and Haime. Flandrin, p. 66; pl. 7, figs. 35-46,

1962 *Nummulites perforates*, Schaub, p. 327: fig. 7

1963 *Nummulites perforates* (Montfort, 1808). Schaub, p. 286-294, 290: figs. 2 and 7

1963 *Nummulites perforatus* (Montfort). Bieda, p. 193; pl. 13; pl. 15, figs. 6-8

1964 *Nummulites perforatus* (Montfort). Kecskeméti, pl. 11, fig. 2

1967 *Nummulites perforatus* (Montfort). Nemkov, p. 181-185; pl. 21, figs. 6-8; pl. 22, figs. 1-7

1971 *Nummulites perforatus* (Montfort). Ferrer, p. 34; pl. 4, figs. 1-5

1972 *Nummulites perforatus* (Montfort). Kecskeméti and Vanová, p. 131-133; pl. 29, figs. 8-9; pl. 30, figs. 1, 6; pl. 31, figs. 1-2; pl. 32, figs. 1-2

1972 *Nummulites perforatus* (Montfort). Blondeau, p. 15, 23, 25, 27, 39, 54-56, 63, 82, 88, 90, 94, 102, 161; pl. 34, figs. 6-11

1973 *Nummulites perforatus* (Montfort). Kecskeméti, p. 38-39; pl. 2

1975 *Nummulites perforatus* (Montfort). Bombita, p. 165; pl. 34, figs. 6-11

1976 *Nummulites perforatus* (Montfort). Rahaghi and Schaub, p. 775; pl. 4, fig. 5; pl. 5, fig. 1

1977 *Nummulites perforatus perforatus* (Montfort, 1808), Nemkov and Vanová, pl. 24, figs. 5-7

1981 *Nummulites perforatus* (Montfort, 1808). Schaub, pp. 88-90; figs. 76, 77; pl. 17; pl. 18; pl. 19, figs. 1-8; tbl. 2, fig. m

1984 *Nummulites perforatus* (Montfort, 1808). Serra-Kiel, p. 124-128; figs. IV-148-IV-150; pl. 23, figs. 1-7; pl. 24, figs. 1-3.

2013 *Nummulites perforatus* (Montfort, 1808). Costa *et al.*, on-line Supplementary Material, Figs. A10 (6-10)

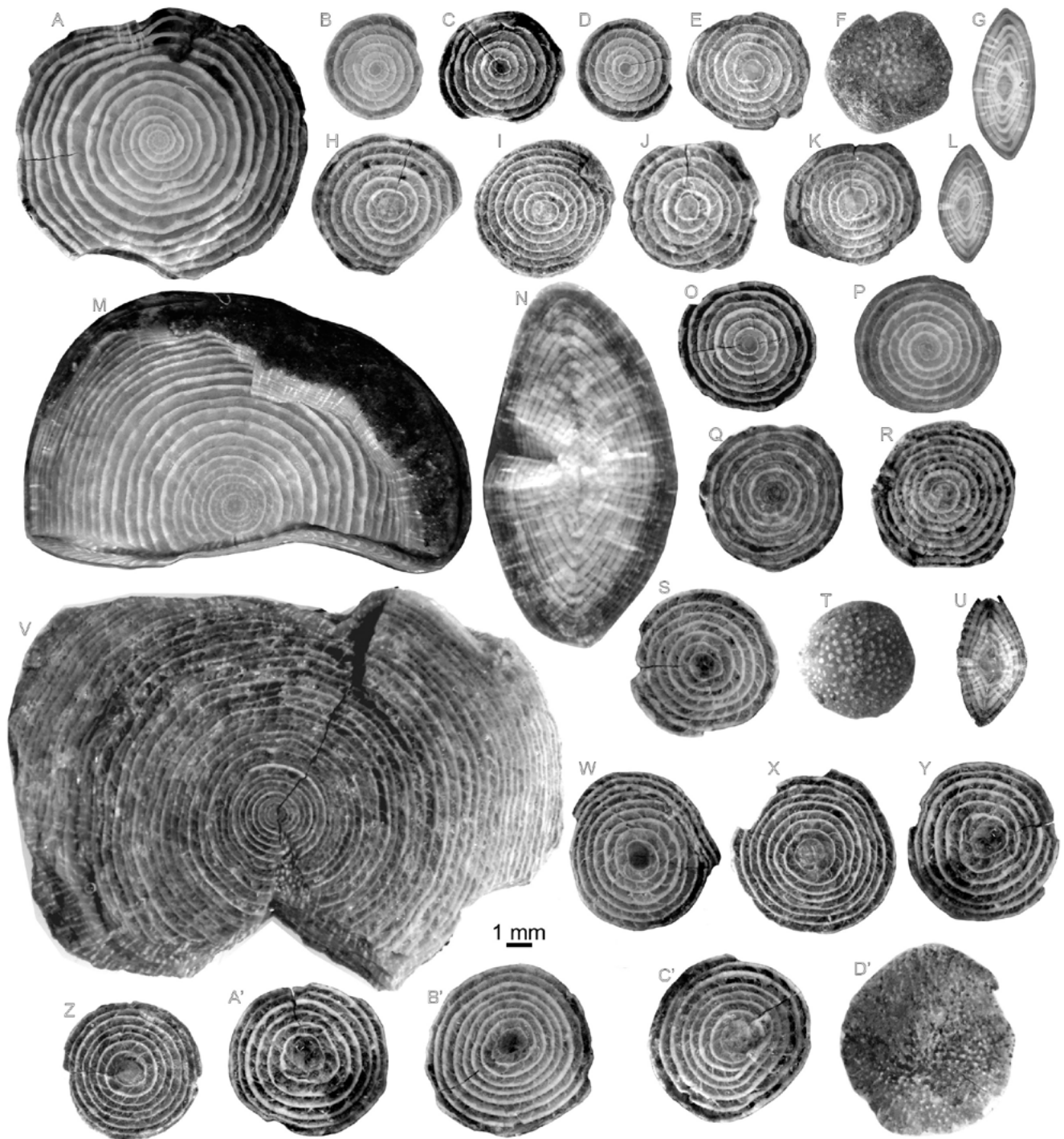


**FIGURE 29.** A-L) *Nummulites aff. deshayesi*. A: equatorial section, microspheric form. B-E: equatorial sections, megalospheric forms. F: external view, megalospheric form. G: axial sections, megalospheric forms. H-K: equatorial sections, megalospheric forms. L: axial sections, megalospheric forms. Specimens A-D: sample I 52; E-F, H-K: sample E 30 and G, L: from sample SC 38. M-U) *Nummulites deshayesi*. M: equatorial section, microspheric form. N: axial section, microspheric form. O-S: equatorial sections, megalospheric forms. T: external view, megalospheric form. U: axial section, megalospheric form. Specimens M, O, P: sample I 54; N, Q, R, T, U: sample SC 50 and S: sample SM 5. V-D') *Nummulites perforatus*. V: equatorial section, microspheric form. W-C': equatorial sections, megalospheric forms. D': external view, megalospheric form. All specimens from sample SM 6.

**Material.** This species is present in the Santa Marina section (Fig. 2).

**Description.** Microspheric forms of large size, inflated lenticular to spherical morphology and rounded periphery. Diameter of the test is 22mm for 42 whorls, 12.5mm for 22 whorls and 8.8mm for 17 whorls. Spiral growth divided in three zones; the first zone comprising 9-10 tight whorls, the second zone comprising 14-17 looser whorls and the third zone formed of at least 20 very tightly closed whorls. Megalospheric forms of inflated lenticular morphology. For 6-7 whorls the diameter of the test is 6.4-6.75mm and the thickness 3.2-3.4mm, and for 7 whorls the diameter can reach 6.85mm. Proloculus is 960-1.280 $\mu$ m in diameter.

In both generations the chambers change from isometric in the inner whorls to longer than high in the other whorls. Ornamentation formed of meandriform filaments and granules on and between the filaments. Spiral growth almost regular. Marginal cord thin. Septa inclined and curved backwards at the top.

**Remarks.** This species differs from *N. aturicus* in the thinner marginal cord, the more irregular spiral growth, the larger diameter of the proloculus and the higher morphological variability in the microspheric forms, which ranges from inflated lenticular to flattened lenticular.

**Age.** In the study area this species occurs in the Arguis Fm. (sample SM 6; Fig. 2). According to Schaub (1981) this species is a biomarker of the *N. brongniarti*-*N. perforatus* Zone, early Bartonian, or SBZ17.

*Nummulites boussaci* ROZLOZSNIK, 1924

Fig. 30A-C

1929 *Nummulites Boussaci* Rozlozsnik. Rozlozsnik, p. 161; pl. 4, figs. 7, 9; pl. 6, fig. 9

1981 *Nummulites boussaci* Rozlozsnik. Schaub, p. 111-112; pl. 32, figs 9, 20, 21, 23, 23-31, 35-39, 41-46, 49, 50; pl. 33, figs. 1-13, 15, 16; pl. 34, figs. 1-11; table 5, fig. g

**Material.** This species is present in the Santa Marina section (Fig. 2).

**Description.** Microspheric forms of inflated lenticular morphology. Diameter 12.7mm for 15 whorls. Spiral growth regular. Marginal cord thick. Septa inclined, slightly flexuous and curved backwards at the top. Megalospheric forms of lenticular morphology with a diameter around 2.8mm for 3 whorls. Ornamentation consisting of large granules in spiral distribution. Chambers are first isometric and change to longer than high in later growth stages.

**Age.** This species is associated with *N. beneharnensis* (samples SM 1 and SM 2; Fig. 2), indicating middle

Lutetian 1 (*N. gratus*-*N. beneharnensis* Zone) or SBZ14.

*Nummulites* aff. *bullatus* AZZAROLI, 1952

Fig. 30D-F

1981 *Nummulites* aff. *bullatus* Azzaroli, 1952. Schaub, p. 125; pl. 49, figs 25a-b

2012a *Nummulites bullatus* Azzaroli, 1952. Rodríguez-Pintó *et al.*, on-line Supplementary Material, pl. 2, figs. 22, 23

**Material.** This species is present in the Isuela section (Fig. 4).

**Description.** Microspheric forms not found. Megalospheric forms of flattened lenticular morphology and sharp periphery. Test small with a diameter of 2.3-2.7mm for 3 whorls. Ornamentation formed of granules in spiral distribution on filaments, that form an irregular network more pronounced in the polar zone. Spiral growth regular. Proloculus is 200-250 $\mu$ m in diameter. Chambers isometric in early growth stages and longer than high in later growth stages. Septa straight and curved backward on the chamber roof. Equatorial section shows values as in Table 9.

**Remarks.** A similar species was described by Schaub (1981) from middle Lutetian rocks from the South Pyrenean Basin (p. 125, *op. cit.*). This species differs from *N. bullatus* in the larger size of the proloculus and in the thicker marginal cord.

**Age.** This species occurs associated with *N. aff. deshayesi* (sample I 52; Fig. 4), indicating middle Lutetian 2 (*N. sordensis*-*N. crassus* Zone) or SBZ15.

*Nummulites migiurtinus* AZZAROLI, 1952

Fig. 30G-H

1952 *Nummulites migiurtinus* n. sp., Azzaroli, p. 120; pl. 10, figs. 1-4

1981 *Nummulites migiurtinus* Azzaroli, 1952. Schaub, p. 135; pl. 53, figs. 7-16, 20, 21; tbl. 14, fig. o

2012a *Nummulites migiurtinus* Azzaroli, 1952. Rodríguez-Pintó *et al.*, on-line Supplementary Material, pl. 2, figs. 24 and 25

**Material.** This species is present in the Santa Marina, Isuela, Sierra Caballera, La Foz de Escalete, La Peña and Murillo de Gállego sections (Figs. 2; 4; 5).

**Description.** Microspheric forms not found. Megalospheric forms of small size, biconical in morphology and sharp periphery. Diameter 2.5mm and thickness 1.3mm for 5-6 whorls. Ornamentation formed of one large granule at the polar zone and radial slightly

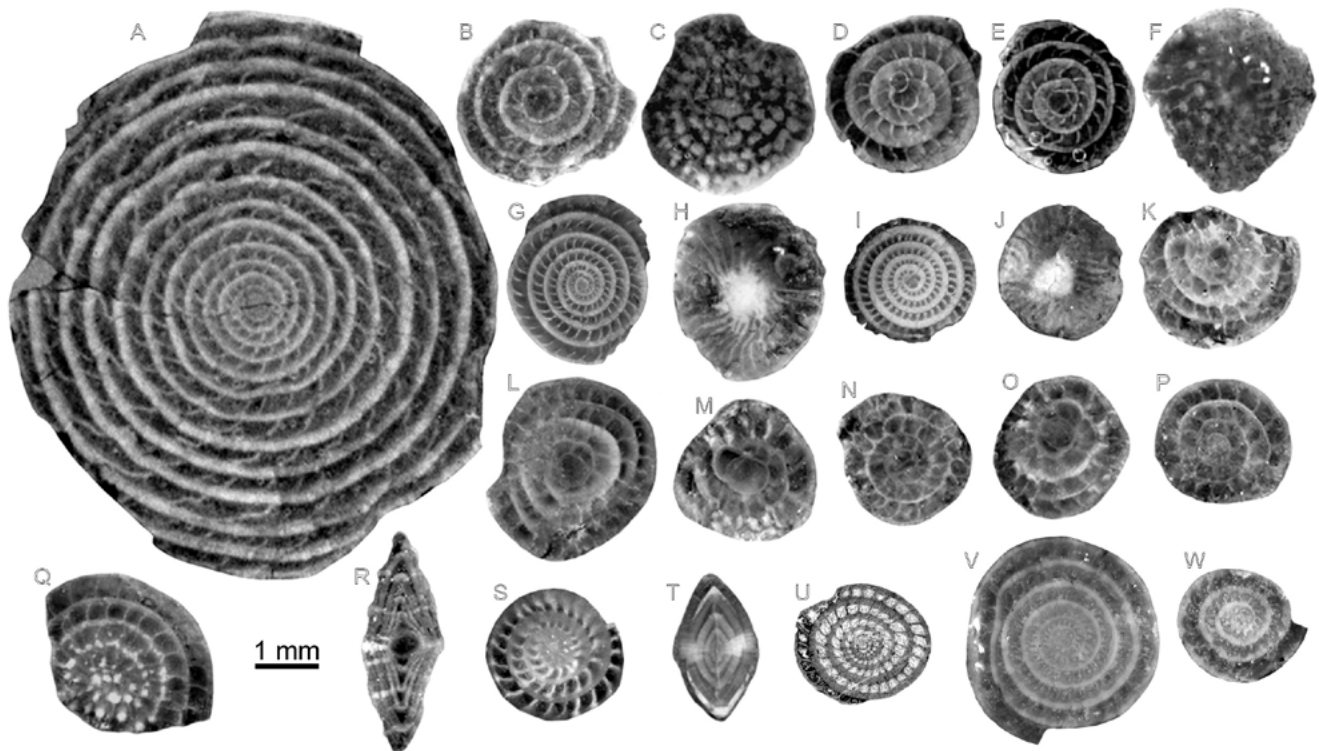


**FIGURE 30.** A-C) *Nummulites boussaci*. A: equatorial section, microspheric form. B: equatorial section, megalospheric form. C: external view, megalospheric form. All specimens from sample SM 2. D-F) *Nummulites aff. bullatus*. D, E: equatorial sections, megalospheric forms. F: external view, megalospheric form. All specimens from sample I 52. G-H) *Nummulites migiurtinus*. G: equatorial section, megalospheric form. H: external view, megalospheric form. Specimens from sample I 18. I-J): *Nummulites praediscorbinus*. I: equatorial section, megalospheric form. J: external view. Specimen from sample I 7. K-R) *Nummulites praepuschi*. K-O: centered slightly oblique equatorial sections, megalospheric forms. P-Q: subequatorial section. R: centered axial section, megalospheric form. All specimens from sample M 24. S-U) *Nummulites beaumonti*. S: equatorial section. T: axial section. U: equatorial section. All specimens megalospheric forms. Specimen S: sample E 40, T: sample P 29 and U: sample I 50. V-W) *Nummulites biarritzensis*. V: equatorial section, microspheric form. W: equatorial section, megalospheric form. Specimens from sample CF 5.

sinuous filaments. Spiral growth regular. Proloculus is 90–140 $\mu$ m in diameter. Chambers begin being isometric and change to higher than long. Straight and backward curved septa on chamber roof.

**Age.** The biostratigraphic range of this species extends from SBZ13 to SBZ14. In SBZ13 this species occurs intercalated with samples of *Alveolina callosa* (sample SC 8; Fig. 5), indicating early Lutetian (A. stipes Zone). The SBZ14 is characterized by the association of *N. migiurtinus* with *N. aspermontis* and *N. beneharnensis* (samples I 18 and SM 3; Figs. 2; 4), indicating middle Lutetian 1 (N. gratus-N. beneharnensis Zone).

***Nummulites praediscorbinus* SCHAUB, 1981**

**Fig. 30I-J**

1981 *Nummulites praediscorbinus* n. sp. Schaub, 1981, p. 165; pl. 52, figs. 28-50; tbl. 14, fig. 1

2012a *Nummulites praediscorbinus* Schaub, 1981. Rodríguez-Pintó *et al.*, on-line Supplementary Material, pl. 2, figs. 16 and 17

**Material.** This species is present in the Isuela section (Fig. 4).

**Description.** Microspheric forms not found. Megalospheric forms of biconical morphology and sharp periphery. Diameter 1.9mm and thickness 2mm for 4-5 whorls. Ornamentation composed of one large granule at the polar zone and radial filaments. The diameter of the proloculus is around 150 $\mu$ m. Spiral growth tight and regular. The thickness of the marginal cord equals the height of the chambers. Chambers isometric or slightly higher than long.

**Age.** This species occurs associated with *N. aspermontis* and *N. beneharnensis* (sample I 8; Fig. 4), indicating early Lutetian (A. stipes and A. spira abrardi zones) or SBZ13.

***Nummulites praepuschi* SCHAUB, 1981**

**Fig. 30K-R**

1981 *Nummulites praepuschi* n. sp. Schaub, p. 165; fig. 100; pl. 61, figs. 1-5; tbl. 8, fig. e

**Material.** This species is present in the Murillo de Gállego section (Fig. 8).

**Description.** Although megalospheric forms have only been studied in non-oriented sections, the following

features were observed. Regular spiral growth. Isometric chambers with curved septa. Diameter of the proloculus between 540-600 $\mu$ m. Ornamentation formed of granules in spiral distribution on the marginal cord and filaments forming a subreticular network.

**Age.** This species occurs in the Murillo de Gállego section (sample M 24; Fig. 8). According to Schaub (1981) it characterizes the late Lutetian (N. herbi-N. aturicus Zone) or SBZ16.

*Nummulites beaumonti* D'ARCHIAC AND HAIME, 1853  
Fig. 30S-U

1952 *Nummulites Beaumonti* d'Archiac and Haime. Azzaroli, P 121; PL. 9, FIG. 3, 6, 12 AND 13.

1981 *Nummulites beaumonti* d'Archiac and Haime, 1853. Schaub, p. 135; pl. 53, figs. 17-19, 22-25; tbl. 14 p

1995 *Nummulites beaumonti* d'Archiac and Haime, 1853. Racey, p. 34; pl. 5, figs. 15-17, and 19.

2013 *Nummulites beaumonti* d'Archiac and Haime, 1853. Serra-Kiel in Costa *et al.*, on-line Supplementary Material, Figs. A2 1-4 and A9 1-8.

**Material.** This species is present in the Isuela, Sierra Caballera, La Foz de Escalate and Campo Fenero sections (Figs. 4; 6; 12).

**Description.** Microspheric forms not found. The megalospheric forms show an inflated biconical morphology and rounded periphery. The test diameter for 6 whorls is around 2.8mm. Ornamentation composed of a large granule at the polar zone and sinuous filaments. Diameter of the proloculus around 100 $\mu$ m. Chambers higher than long in the inner whorls, and isometrical and higher than long in the outer whorls. Septa inclined.

**Age.** According to Serra-Kiel *et al.* (1998) this species occurs in SBZ15-SBZ17. Here this species occurs overlying beds with *N. crassus* and *N. aff. deshayesi* and underlying beds with *N. deshayesi* (Fig. 6), indicating middle Lutetian 2 (SBZ15), or associated with *N. biarrizensis* (sample CF 5; Fig. 12), indicating early Bartonian or SBZ 17. Thus, the biostratigraphic range of this species extends from middle Lutetian 2 (SBZ15) to early Bartonian (SBZ17).

*Nummulites biarrizensis* D'ARCHIAC AND HAIME, 1853  
Fig. 30V-W

1981 *Nummulites biarrizensis* d'Archiac and Haime, 1853. Schaub, p. 123; pl. 51, figs. 30-46, tbl. 15, figs. c, d

2013 *Nummulites biarrizensis* d'Archiac and Haime, 1853. Serra-Kiel in Costa *et al.*, on-line Supplementary Material, Fig. 2A 5-8; Fig. A9 (9-13)

**Material.** This species is present in the Campo Fenero section (Fig. 12).

**Description.** Microspheric forms not found. The megalospheric forms show a lenticular shape and rounded periphery. Diameter of the proloculus around 270 $\mu$ m. The test diameter for 6 whorls is around 2.2mm. Ornamentation formed of filaments radiating S-shaped and a large granule at the polar zone. Septa inclined.

**Age.** This species occurs associated with *N. beaumonti* (sample CF 5; Fig. 12). According to Schaub (1981) and Serra-Kiel (in Costa *et al.*, 2013) this species indicates SBZ17 (early Bartonian).

## DISCUSSION

### Magnetostratigraphic calibration

The biostratigraphic distribution of larger foraminiferal index species in the studied sections has been based on the the alveolinid zones of Hottinger (1960) and Hottinger and Drobné (1988), the nummulitid zones of Schaub (1981) and the Shallow Benthic Zones (SBZ) of Serra Kiel *et al.* (1998). The biostratigraphy of *Alveolina*, *Nummulites* and *Assilina* species in the Boltaña, Guara and Arguis formations in the study area is synthesized in Table 10.

The stratigraphic distribution of the taxa described above allowed recognition and calibration of late Ypresian (SBZ 11) to early Bartonian (SBZ 17) shallow benthic zones. SBZ11 was identified by the presence of *Alveolina decastroii* and *A. cremae*. No taxa were found in the studied material representing SBZ 12, and thus the upper and lower boundaries of this zone could not be established precisely. SBZ 13 is well identified by the concurrence of *Assilina spira abrardi*, *Nummulites lehneri*, *Alveolina stipes*, *A. callosa* and *A. obtuse*. The lower boundary of SBZ 13 was not determined in the studied sections, but the lowermost biostratigraphic markers associated to this zone correlate with the upper part of Chron C21r. The boundary between SBZ 13 and SBZ 14 was pinpointed at 145m from the base of the Isuela section (Fig. 4), in the lower half of Chron C20r. According to this calibration, the age of this boundary is *ca.* 45 Ma. SBZ 14 is also well represented by the occurrence of *A. munieri*, *N. boussaci*, *N. aspermontis* and *N. beneharnensis*. SBZ14 is correlated with Chron C20r and the lowermost part of C20n (Fig. 4). SBZ 15 was determined by the occurrence of *N. crassus*, *N. aff. deshayesi* and *N. taverdetensis*. The boundary between SBZ 14 and SBZ 15 was not accurately defined, but the transition interval was constrained by Rodríguez-Pintó *et al.* (2012a) thanks to the identification of *N. crassus* in the lower part of Chron C19r in La Foz de Escalate section (Fig. 6). Thus, SBZ 15 embraces the lower half of the C19r magnetozone, and the time span not covered by any characteristic taxa assemblage

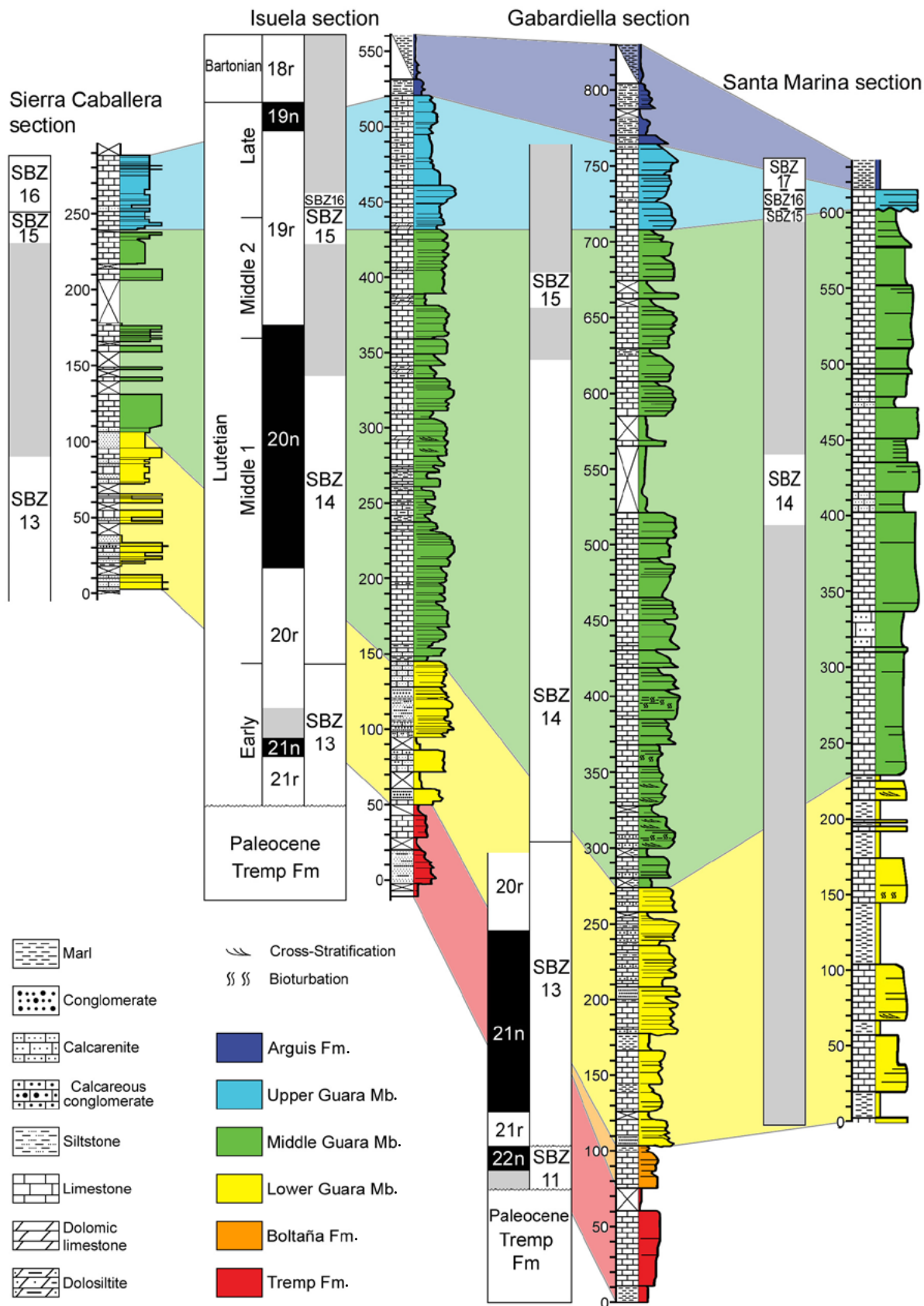


**FIGURE 31.** Correlation between lithostratigraphic units, magnetostratigraphy and SBZ of stratigraphic sections from the central part of Sierras Exteriores (Santa Marina, Gabardiella, Isuela and Sierra Caballera sections, Figs. 2-5).

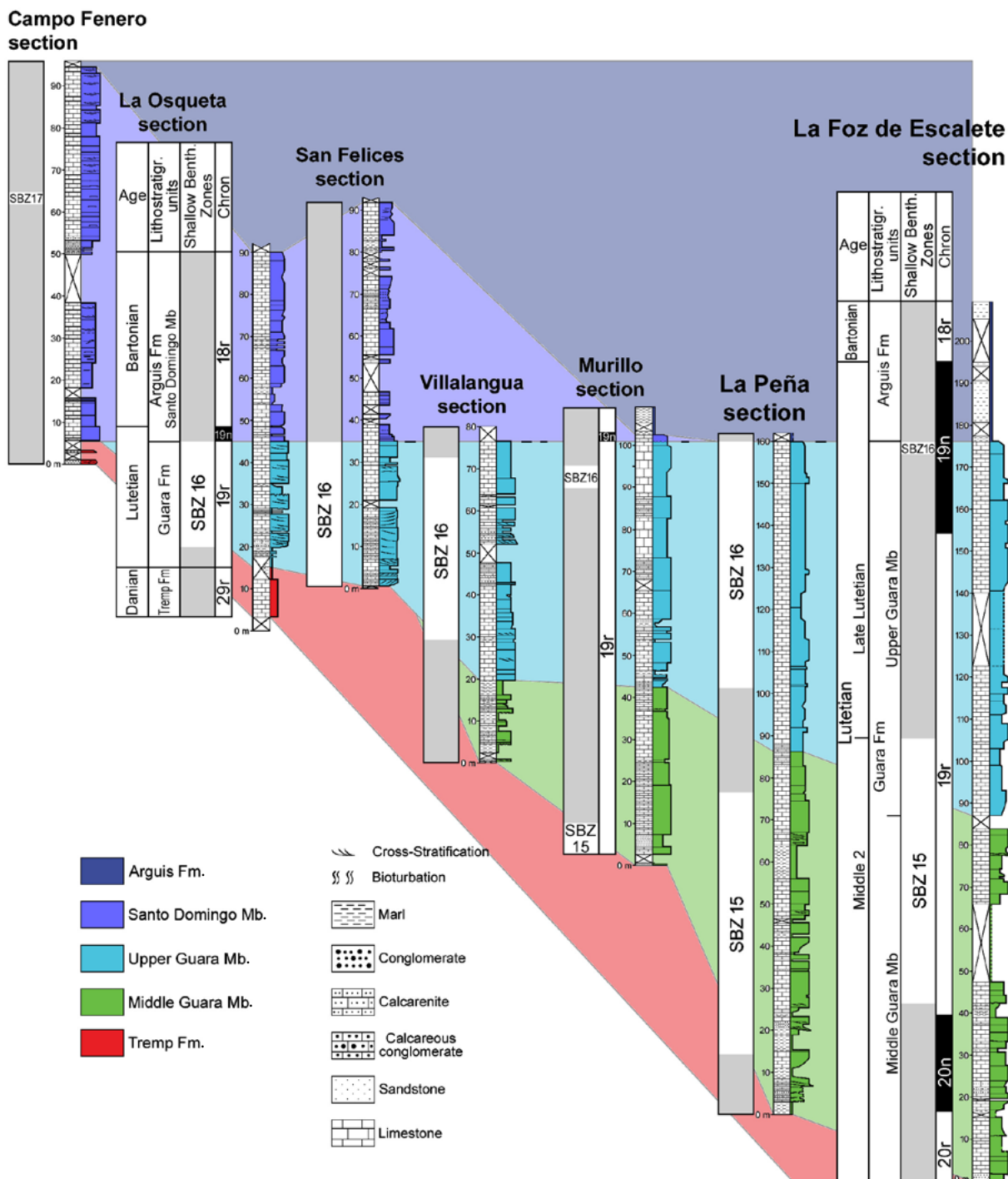
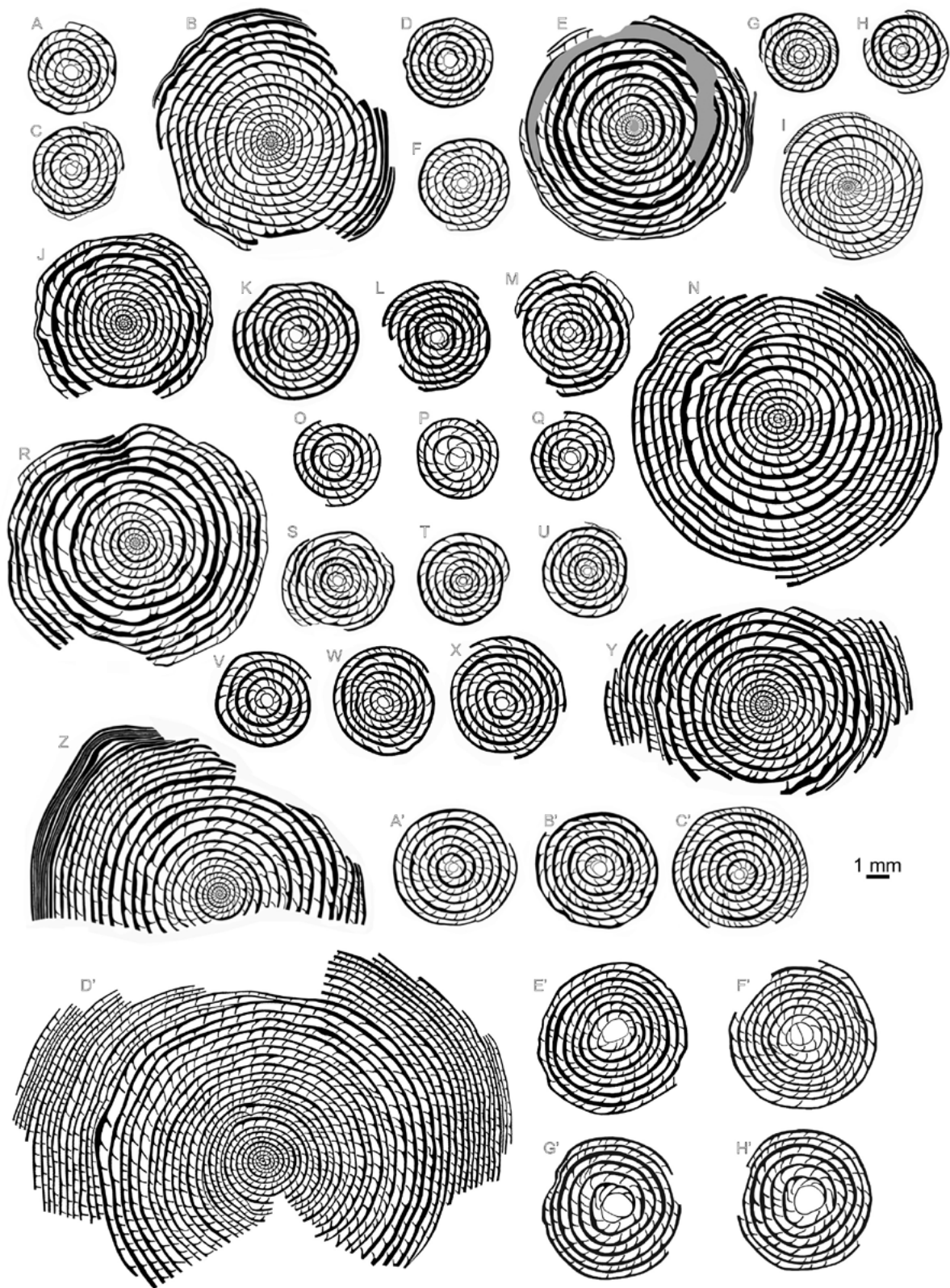


FIGURE 32. Correlation between lithostratigraphic units, magnetostratigraphy and SBZ of stratigraphic sections from the western part of Sierras Exteriores (La Foz de Escalete, La Peña, Murillo de Gállego, Villalangua, San Felices, La Osqueta and Campo Fenero sections Figs. 6-12).

extends/extended from 43.1 to 42.3 Ma. SBZ 16 is well characterized by the presence of *N. deshaysi*, *N. aturicus* and *N. praepuschi*. This zone correlates with the upper half of Chron C19r and C19n. The lower boundary of this SBZ was pinpointed in the Sierra Caballera section at 255m (Fig. 5). This boundary was identified in the Isuela section around 450m and calibrated with

magnetostratigraphy, obtaining an age of about 41.7Ma (Fig. 4). The upper boundary of SBZ 16 was not well constrained. SBZ 17 is represented in the Campo Fenero section (*N. biarritzensis*, Fig. 12) and Santa Marina section (*N. perforatus*, Fig. 2). The boundary between SBZ 16 and SBZ 17 was determined in this section, but precise magnetostratigraphic calibration was not possible.



**FIGURE 32.** Correlation between lithostratigraphic units, magnetostratigraphy and SBZ of stratigraphic sections from the western part of Sierras Exteriores (La Foz de Escalete, La Peña, Murillo de Gállego, Villalangua, San Felices, La Osqueta and Campo Fenero sections [Figs. 6-12](#)).

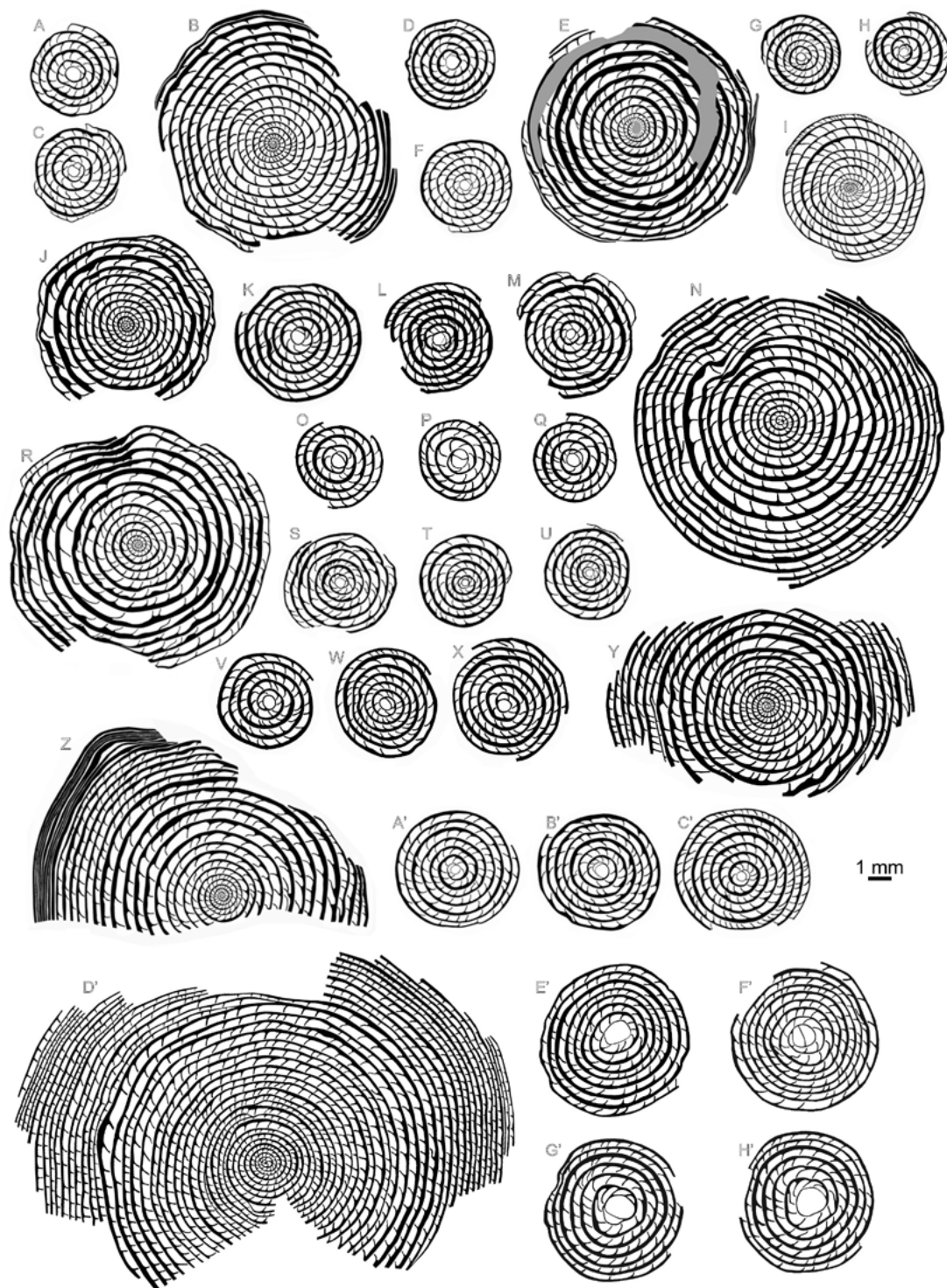


**FIGURE 33.** Nummulites of the Group *N. burdigalensis* used as biostratigraphic markers. A-C) *N. benehamensis*. A, C: specimens from sample I 18. B: drawing from Figure 28X. D-F) *N. aspermontis*. D: drawing from Figure 28R. E: drawing from Figure 28M. F: specimens from sample I 8. G-I) *N. lehneri*. All specimens from sample G 5. J-M) *N. crassus*. J: specimen from sample SM 4. K: drawing from Figure 28F'. L: drawing from Figure 28H'. M: drawing from Figure 28L'. N-Q) *N. tavertetensis*. N: drawing from Figure 28M'. O: drawing from Figure 28Q'. P: specimen from sample SM 4. Q: drawing from Figure 28O'. R-U) *N. aff. deshayesi*. R: drawing from Figure 29A. S: drawing from Figure 29C. T: specimen from sample I 52. U: drawing from Figure 29D. V-Y) *N. aturicus*. V-X: specimens from sample SC 39. Y: drawing from Figure 28T'. Z-C') *N. deshayesi*. Z: drawing from Figure 29M. A': drawing from Figure 29P. B': drawing from Figure 29O. C': specimen from sample I 54. D'-H') *N. perforatus*. D': drawing from Figure 29V. E': drawing from Figure 29B'. F': drawing from Figure 29X. G': drawing from Figure 29A'. H': drawing from Figure 29Y.

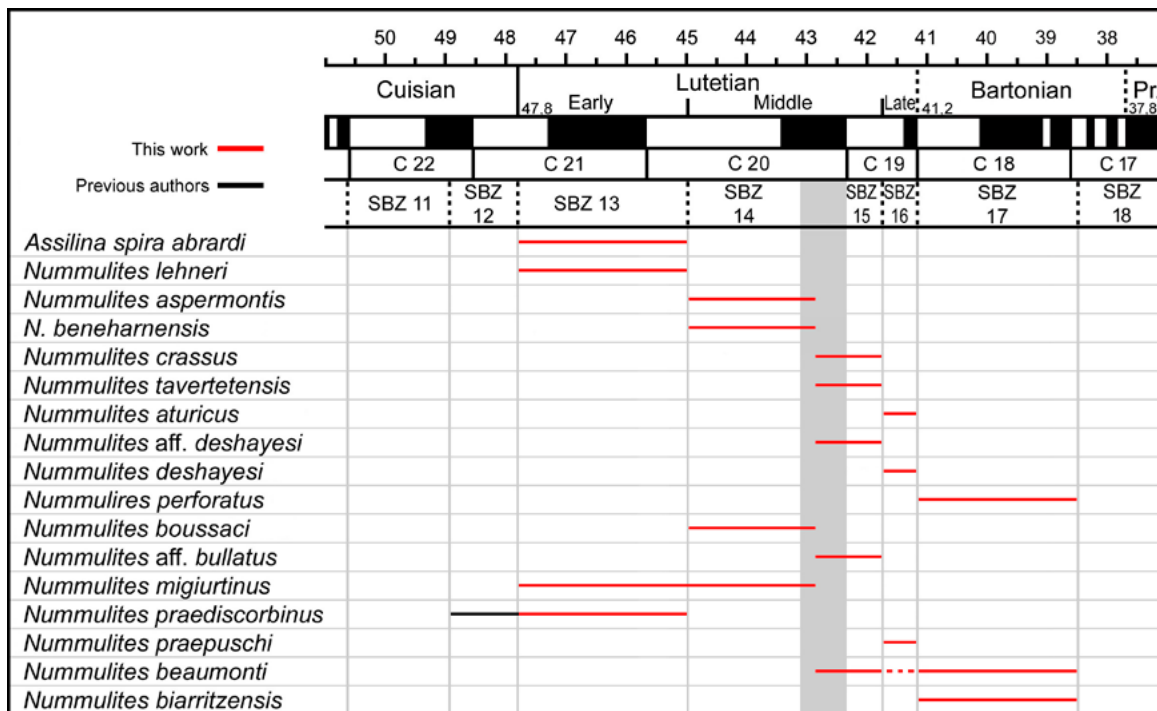


**FIGURE 34.** Biostratigraphic range of the *Nummulites* and *Assilina* species. The ranges shown with red lines are according to this study, whereas those in black lines are according to [Serra-Kiel et al. \(1998\)](#). Chronostratigraphy in accordance with Shallow Benthic Zones of [Serra-Kiel et al. \(1998\)](#), recalibrated according to [Rodríguez-Pintó et al. \(2012a\)](#) and [Costa et al. \(2013\)](#). Magnetostratigraphic data from [Rodríguez-Pintó et al. \(2012a\)](#) recalibrated to the GPTS 2012 according to [Ogg \(2012\)](#). The grey band represents the transition interval (no accurate boundary) between SBZ 14 and SBZ 15.

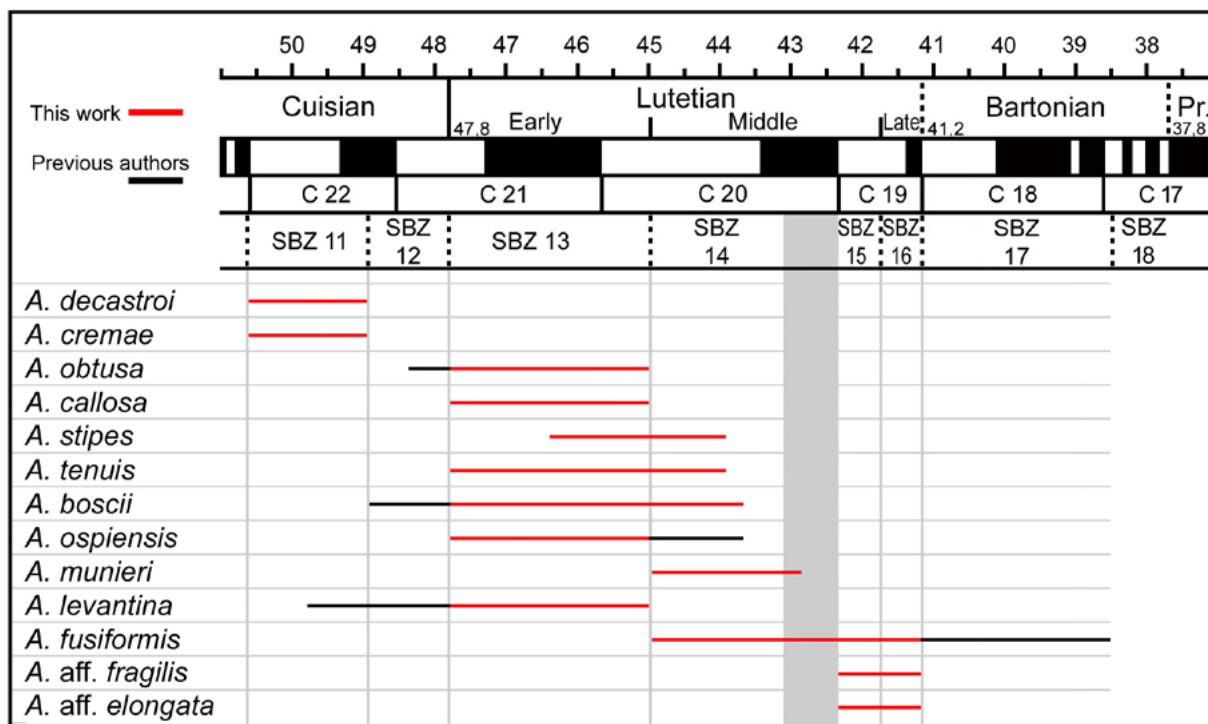


**FIGURE 35.** Biostratigraphic range of the *Alveolina* species studied in this work. The ranges shown with red lines are according to this study, whereas those in black lines are according to [Serra-Kiel et al. \(1998\)](#). Chronostratigraphy is in accordance with Shallow Benthic Zones of [Serra-Kiel et al. \(1998\)](#), recalibrated according to [Rodríguez-Pintó et al. \(2012a\)](#) and [Costa et al. \(2013\)](#). The boundaries of the SBZs in [Rodríguez-Pintó et al. \(2012a, Fig. 8\)](#) are recalibrated to GPTS 2012 according to [Ogg \(2012\)](#). The grey band represents the transition interval (no accurate boundary) between SBZ 14 and SBZ 15.

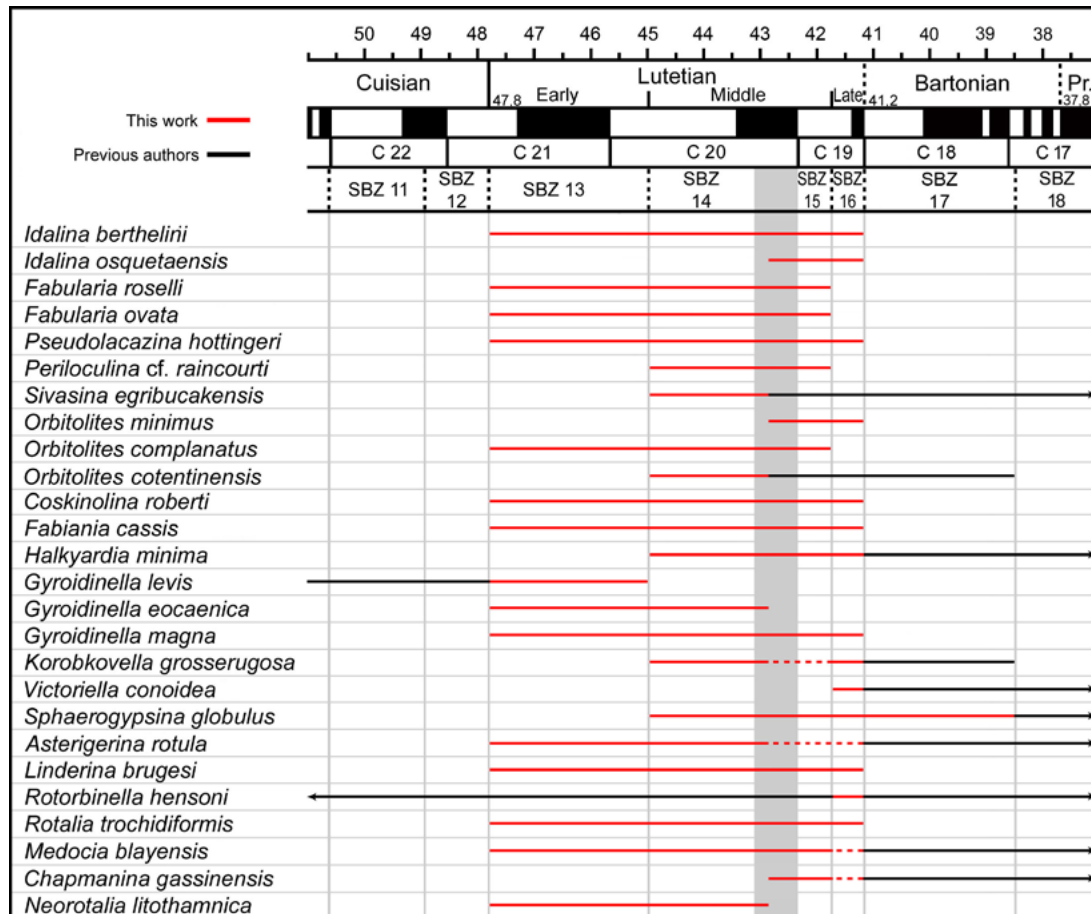


**FIGURE 36.** Biostratigraphic range of several taxa studied in this work. The ranges shown with red lines are according to this study, whereas those in black lines are according to [Serra-Kiel \*et al.\* \(1998\)](#). Chronostratigraphy in accordance with Shallow Benthic Zones of [Serra-Kiel \*et al.\* \(1998\)](#), recalibrated according to data by [Rodríguez-Pintó \*et al.\* \(2012a\)](#) and [Costa \*et al.\* \(2013\)](#). The boundaries of the SBZs in [Rodríguez-Pintó \*et al.\* \(2012a, Fig. 8\)](#) are recalibrated to the GPTS 2012 according to [Ogg \(2012\)](#). The grey band represents the transition interval (no accurate boundary) between SBZ 14 and SBZ 15.

The calibration of the biostratigraphic data of this study with magnetostratigraphic data ([Rodríguez-Pintó \*et al.\*, 2012a, b](#); [Rodríguez-Pintó \*et al.\*, 2017](#); [Silva-Casal \*et al.\*, 2019](#)) allowed the correlation of the late Ypresian–lower Bartonian shallow marine successions (*i.e.* Boltaña, Guara and Arguis formations) throughout the central ([Fig. 31](#)) and western parts ([Fig. 32](#)) of the Sierras Exteriores.

### Contributions to the biostratigraphy of Larger Foraminifera

Most of the biostratigraphic markers used in this study belong to genera *Nummulites* and *Alveolina*. Genus *Nummulites*, widely studied by [Schaub \(1981\)](#), is represented in this study by several phyletic lines, some included in the Group of *Nummulites burdigalensis*, with five evolutionary branches. This group, diversified from the base of the Lutetian, includes most of the biostratigraphic markers used here, *i.e.* *N. taverdetensis*, *N. lehneri*, *N. aspermontis*, *N. crassus*, *N. aturicus*, *N. beneharnensis*, *N. aff. deshayesi*, *N. deshayesi*,

*N. perforatus* ([Fig. 33](#)). The Group of *N. laevigatus* (*N. praepuschi*), and the lineages of *N. leupoldi* (*N. biarrizensis*), *N. fabianii* (*N. aff. bullatus*), *N. partschi* (*N. boussaci*) and *N. beaumonti* (*N. migiurtinus*, *N. beaumonti*) are also present. The nummulitid *Assilina spira abrardi* is another important biostratigraphic marker used in this study. The biostratigraphic range and magnetostratigraphic calibration of the studied *Nummulites* and *Assilina* species are represented in [Figure 34](#).

*Nummulites* facies are not abundant in the studied sections, and the *Nummulites* specimens were collected from discrete levels. *Nummulites* data was complemented with species of *Alveolina* of biostratigraphic interest, which are abundant in facies rich in porcellaneous foraminifera in the Boltaña and Guara formations. The specific diversity of the genus *Alveolina* in the Sierras Exteriores is represented by six lineages that include elongated and fusiform morphotypes ([Hottinger and Drobne, 1988](#)). The best represented lineages are from the Group of *Alveolina callosa* (*A. obtusa*, *A. callosa*, *A. ospiensis*) and the Group

Age	Polarity	Chron	Biozones	Lithostratigraphic units	Biostratigraphic markers
39				Arguis FM	<i>N. perforatus</i> <i>N. biarritzensis</i>
40		C-18	SBZ 17		
41				Santo Domingo Member	
41				Glaucocenic level	
42		C-19	SBZ 15, 16	Upper Guara Mb.	<i>N. aturicus</i> <i>N. deshayesi</i> <i>N. praepuschi</i>
43				Middle Guara Mb.	<i>N. crassus</i> <i>N. taverdetensis</i> <i>N. aff. deshayesi</i>
44		C-20	SBZ 14		
45				Lower Guara Mb.	<i>A. stipes</i> <i>A. callosa</i> <i>N. lehneri</i> <i>A. spira abrardi</i>
46		C-21	SBZ 13		
47				Hiatus	Hiatus
48			SBZ 12	Boltaña Fm.	<i>A. decastroi</i> <i>A. cremae</i>
49		C-22	SBZ 11		
50					

**FIGURE 37.** Correlation between the standard Time Scale, magnetostratigraphy, Shallow Benthic Zones, lithostratigraphic units of the Sierras Exteriores and biomarker taxa used in this study, in accordance with the International Chronostratigraphic Chart 2017 (Vandenberghe *et al.*, 2012; Cohen *et al.*, 2013).

of *Alveolina munieri* (*A. stipes*, *A. tenuis*, *A. munieri* and *A. aff. fragilis*). However, *Alveolina prorrecta* was not found. Interestingly, *A. aff. fragilis*, which is the predecessor of the Bartonian species *A. fragilis*, fills in the gap in SBZ 16 for this lineage, with a biostratigraphic distribution ranging from upper middle Lutetian (SBZ15) to late Lutetian (SBZ16). Similarly, *A. aff. elongata* complements the significant gap existing in the Group of *Alveolina gigantea*, as a predecessor of the Bartonian *A. elongata*. Other groups represented are the group of *A. minuta* (*A. decastroi*, *A. boscii* and *A. frumentiformis*) and the group of *A. levantina* (*A. levantina* and *A. fusiformis*). According to the revision of *A. fusiformis* presented here, the biostratigraphic range of this species expands from middle-late Lutetian (SBZ14-16) to early Bartonian (SBZ17). The biostratigraphic distribution of the studied *Alveolina* species and their calibration to the GPTS is represented in Figure 35.

The occurrence of *A. fusiformis*, *A. aff. fragilis* and *A. aff. elongata* in SBZ 15 and SBZ 16 increases the diversity

of *Alveolina* species for this time span. The number of species increases from two to five in the middle Lutetian 2, and from one to four in the late Lutetian (Hottinger and Drobne, 1988; Serra-Kiel *et al.*, 1998).

In addition, two new taxa have been described in the evolutionary lineage of *Idalina berthelini* (Fig. 15). A late Ypresian (middle Cuisian SBZ 11) species, *Idalina* sp., has been considered the predecessor of *I. berthelini*. Unfortunately, it could not formally be defined as a species because of the scarce material available. On the other hand, *I. osquetaensis*, new species, represents a diversification of the *Idalina* genus in the middle Lutetian 2 (SBZ 15), showing an evolutionary trend in this genus towards an increase of the test size and the thickening of the basal layer over time (Fig. 15).

This study highlights the high diversity of larger foraminifera in the Sierras Exteriores, with 17 families, 26 genera and 61 species (see also Appendix II). The biostratigraphic distribution of species belonging to other genera than *Nummulites*, *Assilina* and *Alveolina*, is shown in Figure 36. A summary of the chronostratigraphic data is given in Figure 37.

## CONCLUSIONS

A detailed systematic description of larger foraminifera recorded in the mid-Eocene successions exposed in the Sierras Exteriores (South Pyrenean Basin) has shown a high taxonomic diversity, with 17 families, 26 genera and 61 species. Furthermore, a new species, *Idalina osquetaensis*, has been described in this study. The biostratigraphic analysis of 11 sections widely distributed across the Sierras Exteriores and their correlation with magnetostratigraphic data has led to an accurate calibration of the Lutetian SBZs. The biostratigraphic markers identified in this study permitted the characterization of the following SBZs:

- SBZ 11 (middle Cuisian) characterized by *A. decastroi* and *A. cremae*.
- SBZ 13 (early Lutetian) characterized by *A. callosa*, *A. stipes*, *N. lehneri* and *A. spira abrardi*.
- SBZ 14 (middle Lutetian 1) characterized by *A. munieri*, *N. boussaci*, *N. beneharnensis* and *N. aspermontis*.
- SBZ 15 (middle Lutetian 2) characterized by *N. crassus*, *N. taverdetensis* and *N. aff. deshayesi*.
- SBZ 16 (late Lutetian) characterized by *N. deshayesi*, *N. aturicus* and *N. praepuschi*.
- SBZ 17 (early Bartonian) characterized by *N. perforatus* and *N. biarritzensis*.

The regional scope of this study allows for a correlation between *Alveolina* and *Nummulites* biostratigraphic

**TABLE 6.** Measurements of the ecuatorial section of *Nummulites tavertetensis*.

Whorl (n°)	1	2	3	4
Radius (mm)	0.7-0.9	1.2-1.3	1.5-1.6	1.8-2.0
Septa (n°)	1.8-2.0	17-20	32-35	56-57

**TABLE 7.** Measurements of the ecuatorial section of *Nummulites aturicus*.

Whorl (n°)	1	2	3	4	5	6
Radius (mm)	0.7-1.0	1.0-1.5	1.4-1.9	1.6-2.4	2.2-2.6	2.5-2.8
Septa (n°)	7-8	20-23	48-52	61-65	81-83	102-104

**TABLE 8.** Measurements of the ecuatorial section of *Nummulites deshayesi*.

Whorl (n°)	1	2	3	4	5	6	7
Radius (mm)	0.8-1.2	1.22-1.68	1.52-2.08	1.8-2.4	2.14-2.70	2.42-2.70	2.7-3.04
Septa (n°)	5-9	15-24	32-47	52-73	83-111	118-144	152-184

**TABLE 9.** Measurements of the ecuatorial section of *Nummulites* aff. *bullatus*.**Table 9.** Measurements of the ecuatorial section of *Nummulites* aff. *bullatus*

Whorl (n°)	1	2	3
Radius (mm)	0.5-0.6	0.8-1.0	1.2-1.7
Septa (n°)	7-8	21-22	39-42

markers. An improved definition of the SBZ boundaries and their magnetostratigraphic calibration, led to a revision of the stratigraphic distribution of several larger foraminifera species. This contributed to filling in a former gap of the biostratigraphy of the *Alveolina* biozonation in the middle Lutetian 2 and late Lutetian (SBZ 15 and SBZ 16) intervals. The material found in this work allowed the definition of *A. aff. elongata* and *A. aff. fragilis* as the ancestral representatives of the evolutionary lineages of the Bartonian *A. elongata* and *A. fragilis* respectively.

*Alveolina* aff. *fragilis* and *A. aff. elongata*, together with other biostratigraphic markers of the SBZ 15 (*N. crassus*, *N. aff. deshayesi*) and SBZ 16 (*N. praepuschi*, *N. aturicus* and *N. deshayesi*), sheds light on a previously poorly known middle to late Lutetian alveolinid biostratigraphy. Moreover,

the revision of the systematics and the stratigraphic range of *A. fusiformis* has shown that it can no longer be considered a biostratigraphic marker of the early Bartonian (SBZ 17). This species is common in materials belonging to SBZ 15 and SBZ 16 (along with *A. aff. fragilis* and *A. aff. elongata*), and its association to *A. munieri* confirms the occurrence of *A. fusiformis* at least in the upper part of SBZ 14.

## ACKNOWLEDGMENTS

In memory of Josep Serra-Kiel, who unfortunately passed away during the writing of this article. During part of this work R. Silva-Casal was funded by a predoctoral grant of the Basque Government (BFI-2011-344). This study had financial support from projects PID2019-105670GB-I00, CGL2017-85038-P,

CGL2017-90632-REDT, CGL 2015-69805-P and CGL2014-54118-C2-2-R of the Spanish Ministry of Science and Innovation (FEDER, EU), the Government of Aragón-FEDER 2014-2020 (Groups E18 and E0117R-GeoAp) and the Basque Government (project IT930-16). We are grateful to Josep Tosquella and Esmeralda Caus and the editors for their constructive comments during the peer review process.

## REFERENCES

- Adams, C.G., 1962. *Alveolina* from the Eocene of England. *Micropaleontology*, 8, 45-54.
- d' Archiac, A., Haime, J., 1853. Description des animaux fossiles du groupe nummulitique de l'Inde, précédée d'un résumé géologique et d'une monographie des Nummulites. Paris, Gide et J. Baudry, part. 1.
- Azzaroli, A., 1952. I macroforaminiferi della serie del Carcàr (Eocene medio e superiore) in Somalia e la loro distribuzione stratigrafica. *Palaeontographia Italica*, 17, 99-131.
- Bandy, O.L., 1944. Eocene Foraminifera from Cape Blanco. Oregon. *Journal of Paleontology*, 18(4), 366-377.
- Barnolas, A., Samsó, J.M., Teixell, A., Tosquella, J., Zamorano, M., 1991. Evolución sedimentaria entre la cuenca de Graus-Tremp y la cuenca de Jaca-Pamplona. In: Colombo, F. (ed.). *Libro-Guía de la Excursión*, 1. Vic (Spain), EUMO Gràfic, 123pp.
- Barnolas, A., Pujalte, V., 2004. La Cordillera Pirenaica. Definición, límites y división. In: Vera, J.A. (ed.). *Geología de España*. Sociedad Geológica de España-Instituto Geológico y Minero de España, Madrid, 233-241.
- Bassi, D., 2003. Reassessment of *Solenomeris afonensis* Maslov, 1956 (Foraminifera): formerly considered a coralline red alga. *Revista Española de Micropaleontología*, 35(3), 337-343.
- Benjamini, C., 1980. Stratigraphy and foraminifera of the Qezi'ot and Har'Aqrav formations (latest middle to late Lutetian) of the western Negev Israel. *Israel Journal of Earth Sciences*, 29, 227-244.
- Bermúdez, P.J., 1952. Estudio sistemático de los foraminíferos rotaliformes. Ministerio de Minas e Hidrocarburos (Venezuela). *Boletín de Geología*, 2(4), 1-230.
- Bieda, E., 1963. Duze Otworknice eocenu Tatrzańskiego (Larger Foraminifers of the Tatra Eocene). *Prace Instytut Geologiczny*, 37, 1-215.
- de Blainville, H.M.D., 1825. *Dictionnaire des Sciences Naturelles*. Paris, FG. Levrault, vol. 41.
- Blondeau, A., 1972. Les Nummulites. De l'enseignement à la Recherche - Sciences de la Terre. Paris, Vuibert, 254pp.
- Bombita, Gh., 1975. Macroforaminifères, Eocène moyen-supérieur et Oligocène inférieur des environs de Cluj. Romania, 14th European Micropaleontological Colloquium, Livret-Guide, 163-167.
- Boubée, N., 1831. *Bulletin de nouveaux gisements de France*. Paris, France.
- Boulanger, D., Poignant, A., 1971. Sur quelques foraminifères fixés de l'Éocène supérieur et de l'Oligocène en Aquitaine méridionale. *Revue de Micropaléontologie*, 10(2), 191-204.
- Bozorgnia, F., Kalantari, A., 1965. *Nummulites* of parts of Central and East Iran. National Iran Oil Company, 28pp.
- Brady, H.B., 1881. Notes on some of the reticularian Rhizopoda of the Challenger Expedition. Part III. 1, Classification. 2, Further notes on new species. 3, Note on *Biloculina* mud, *Quarterly Journal of Microscopical Science*, new ser, 21, 31-71.
- Bronn, H.G., 1825. *System der urweltliche Pflanzenthiere durch Diagnose, Analyse und Abbildung der Geschlechter erläutert: zum Gebrauche bey Vorlesungen über Petrefactenkunde und zur Erleichterung des Selbststudiums derselben*. J. C. B. Mohr (Heidelberg), 59pp.
- Bruognatti, M.A., Ungaro, S., 1987. Analogie e differenze tra *Solenomeris* (Alga) e *Gypsina* (Foraminifero). *Annali dell'Università di Ferrara*, 9(5), 1-14.
- Bruguière, J.G., 1792. Camerine. In: *Encyclopédie méthodique: Histoire naturelle des Vers*, 1, 395-400.
- Canudo, J.-I., Molina, E., Riveline, J., Serra-Kiel, J., Sucunza, M., 1988. Les événements biostratigraphiques de la zone prépyréenne d'Aragón (Espagne), de l'Éocène Moyen à l'Oligocène Inférieur. *Revue de Micropaléontologie*, 31(1), 15-29.
- Canudo, J.I., 2018. The collection of type fossils of the Natural Science Museum of the University of Zaragoza (Spain). *Geoheritage*, 10, 385-392.
- Carter, H.J., 1877. On a Melobesian form of foraminifera (*Gypsina melobesoides mihl*), and further observations on *Carpenteria monticularis*. *Annals and Magazine of Natural History*, (4) 20(117), 172-176.
- Caus, E., 1976. Alguns macroforaminífers del Biarritzia català. *Butlletí de la Institució Catalana d'Història Natural*, 40(1), 23-29.
- Caus, E., 1979. *Fabularia roselli* n. sp. et *Pseudolacazina* n. gen. foraminifères de l'Éocène Moyen du Nord-Est de l'Espagne. *Geobios*, 12(1), 29-45.
- Chapman, F., 1898. On *Haddonella*, a new genus of the Foraminifera, from Torres Straits. *Journal of the Linnaean Society of London Zoology*, 26, 452-456.
- Chapman, F., Cressin, I., 1930. Rare foraminifera from deep borings in the Victorian Tertiaries; Part II. *Proceedings of the Royal Society of Victoria*, new ser, 43(1), 96-100.
- Checchia-Rispoli, G., 1905. Sopra alcune Alveoline eoceniche della Sicilia. *Palaeontographia Italica*, 11, 147-167.
- Cimerman, E., 1969. *Halkyardia maxima* n. sp. (Middle Oligocene) and *Halkyardia minima* (Liebus) (Middle Eocene). *Annales de la Société Géologique de Pologne*, 39, 295-304.
- Cohen, K.M., Finney, S.C., Gibbard, P.L., Fan, J.X., 2013. The ICS International Chronostratigraphic Chart. *Episodes*, 36, 199-204.
- Colom, G., 1975. *Geología de Mallorca*. Instituto de Estudios Baleáricos, C.S.I.C., 1, 1-297.
- Costa, E., Garcés, M., López-Blanco, Serra-Kiel, J., Bernaola, G., Cabrera, L., Beamud, E., 2013. The Bartonian-Priabonian marine record of the eastern South Pyrenean Foreland Basin (NE Spain): A new calibration of the larger foraminifera and

- calcareous nannofossil biozonation. *Geologica Acta*, 11(2), 177-193.
- Cushman, J.A., 1927. An outline of a re-classification of the foraminifera. *Contributions from the Cushman Laboratory for Foraminiferal Research*, 3, 1-105.
- Defrance, J.L.M., 1820. *Dictionnaire des Sciences Naturelles*, 16, eup-fik, Paris, FG. Levrault.
- Delage, Y., Hérouard, E., 1896. *Traité de Zoologie Concrète*, 1, La Cellule et les Protozoaires. Paris, Schleicher Frères.
- Deloffre, R., Hamaoui M., 1973. Révision des Chapmaninidae et Cymbaloporidae, *Angotia* et *Fabiania* (Foraminifères). *Bulletin Centre de Recherches, Pau. Société Nationale Elf-Aquitaine (Production (SNPA))*, 7(29), 291-335.
- Deshayes, G.P., 1828. Mémoire sur les Alvéolines, et Monographie sur ce genre de coquilles. *Annales des Sciences Naturelles*, 14, 225-236.
- Di Scotto, C.B., 1966. Le alveoline del Gargano nord-orientale. *Palaeontographia Italica, new series* 31, 65-73.
- Dixon, F., 1850. *The Geology and Fossils of the Tertiary and Cretaceous Formations of Sussex*. London, 422pp.
- Dizer, A., 1965. Sur quelques alvéolines de l'Éocène de Turquie. *Revue de Micropaléontologie*, 7(4), 265-279.
- Drobne, K., 1977. Alvéolines paléogènes de la Slovénie et de l'Istrie. *Mémoires suisses de Paléontologie*, 99, 1-175.
- Drobne, K., Pavlovec, R., Drobne F. 1977. Paleogene larger foraminifera from the area between Mezica and Slovenj Gradec (NW Yugoslavia). *Razprave Slovenska Akademija Znanosti in Umetnosti (SAZU)* 4, 1-88.
- Drobne, K., Pavlovec, R., Drobne, F., 1979. Mikrofossilne karakteristike Starejšega Paleogena na zahodnem obrobju Panonskega Bazena. *Zbornik Radova*, 4, 155-172.
- Drobne, K., 1988. Eléments structuraux et répartition stratigraphique des grands Miliolidés de la famille des Fabulariidae. *Revue de Paléobiologie, volume spécial* 2(2), 643-661.
- Douville, H., 1924. Un nouveau genre d'Algues calcaires. *Compte rendu sommaire des séances de la Société géologique de France*, 4, 169-170.
- Ehrenberg, C.G., 1839. Über die Bildung der Kreidefelsen und des Kreidemergels durch unsichtbare Organismen. *Physikalische Abhandlungen der Königlichen Akademie der Wissenschaften zu Berlin*, 1838 (1840: separate 1839), 59-147pp.
- von Eichwald, C.E., 1830. *Zoologia specialis*. Vilnae, D.E. Eichwaldus, vol. 2, 323pp.
- Escandell, B., Colom, G., 1962. Una revisión del Nummulítico Mallorquín. *Notas y Comunicaciones del Instituto Geológico y Minero de España*, 66, 73-142.
- Ferrández-Cañadell, C., Serra-Kiel, J., 1999. Morphostructure and systematics of *Linderina brugesii* Schlumberger, 1893 (Foraminifera, Eocene). *Geobios*, 32(4), 525-537.
- Ferrer, J., 1971. El Paleoceno y Eoceno del borde-sur-oriental de la depresión del Ebro (Cataluña). *Mémoires suisses de Paléontologie*, 90, 1-70.
- Flandrin, J., 1938. Contribution à l'Étude Paléontologique du Nummulitique Algérien. *Matériaux pour la Carte Géologique de l'Algérie*, 1<sup>ère</sup> Série Paléontologie, 8, 158pp.
- Freudenthal, T., 1969. Stratigraphy of Neogene deposits in the Khania province, Crete, with special reference to foraminifera of the family Planorbulinidae and the genus *Heterostegina*. *Utrecht micropaleontological bulletins*, 1, 1-208.
- Galloway, J.J., 1933. *A manual of Foraminifera*. Bloomington, Principia Press. 483pp.
- Garcés, M., López-Blanco, M., Valero, L., Beamud, E., Muñoz, J.A., Oliva-Urcia, B., Vinyoles, A., Arbués, P., Cabello, P., Cabrera, L., 2020. Paleogeographic and sedimentary evolution of the south-pyrenean foreland basin. *Marine and Petroleum Geology*, 113, 104-105.
- Gradstein, F.M., Ogg, J.G., Schmitz, M., Ogg, G. (eds.), 2012. *The Geologic Time Scale*. Elsevier, 1176pp.
- Grimsdale, T.T., 1952. Cretaceous and Tertiary Foraminifera from the Middle East. *Bulletin of British Museum (Natural History)*, 1, 223-247.
- von Gümbel, C.W., 1870. Beiträge zur Foraminiferenfauna der nordalpinen Eocängebilde. *Abhandlungen der K. Bayerischen Akademie der Wissenschaften, Cl. II* (1868) 10(2), 581-730 (also numbered 1-152).
- Hagn, H., 1968. *Haddonina heissigi* n. sp., ein bemerkenswerter Sandschaler (Foram.) aus dem Obereozän der Bayerischen Kalkalpen. *Mitteilungen der Bayerischen Staatssammlung für Paläontologie und Historische Geologie*, 8, 3-50.
- Hagn, H., Ohmert, W., 1971. Révision de "*Truncatulina*" *grosserugosa* Gümbel et de "*Truncatulina*" *sublobatula* Gümbel (Foraminifères de l'Éocène des Préalpes Bavareses). *Revue de Micropaléontologie*, 14, 131-144.
- Halkyard, E., 1918. The fossil foraminifera of the Blue Marl of the Côte des Basques, Biarritz. *Memoirs and proceedings of the Manchester Literary and Philosophical Society*, 62(6), 1-145.
- Hallock, P., 1985. Why are Larger Foraminifera Large? *Paleobiology*, 11, 195-208.
- Henson, F.R.S., 1950. Middle Eastern Tertiary Peneroplidae (Foraminifera) with remarks on the Phylogeny and Taxonomy of the Family. Wakefield, West Yorkshire Printing Co., 70pp.
- Herb, R., Schaub, H., 1963. Zur Nummuliten fauna des Mitteleozans von Sorde-l'Abbaye (Landes), Frankreich. *Eclogae Geologicae Helveticae*, 56(2), 973-999.
- Hofker, J., 1956. Tertiary foraminifera of coastal Ecuador. Part II Additional notes on the Eocene species. *Journal of Palaeontology*, 30, 891-958.
- Hogan, P.J., Burbank, D.W., 1996. Evolution of the Jaca piggyback and emergence of the External Sierra, southern Pyrenees. In: Friend, P.E., Dabrio, C.J. (eds.). *Tertiary Basins of Spain: The Stratigraphic Record of Crustal Kinematics*. Cambridge University Press, 153-160.
- Hottinger, L., 1960. Recherches sur les Alvéolines du Paléocène et de l'Éocène. *Mémoires suisses de Paléontologie*, 75, 1-243; 76, 1-18pls.
- Hottinger, L., 1963. Quelques Foraminifères porcelanés oligocènes dans la série sédimentaire prébétique de Moratalla (Espagne méridionale). *Eclogae Geologicae Helveticae*, (56), 963-972.
- Hottinger, L., Lehmann, R., Schaub, H., 1964. Données actuelles sur la Biostratigraphie de Nummulitique Méditerranéen.

- Mémoires Bureau Recherches Géologiques (Colloque sur l'Éocène), 611-652.
- Hottinger, L., 1974. Alveolinids, Cretaceous-Tertiary larger Foraminifera. Esso Production Research-European Laboratories, A. Schudel & Co. AG. Riehen/Basle, 84pp.
- Hottinger, L., Drobne, K., 1980. Early Tertiary conical Imperforata Foraminifera. *Razprave Slovenske Akademije Znanosti in Umetnosti*, 22(3), 169-276.
- Hottinger, L., 1983. Processes determining the distribution of larger foraminifera in space and time. *Utrecht Micropaleontological Bulletin*, 30, 239-253.
- Hottinger, L., Drobne, K. 1988. Alveolines Tertiaires: Quelques problèmes liés à la conception de l'espèce. *Revue de Paléobiologie*, volume spécial, 2, 665-681.
- Hottinger, L., 2006. Illustrated glossary of terms used in foraminiferal research. Brest, Carnets de Géologie/Notebooks on Geology, Memoir 2006/02, 126pp.
- Hottinger, L., 2007. Revision of the foraminiferal genus *Globoreticulina* Rahaghi, 1978, and of its associated fauna of larger foraminifera from the late Middle Eocene of Iran. *Carnets de Géologie/Notebooks on Geology*, Article 2007/06 (CG2007\_A06), 51pp.
- Hottinger, L., 2014. Paleogene larger rotaliid foraminifera from the western and central Neotethys. Springer International Publishing Switzerland, 196pp.
- Joly, N., Leymerie, A., 1848. Mémoire sur les Nummulites, considérées zoologiquement et géologiquement. *Mémoires de l'Académie des Sciences de Toulouse*, 3(4), 149-218.
- Kaufmann, F.J., 1867. Der Pilatus, geologisch untersucht und beschrieben. *Beiträge zur Geologischen Karte der Schweiz*, 5, 1-166.
- Keckskeméti, T., 1964. A Nummulitesek Dimorfizmusáról. *Bulletin de la Société Géologique de Hongrie*, 94, 112-120.
- Keckskeméti, T., Vanová, M., 1972. *Nummulites* of the Drog-Stúrovo basin. *Západné-Karpaty*, 17, 105-145.
- Keckskeméti, T., 1973. Entwicklungsgeschichte der Nummuliten fauna des Bakonygebirges in Ungarn. *Annales Musei historico-naturalis hungarici*, 65, 31-48.
- Kodama, K.P., Anastasio, D.J., Newton, M.L., Pares, J.M., Hinnov, L.A., 2010. High-resolution rock magnetic cyclostratigraphy in an Eocene flysch, Spanish Pyrenees. *Geochemistry, Geophysics, Geosystems*, 11, Q0AA07. DOI: 10.1029/2010GC003069
- Kudo, R.R., 1931. *Handbook of Protozoology*. Baltimore, Charles C. Thomas.
- Lamarck, J.B., 1801. *Système des animaux sans vertèbres*. Paris, The Author, 432pp.
- Lamarck, J.B., 1804. Suite des mémoires sur les fossiles des environs de Paris. *Annales Muséum National d'Histoire Naturelle*, 5, 349-357.
- Le Calvez, Y., 1949. Révision des foraminifères lutétiens du Bassin de Paris II, Rotaliidae et familles affines. Paris, Imprimerie nationale, 54pp., VI pl.
- Le Calvez, Y., Blondeau, A. 1978. La microfaune «Biarritzienne» du Lutétien du Cotentin. *Bulletin d'Information des Géologues du Bassin de Paris*, 15(2), 21-31.
- Lehmann, R., 1961. Strukturanalyse einiger Gattungen der Subfamilie Orbitolininae. *Eclogae geologicae Helvetiae*, 54(2), 597-667.
- Liebus, A., 1911. Die Foraminiferenfauna der mitteleocänen Mergel von Norddalmatien. *Sitzungsberichte der mathematisch-naturwissenschaftlichen Klasse der kaiserlichen Akademie der Wissenschaften*, 120 (part 1), 1-10, 865-956.
- Loeblich, A.R., Tappan, H., 1986. Some new and redefined genera and families of Textulariina, Fusulinina, Involutinina and Miliolina (Foraminiferida). *The Journal of Foraminiferal Research*, 16(4), 334-346.
- Loeblich, A.R.Jr., Tappan, H., 1987. Foraminiferal genera and their classification. New York, Van Nostrand Reinhold Co, vol. 1, 970pp., vol. 2, 212pp., 847pls.
- Matteucci, R., 1978. Foraminiferi epibionti e criptobionti in gusci di Nummuliti dell'Eocene Medio del Gargano (Puglia). *Geologica Romana*, 17, 389-419.
- Mey, P.H.W., Nagtegaal, P.J.C., Roberti, K.J., Hartevelt, J.J.A., 1968. Lithostratigraphic subdivision of post-hercynian deposits in the south-central Pyrenees, Spain. *Leidse Geologische Mededelingen*, 41, 221-228.
- Millán, H., Aurell, M., Melendez, A., 1994. Synchronous detachment folds and coeval sedimentation in the Prepyrenean External Sierras (Spain): a case study for a tectonic origin of sequences and systems tracts. *Sedimentology*, 41, 1001-1024.
- Millán, H., Pueyo, E.L., Pocoví, A., 1996. Estimación del acortamiento en áreas afectadas por rotaciones y su contrastación con datos paleomagnéticos. *Geogaceta* 20(4), 755-758.
- Mochales, T., Barnolas, A., Pueyo, E.L., Serra-Kiel, J., Casas, A.M., Samsó, J.M., Ramajo, J., Sanjúan, J., 2012. Chronostratigraphy of the Boltaña anticline and the Ainsa Basin (southern Pyrenees). *Geological Society of America Bulletin*, 124, 1229-1250. DOI: <https://doi.org/10.1130/B30418.1>
- Montanari, L., 1964. *Alveolina obtusa*, nuova specie nel Luteziano. *Rivista Italiana di Paleontologia*, 70(3), 547-552.
- de Montfort, P.D., 1808-1810. *Conchyliologie systématique et classification méthodique des coquilles*. Paris, Schoell., Vol. 1.
- Morsilli, M., Bosellini, F.R., Pomar, L., Hallock, P., Aurell, M., Papazzoni, C., 2012. Mesophotic coral buildups in a prodelta setting (Late Eocene, southern Pyrenees, Spain): A mixed carbonate-siliciclastic system. *Sedimentology*, 59, 766-794.
- Moullade, M., 1965. Contribution au problème de la classification des Orbitolinidae (Foraminiferida, Lituolacea). *Comptes Rendus Hebdomadaires des Séances, Paris, Académie des Sciences*, 260, 4031-4034.
- Munier-Chalmas, E., Schlumberger, C., 1885. Note sur les Miliolidées trématophorées. *Bulletin de la Société Géologique de France* (1884-1885), sér. 3, 13, 273-323.
- Müller-Merz, E., 1980. Strukturanalyse ausgewählter rotaloidre Foraminiferen. *Schweizerische Paläontologische Abhandlungen*, 101, 5-68.
- Muñoz, J.A., 1992. Evolution of a continental collision belt: ECORS-Pyrenees crustal balanced crosssection. In: McClay K.R. (ed.). *Thrust Tectonics*. Dordrecht, Springer, 235-246.

- Nemkov, G.I., 1967. Nummulitides of the Soviet Union and their biostratigraphic significance. *Proceedings of the Study of the Geological Structure of the USSR, New Series*, 16, 312pp.
- Nemkov, G.I., Vanová, M., 1977. Redeposition of larger Foraminifers in East Slovakian Flisc Belt. *Geologische Práce*, 67, 105-134.
- Nuttall, W.L.F., 1928. Notes on the Tertiary Foraminifera of southern Mexico. *Journal of Paleontology*, 2(4), 372-376.
- Ogg, J., 2012. Geomagnetic Polarity Time Scale. In: Gradstein, F.M., Ogg, J.G., Schmitz, M., Ogg, G. (eds.). *The Geologic Time Scale*. Elsevier, 85-113.
- Oliva-Urcia, B., Beamud, E., Arenas, C., Pueyo, E.L., Garcés, M., Soto, R., Valero, L., Pérez-Rivarés, F.J., 2019. Dating the northern deposits of the Ebro foreland basin; implications for the kinematics of the SW Pyrenean front. *Tectonophysics*, 765, 11-34. DOI: <https://doi.org/10.1016/j.tecto.2019.05.007>
- Oppenheim, P., 1896. Die Eocaenfauna des Monte Postale bei Bolca im Veronesischen. *Palaeontographica*, 43, 125-221.
- d'Orbigny, A., 1826. Tableau méthodique de la classe des Céphalopodes. *Annales des Sciences Naturelles*, 7, 245-314.
- d'Orbigny, A., 1839. Voyage dans l'Amérique Méridionale. Foraminifères, 5(5), 1-86.
- d'Orbigny, A., 1839. Foraminifères, in de la Sagra R., *Histoire physique, politique et naturelle de l'île de Cuba*. A. Bertrand, 224pp.
- d'Orbigny, A., 1846. Foraminifères fossiles du bassin tertiaire de Vienne. Paris, Gide et Compe, 312pp.
- d'Orbigny, A., 1850-1852. *Prodrome de paléontologie stratigraphique universelle des animaux mollusques et rayonnés faisant suite au cours élémentaire de paléontologie et de géologie stratigraphiques*. Paris, Masson, vol. 1, 394pp., vol. 2, 427pp., vol. 3, 389pp.
- Parvati, S., 1971. A study of some rotaliid Foraminifera. *Koninklijke Nederlandse Akademie van Wetenschappen Proceedings, Serie B*, 74(1), 1-26.
- Pawlowski, J., Holzmann, M., Tyska, J., 2013. New supraordinal classification of Foraminifera: Molecules meet morphology. *Marine Micropaleontology*, 100(1-10), 1-18.
- Perrin, C., 1987. *Solenomeris*: un Foraminifère Acervulinidae constructeur de récifs. *Revue de Micropaléontologie*, 30, 197-206.
- Perrin, C., 1994. Morphology of encrusting and free living acervulinid Foraminifera: *Acervulina*, *Gypsina* and *Solenomeris*. *Paleontology*, 37(2), 425-458.
- Pignatti, J.S., 1994. Biostratigrafia dei macroforaminiferi del Paleogene della Maiella nel quadro delle piattaforme periadriatiche. *Studi Geologici Camerti, Special Volume "Biostratigrafia dell'Italia Centrale"*, 359-405.
- Pignatti, J., Papazzoni, C.A., 2017. Opelezones and their heritage in current larger foraminiferal biostratigraphy. *Lethaia*, 50, 369-380. DOI: <https://doi.org/10.1111/let.12210>
- Plaziat, J.-C., 1981. Late Cretaceous to late Eocene palaeogeographic evolution of southwest Europe. *Palaeogeography, Palaeoclimatology, Palaeoecology*, 36, 211-234.
- Plaziat, J.-C., Perrin, C., 1992. Multikilometer-sized reefs built by foraminifera (*Solenomeris*) from the early Eocene of the Pyrenean domain (S. France, N. Spain): Palaeoecologic relations with coral reefs. *Palaeogeography, Palaeoclimatology, Palaeoecology*, 96, 195-231.
- Pueyo, E.L., Millán, H., Pocoví, A., 2002. Rotation velocity of a thrust: a paleomagnetic study in the External Sierras (Southern Pyrenees). *Sedimentary Geology*, 146, 191-208.
- Puigdefàbregas, C., 1975. La Sedimentación Molásica en la Cuenca de Jaca. *Pirineos*, 114, 1-188.
- Puigdefàbregas, C., Souquet, P., 1986. Tecto-sedimentary cycles and depositional sequences of the Mesozoic and Tertiary from the Pyrenees. *Tectonophysics*, 129, 173-203.
- Racey, A., 1995. Lithostratigraphy and larger foraminiferal (Nummulitid) biostratigraphy of the Tertiary of northern Oman. *Micropaleontology*, 41, 1-123.
- Rahaghi, A., Schaub, H., 1976. Nummulites et Assilines du NE de l'Iran. *Eclogae geologicae Helvetiae*, 69, 765-782.
- Reguant, S., 1967. El Eoceno de Vic (Barcelona). *Memorias del Instituto Geológico y Minero de España*, 68, 1-350.
- Reguant, S., Clavell, E. 1967. Descripción de algunos *Nummulites* afines al *Nummulites perforatus* (Montfort) del Eoceno de Vic (Barcelona). *Notas y Comunicaciones del Instituto Geológico y Minero de España*, 101-102, 41-56.
- Reiss, Z., 1963. Reclassification of perforate Foraminifera. *Bulletin Geological Survey of Israel*, 36, 1-111.
- Reuss, A.E., 1848. Die Fossilien Polyparien des Wiener Tertiärbeckens. *Haidingers Naturwissenschaftlichen Abhandlungen*, 2(1), 1-109.
- Robinson, E., Wright, R.M., 1993. Jamaican Paleogene larger foraminifera. In: Wright, R.M., Robinson, E. (eds.). *Biostratigraphy of Jamaica*. Boulder, Colorado, Geological Society of America, 182 (Memoir), 283-345.
- Rodríguez-Pintó, A., Pueyo, E.L., Serra-Kiel, J., Samsó, J.M., Barnolas, A., Pocoví, A., 2012a. Lutetian magnetostratigraphic calibration of larger foraminifera zonation (SBZ) at the Southern Pyrenees: The Isuela Section. *Palaeogeography, Palaeoclimatology, Palaeoecology*, 333-334, 107-120.
- Rodríguez-Pintó, A., Pueyo, E.L., Barnolas, A., Samsó, J.M., Pocoví, A., Gil-Peña, I., Mochales, T., Serra-Kiel, J., 2012b. Lutetian magnetostratigraphy in the Santa Marina section (Balzes anticline, Southwestern Pyrenees). *Geotemas*, 13, 1184-1187.
- Rodríguez-Pintó, A., Pueyo, E.L., Serra-Kiel, J., Barnolas, A., Samsó, J.M., Pocoví, A., 2013a. The Upper Ypresian and Lutetian in San Pelegrín (Southwestern Pyrenean Basin): Magnetostratigraphy and larger foraminifera. *Palaeogeography, Palaeoclimatology, Palaeoecology*, 370, 13-29.
- Rodríguez-Pintó, A., Pueyo, E.L., Pocoví, A., Ramón, M.J., Oliva-Urcia, B., 2013b. Structural control on overlapped paleomagnetic vectors: A case study in the Balzes anticline (Southern Pyrenees). *Physics of the Earth and Planetary Interiors*, 215, 43-57.
- Rodríguez-Pintó, A., Sanchez, E., Barnolas, A., Serra-Kiel, J., Samsó, J.M., Mochales, T., Pueyo, E.L., Scholger, R., 2017.

- Magnetostratigraphic data from lower part of Gabardiella section: Early - Middle Eocene, Southern Pyrenees. Reunión de la Comisión de Paleomagnetismo de la Sociedad Geológica de España- MAGIBER-X (Valle del Grío) ISBN: 978-84-16723-40-9, 30-33.
- Rodríguez-Pintó, A., Sánchez-Moreno, E., Pueyo, E.L., Oliva-Urcia, B., Barnolas, A., Izquierdo-Llavall, E., 2019. Límite Luteciense/Bartoniense en la sección de Isuela (revisada), Pirineos suroccidentales. In: Font, E., Beamud, E., Oliva-Urcia, B., Pueyo, E.L., Lopes, F.C. (eds.). MAGIBER XI- Paleomagnetismo Em Espanha E Portugal (Livro de Resumos). Universidade de Coimbra, ISBN 978-989-98914-7-0, 121-124.
- de Roissy, F., 1805. Histoire naturelle, générale et particulière des Mollusques (Buffon et Sonnini), vol. 5. Paris, Dufart, 450pp
- Romero, J., 2001. Los macroforaminíferos del Eoceno Medio del borde suroriental de la cuenca paleógena surpirenaica. Doctoral Thesis. Cerdanyola del Vallès, Universitat Autònoma de Barcelona, 1-274pp.
- Rozlozsnik, P., 1924. Nummulites paléogènes d'Hongrie. Description des planches posthumes de Max von Hantken et Sigmund Madarasz, hongrois. - Fô ldt. Szemle 1(4), 159-189, pLI-V
- Rozlozsnik, P., de la Harpe, P., 1926. Matériaux pour servir à une monographie des Nummulines et Assilines. D'après les manuscrits inédits de Prof. Philippe de La Harpe. Magyar Királyi Földtani Intézet évkönyve, 27(1), 1-102.
- Rozlozsnik, P., 1929. Studien über Nummulinen. Geologica Hungarica, 2, 1-248.
- Rutten, L.M.R., 1914. Foraminiferen-führende Gesteine von niederländisch Neu-Guinea. Résultats de l'expédition scientifique néerlandaise à la Nouvelle-Guinée, 6(2) [1913], 21-51.
- Sacal, V., Debourle, A., 1957. Foraminifères d'Aquitaine. 2e partie – Peneroplidae à Victoriellidae. Mémoires de la Société géologique de France (nouvelle série), 78(36), 1-87.
- Samsó, J.M., Sanz Lopez, J., Garcia Senz, J., Serra-Kiel, J., Tosquella, J., 1992. Mapa Geológica y Memoria de la Hoja nº 248 (Apiés). Mapa Geológico de España 1:50.000, Segunda Serie (Magna), Primera edición, Instituto Geológico y Mineo de España, (IGME).
- Samsó, J.M., Serra-Kiel, J., Tosquella, J., Travé, A., 1994. Cronoestratigrafía de las plataformas lutecienses de la zona central de la cuenca Surpirenaica. In: Gonzalez Rodriguez, A. (ed.). II Congreso Del Grupo Español Del Terciario. Jaca, Universidad de Zaragoza, 205-208.
- Samuel, O., Borza, K., Köhler, E., 1972. Microfauna and Lithostratigraphy of the Paleogene. Bratislava, Geologický ústav Dionýza Stura, 246pp.
- Schaub, H., 1962. Über einige stratigraphische wichtige Nummuliten-Arten. Eclogae Geologicae Helveticae, 55(2), 529-551.
- Schaub, H., 1963. Über einige entwicklungsreihen von Nummulites und Assilina und ihre Stratigraphische Bedeutung. In: von Koenigswald, G.H.R., Emeis, J.D., Buning, W.L., Wagner, C.W. (eds.). Evolutionary trends in Foraminifera, Elsevier, 282-297.
- Schaub, H., 1966. Über die Grossforaminiferen im Untereocaen von Campo (Ober-Aragonien). Eclogae Geologicae Helveticae, 59(1), 355-377.
- Schaub, H., 1981. Nummulites et Assilines de la Tethys paléogène. Taxinomie, phylogénèse et biostratigraphie. Mémoires suisses de Paléontologie, 104, 236pp, 105-106, 97pls.
- Schlumberger, C., Munier-Chalmas, E., 1884. Note sur les Miliolidées trématophorées. Bulletin de la Société géologique de France (1883-1884), série 3, 12, 629-630.
- Schlumberger, C., 1893. Note sur les genres *Trillina* et *Linderina*. Bulletin de la Société géologique de France, série 3, 21(2), 118-123.
- Schlumberger, C., 1905. Deuxième note sur les Miliolidées trématophorées. Bulletin Société géologique de France, série 4, 5, 115-134.
- Schmidt, U., Jäger R., 1993. Bestimmungstabelle für einige inkrustierende Foraminiferen aus den Unterordnungen Textulariina und Rotaliina. Zitteliana, 20, 171-178.
- Schultze, M.S., 1854. Über den Organismus der Polythalamien (Foraminiferen), nebst Bemerkungen über die Rhizopoden im Allgemeinen. Leipzig, Wilhem Engelmann, 68pp
- Schwager, C., 1876. Saggio di una classificazione dei foraminiferi avuto riguardo alle loro famiglie naturali. Bolletino Reale Comitato Geologico d'Italia, 7, 475-485.
- Schwager, C., 1877. Quadro del proposto Sistema di classificazione dei foraminiferi con guscio. Bolletino Reale Comitato Geologico d'Italia, 8, 18-27.
- Scotto di Carlo, B., 1966. Le alveoline del Gargano nord-orientale. Palaeontographia Italica, vol. LXI (n. serie Vol. XXXI), 65-73.
- Serra-Kiel, J., 1984. Estudi dels *Nummulites* del grup de *N. perforatus* (Montfort). Treballs de la Institució Catalana d'Història Natural, 11, 1-244.
- Serra-Kiel, J., Hottinger, L., Caus, E., Drobne, K., Ferràndez, C., Jauhari, A.K., Less, G., Pavlovec, R., Pignatti, J., Samsó, J.M., Schaub, H., Sirel, E., Strougo, A., Tambareau, Y., Tosquella, J., Zakrevskaya, E., 1998. Larger foraminiferal biostratigraphy of the Tethyan Paleocene and Eocene. Bulletin de la Société géologique de France, 169(2), 281-299.
- Serra-Kiel, J., Ferràndez-Cañadell, C., García-Senz, J., Hernaiz Huerta, P.P., 2007. Cainozoic larger foraminifers from Dominican Republic. Boletín Geológico y Minero, 118(2), 359-384.
- Serra-Kiel, J., Gallardo-García, A., Razin, Ph., Robinet, J., Roger, J., Grelaud, C., Leroy, S., Robin, C., 2016. Middle Eocene – Early Miocene larger foraminifera from Dhofar (Oman) and Socotra Island (Yemen). Arabian Journal of Geosciences, 9, 1-95.
- Silva-Casal R., 2017. Las plataformas carbonatadas del Eoceno medio de la cuenca de Jaca-Pamplona (Formación Guara, Sierras Exteriores): análisis estratigráfico integral y evolución sedimentaria. PhD Thesis. Zaragoza, Universidad de Zaragoza, 345pp.
- Silva-Casal, R., Aurell, M., Payros, A., Pueyo, E.L., Serra-Kiel, J., 2019. Carbonate ramp drowning caused by flexural

- subsidence: The South Pyrenean middle Eocene foreland basin. *Sedimentary Geology*, 393-394, 105538.
- Silvestri, A., 1905. Sul *Dictyoconus aegyptiensis* (Chapman). Roma, Atti della Pontificia Accademia Romana dei Nuovi Lincei, 58, 129-131.
- Silvestri, A., 1924. Revisione di fossili della Venezia e Venezia Giulia. Padova (1923), Atti dell'Accademia Scientifica Veneta-Trentino-Istriana, serie 3, 14, 7-12
- Sirel, E., 2000. Biostratigraphy of the Middle/Upper Eocene/Oligocene boundaries at the eastern Turkey. *Annali del Museo Civico di Storia Naturale di Ferrara*, 3, 61-70.
- Sirel, E., 2003. Foraminiferal description and biostratigraphy of the Bartonian, Priabonian and Oligocene shallow-water sediments of the southern and eastern Turkey. *Revue de Paléobiologie*, 22(1), 269-339.
- Sirel, E., Acar, S., 2008. Description and Biostratigraphy of the Thanetian-Bartonian Globulvalveolids and Alveolids of Turkey. The Chamber of Geological Engineers Publication (UCTEA), Scientific Synthesis of the Lifelong Achievement Special Volume, 2, 108pp.
- Sirel, E., Özgen-Erdem, N., Kangal, Ö., 2013. Systematics and biostratigraphy of Oligocene (Rupelian-Early Chattian) foraminifera from lagoonal-very shallow water limestone in the eastern Sivas Basin (central Turkey). *Geologia Croatica*, 66(2), 83-109.
- Smout, A.H., 1954. Lower Tertiary foraminifera of the Qatar Peninsula. London, British Museum (Natural History), 96pp.
- Stache, G., 1875. Neue Beobachtungen in den Schichten der liburnischen Stufe. *Verhandlungen der Geologischen Reichsanstalt*, 1875, 334-338.
- Sztràkos, K., 2000. Les foraminifères de l'Éocène du Bassin de l'Adour (Aquitaine, France). *Biostratigraphie et Taxonomie. Revue de Micropaléontologie*, 1-2, 71-172.
- Thalman, H.E., 1938. Protozoa. *Geologisches Zentralblatt, Abteilung B, Palaeontologie*, 11, 203-211.
- Thalman, H.E., 1951. Mitteilungen über Foraminiferen IX. *Eclogae Geologicae Helveticae*, 43(1950), 221-225.
- Tomás, S., Frijia, G., Bömelburg, E., Zamagni, J., Perrin, C., Mutti, M., 2016. Evidence for seagrass meadows and their response to paleoenvironmental changes in the early Eocene (Jafnayn Formation, Wadi Bani Khalid, N Oman). *Sedimentary Geology*, 341, 189-202. DOI: <https://doi.org/10.1016/j.sedgeo.2016.05.016>
- Tomassetti, L., Benedetti, A., Brandano, M., 2016. Middle Eocene seagrass facies from Apennine carbonate platforms (Italy). *Sedimentary Geology*, 335, 136-149. DOI: <https://doi.org/10.1016/j.sedgeo.2016.02.002>
- Tosquella, 1995. Els Nummulitinae del Paleocè-Eocè inferior de la Conca Sudpirenaica. Doctoral Thesis. Barcelona, University of Barcelona, 581pp.
- Uhlig, V., 1886. Ueber eine Mikrofauna aus dem Alttertiär der westgalizischen Karpathen. *Jahrbuch der Geologischen Bundesanstalt*, 036, 141-214.
- Vandenbergh, N., Hilgen, F.J., Speijer, R.P., 2012. The Paleogene Period. In: Gradstein, F.M., Ogg J.G., Schmitz, M., Ogg, G. (eds.). *The Geologic Time Scale*, Elsevier, 856-921.
- Vanová, M., 1972. Nummulites from the area of Bojnice, the Upper Hron Depression, and the Budin paleogene around Stúrovo. *Zborník GeologickýchVied západné karpáty*, 17, 5-104.
- Vecchio, E., Barattolo, E., Hottinger, L., 2007. Alveolina horizons in the Trentinara Formation (Southern Apennines, Italy): Stratigraphic and paleogeographic implications. *Rivista Italiana di Paleontologia e Stratigrafia*, 113(1), 21-42.
- Vella, P., 1957. Studies in New Zealand foraminifera. *Paleontological Bulletin of Wellington*, 28, 1-64.

**Manuscript received January 2020;**  
**revision accepted February 2021;**  
**published Online June 2021.**

# APPENDIX I

Specimen	Species	Sample name in this work	Sample name in the repository	Repository	Catalogue numbers	Stratigraphic Section
Fig. 13A/ Fig. 14A	<i>Idalina</i> sp.	G 1	L 20	Instituto Geológico y Minero de España (IGME)		Gabardiella / Lusera*
Fig. 13B/ Fig. 14B	<i>Idalina</i> sp.	G 2	L 23	Instituto Geológico y Minero de España (IGME)		Gabardiella / Lusera*
Fig. 13C/ Fig. 14C	<i>Idalina</i> sp.	G 1	L 21	Instituto Geológico y Minero de España (IGME)		Gabardiella / Lusera*
Fig. 13D	<i>Idalina</i> sp.	G 2	L 23	Instituto Geológico y Minero de España (IGME)		Gabardiella / Lusera*
Fig. 13E	<i>Idalina</i> sp.	G 1	L 20	Instituto Geológico y Minero de España (IGME)		Gabardiella / Lusera*
Fig. 13F/ Fig. 14N	<i>Idalina berthelini</i>	G 28	L 91	Instituto Geológico y Minero de España (IGME)		Gabardiella / Lusera*
Fig. 13G/ Fig. 14D	<i>Idalina berthelini</i>	I 45	A 78	Instituto Geológico y Minero de España (IGME)		Isuela / Arguis*
Fig. 13H/ Fig. 14M	<i>Idalina berthelini</i>	I 47	A 81	Instituto Geológico y Minero de España (IGME)		Isuela / Arguis*
Fig. 13I	<i>Idalina berthelini</i>	I 45	A 78	Instituto Geológico y Minero de España (IGME)		Isuela / Arguis*
Fig. 13J/ Fig. 14G	<i>Idalina berthelini</i>	I 42	A 74	Instituto Geológico y Minero de España (IGME)		Isuela / Arguis*
Fig. 13K	<i>Idalina berthelini</i>	I 38	A 70	Instituto Geológico y Minero de España (IGME)		Isuela / Arguis*
Fig. 13L/ Fig. 14J	<i>Idalina berthelini</i>	G 60	L 141	Instituto Geológico y Minero de España (IGME)		Gabardiella / Lusera*
Fig. 13M/ Fig. 14L	<i>Idalina berthelini</i>	I 22	A 46	Instituto Geológico y Minero de España (IGME)		Isuela / Arguis*
Fig. 13N/ Fig. 14K	<i>Idalina berthelini</i>	G 13	L 52	Instituto Geológico y Minero de España (IGME)		Gabardiella / Lusera*
Fig. 13O	<i>Idalina berthelini</i>	I 44	A 77	Instituto Geológico y Minero de España (IGME)		Isuela / Arguis*
Fig. 13P	<i>Idalina berthelini</i>	G 35	L 104	Instituto Geológico y Minero de España (IGME)		Gabardiella / Lusera*
Fig. 13Q	<i>Idalina berthelini</i>	I 39	A 71	Instituto Geológico y Minero de España (IGME)		Isuela / Arguis*
Fig. 13R	<i>Idalina berthelini</i>	I 37	A 69	Instituto Geológico y Minero de España (IGME)		Isuela / Arguis*
Fig. 13S/ Fig. 14F	<i>Idalina berthelini</i>	G 36	L 105	Instituto Geológico y Minero de España (IGME)		Gabardiella / Lusera*
Fig. 13T	<i>Idalina berthelini</i>	I 40	A 72	Instituto Geológico y Minero de España (IGME)		Isuela / Arguis*
Fig. 13U/ Fig. 14E	<i>Idalina berthelini</i>	G 27	L 88	Instituto Geológico y Minero de España (IGME)		Gabardiella / Lusera*
Fig. 13V	<i>Idalina berthelini</i>	I 17	A 40	Instituto Geológico y Minero de España (IGME)		Isuela / Arguis*
Fig. 14H	<i>Idalina berthelini</i>	I 38	A 70	Instituto Geológico y Minero de España (IGME)		Isuela / Arguis*
Fig. 14I	<i>Idalina berthelini</i>	I 9	A 18	Instituto Geológico y Minero de España (IGME)		Isuela / Arguis*
Fig. 14O	<i>Idalina osquetaensis</i>	O 12	Os-13	Natural Science Museum of the University of Zaragoza	MPZ 2020/506	La Osqueta
Fig. 14W	<i>Idalina osquetaensis</i>	O 5	Os-6	Natural Science Museum of the University of Zaragoza	MPZ 2020/511	La Osqueta
Fig. 15A/ Fig. 14P	<i>Idalina osquetaensis</i>	O 3	Os-4	Natural Science Museum of the University of Zaragoza	Holotype, MPZ 2019/1681	La Osqueta
Fig. 15B/ Fig. 14V	<i>Idalina osquetaensis</i>	P 21	P-10	Natural Science Museum of the University of Zaragoza	MPZ 2020/515	La Peña
Fig. 15C/ Fig. 14A'	<i>Idalina osquetaensis</i>	V 9	Vi-10	Natural Science Museum of the University of Zaragoza	MPZ 2020/554	Villalangua
Fig. 15D/ Fig. 14Q	<i>Idalina osquetaensis</i>	O 2	Os-3	Natural Science Museum of the University of Zaragoza	MPZ 2020/508	La Osqueta
Fig. 15E/ Fig. 14R	<i>Idalina osquetaensis</i>	O 3	Os-4	Natural Science Museum of the University of Zaragoza	Paratype, MPZ 2019/1683	La Osqueta

## APPENDIX I. Continued.

Specimen	Species	Sample name in this work	Sample name in the repository	Repository	Catalogue numbers	Stratigraphic Section
Fig. 15F/ Fig. 14S	<i>Idalina osquetaensis</i>	O 3	Os-4	Natural Science Museum of the University of Zaragoza	Paratype, MPZ 2019/1682	La Osqueta
Fig. 15G/ Fig. 14U	<i>Idalina osquetaensis</i>	E 33	Es-30	Natural Science Museum of the University of Zaragoza	MPZ 2020/488	La Foz de Escalete
Fig. 15H/ Fig. 14Z	<i>Idalina osquetaensis</i>	M 16	Mu-15	Natural Science Museum of the University of Zaragoza	MPZ 2020/495	Murillo de Gállego
Fig. 15I/ Fig. 14T	<i>Idalina osquetaensis</i>	SC 52	Sc-39	Natural Science Museum of the University of Zaragoza	MPZ 2020/538	Sierra Caballera
Fig. 15J/ Fig. 14Y	<i>Idalina osquetaensis</i>	V 15	Vi-17	Natural Science Museum of the University of Zaragoza	MPZ 2020/548	Villalangua
Fig. 15K	<i>Idalina osquetaensis</i>	M 16	Mu-15	Natural Science Museum of the University of Zaragoza	MPZ 2020/494	Murillo de Gállego
Fig. 15L	<i>Idalina osquetaensis</i>	O 17	Os-18	Natural Science Museum of the University of Zaragoza	MPZ 2020/507	La Osqueta
Fig. 15M	<i>Idalina osquetaensis</i>	E 40	Es-38	Natural Science Museum of the University of Zaragoza	MPZ 2020/490	La Foz de Escalete
Fig. 15N	<i>Idalina osquetaensis</i>	P 33	P-34	Natural Science Museum of the University of Zaragoza	MPZ 2020/520	La Peña
Fig. 15O	<i>Idalina osquetaensis</i>	SC 52	Sc-39	Natural Science Museum of the University of Zaragoza	MPZ 2020/537	Sierra Caballera
Fig. 15P	<i>Idalina osquetaensis</i>	M 8	Mu-24	Natural Science Museum of the University of Zaragoza	MPZ 2020/505	Murillo de Gállego
Fig. 15Q	<i>Idalina osquetaensis</i>	V 14	Vi-16	Natural Science Museum of the University of Zaragoza	MPZ 2020/547	Villalangua
Fig. 15R	<i>Idalina osquetaensis</i>	V 7	Vi-8	Natural Science Museum of the University of Zaragoza	MPZ 2020/549	Villalangua
Fig. 15S	<i>Idalina osquetaensis</i>	M 15	Mu-16	Natural Science Museum of the University of Zaragoza	MPZ 2020/493	Murillo de Gállego
Fig. 16A	<i>Fabularia roselli</i>	G 21	L 73	Instituto Geológico y Minero de España (IGME)		Gabardiella / Lusera*
Fig. 16B	<i>Fabularia roselli</i>	G 20	L 71	Instituto Geológico y Minero de España (IGME)		Gabardiella / Lusera*
Fig. 16C	<i>Fabularia roselli</i>	I 1	A 1	Instituto Geológico y Minero de España (IGME)		Isuela / Arguis*
Fig. 16D	<i>Fabularia roselli</i>	G 21	L 73	Instituto Geológico y Minero de España (IGME)		Gabardiella / Lusera*
Fig. 16E	<i>Fabularia roselli</i>	G 12	L 51	Instituto Geológico y Minero de España (IGME)		Gabardiella / Lusera*
Fig. 16F	<i>Fabularia roselli</i>	G 18	L 66	Instituto Geológico y Minero de España (IGME)		Gabardiella / Lusera*
Fig. 16G	<i>Fabularia roselli</i>	G 16	L 60	Instituto Geológico y Minero de España (IGME)		Gabardiella / Lusera*
Fig. 16H	<i>Fabularia roselli</i>	G 19	L 69	Instituto Geológico y Minero de España (IGME)		Gabardiella / Lusera*
Fig. 16I	<i>Fabularia roselli</i>	G 21	L 72	Instituto Geológico y Minero de España (IGME)		Gabardiella / Lusera*
Fig. 16J	<i>Fabularia roselli</i>	I 2	A 2	Instituto Geológico y Minero de España (IGME)		Isuela / Arguis*
Fig. 16K	<i>Fabularia roselli</i>	G 21	L 72	Instituto Geológico y Minero de España (IGME)		Gabardiella / Lusera*
Fig. 16L	<i>Fabularia roselli</i>	G 21	L 72	Instituto Geológico y Minero de España (IGME)		Gabardiella / Lusera*
Fig. 16M	<i>Fabularia roselli</i>	G 21	L 72	Instituto Geológico y Minero de España (IGME)		Gabardiella / Lusera*
Fig. 16N	<i>Fabularia roselli</i>	G 18	L 66	Instituto Geológico y Minero de España (IGME)		Gabardiella / Lusera*
Fig. 16O	<i>Fabularia roselli</i>	G 19	L 69	Instituto Geológico y Minero de España (IGME)		Gabardiella / Lusera*
Fig. 16P	<i>Fabularia ovata</i>	G 18	L 66	Instituto Geológico y Minero de España (IGME)		Gabardiella / Lusera*
Fig. 16Q	<i>Fabularia ovata</i>	G 9	L 47	Instituto Geológico y Minero de España (IGME)		Gabardiella / Lusera*

## APPENDIX I. Continued.

Specimen	Species	Sample name in this work	Sample name in the repository	Repository	Catalogue numbers	Stratigraphic Section
Fig. 16R	<i>Fabularia ovata</i>	G 9	L 47	Instituto Geológico y Minero de España (IGME)		Gabardiella / Lusera*
Fig. 16S	<i>Fabularia ovata</i>	V 9	Vf-10	Natural Science Museum of the University of Zaragoza	MPZ 2020/553	Villalangua
Fig. 16T	<i>Fabularia ovata</i>	E 16	Es2-17	Natural Science Museum of the University of Zaragoza	MPZ 2020/486	La Foz de Escalote
Fig. 16U	<i>Fabularia ovata</i>	V 9	Vf-10	Natural Science Museum of the University of Zaragoza	MPZ 2020/552	Villalangua
Fig. 16V	<i>Fabularia ovata</i>	P 22	P-12	Natural Science Museum of the University of Zaragoza	MPZ 2020/516	La Peña
Fig. 16W	<i>Fabularia ovata</i>	V 9	Vf-10	Natural Science Museum of the University of Zaragoza	MPZ 2020/551	Villalangua
Fig. 16X	<i>Fabularia ovata</i>	I 32	A 56	Instituto Geológico y Minero de España (IGME)		Isuela / Arguis*
Fig. 16Y	<i>Fabularia ovata</i>	G 9	L 47	Instituto Geológico y Minero de España (IGME)		Gabardiella / Lusera*
Fig. 17A	<i>Pseudolacazina hottigeri</i>	G 18	L 67	Instituto Geológico y Minero de España (IGME)		Gabardiella / Lusera*
Fig. 17B	<i>Pseudolacazina hottigeri</i>	G 14	L 55	Instituto Geológico y Minero de España (IGME)		Gabardiella / Lusera*
Fig. 17C	<i>Pseudolacazina hottigeri</i>	G 16	L 61	Instituto Geológico y Minero de España (IGME)		Gabardiella / Lusera*
Fig. 17D	<i>Pseudolacazina hottigeri</i>	G 18	L 65	Instituto Geológico y Minero de España (IGME)		Gabardiella / Lusera*
Fig. 17E	<i>Pseudolacazina hottigeri</i>	G 18	L 65	Instituto Geológico y Minero de España (IGME)		Gabardiella / Lusera*
Fig. 17F	<i>Pseudolacazina hottigeri</i>	G 18	L 65	Instituto Geológico y Minero de España (IGME)		Gabardiella / Lusera*
Fig. 17G	<i>Pseudolacazina hottigeri</i>	I 34	A 59	Instituto Geológico y Minero de España (IGME)		Isuela / Arguis*
Fig. 17H	<i>Pseudolacazina hottigeri</i>	M 2	Mu-30	Natural Science Museum of the University of Zaragoza	MPZ 2020/496	Murillo de Gállego
Fig. 17I	<i>Pseudolacazina hottigeri</i>	I 28	A 52	Instituto Geológico y Minero de España (IGME)		Isuela / Arguis*
Fig. 17J	<i>Pseudolacazina hottigeri</i>	I 31	A 55	Instituto Geológico y Minero de España (IGME)		Isuela / Arguis*
Fig. 17K	<i>Pseudolacazina hottigeri</i>	G 18	L 65	Instituto Geológico y Minero de España (IGME)		Gabardiella / Lusera*
Fig. 17L	<i>Pseudolacazina hottigeri</i>	I 28	A 52	Instituto Geológico y Minero de España (IGME)		Isuela / Arguis*
Fig. 17M	<i>Pseudolacazina hottigeri</i>	G 14	L 55	Instituto Geológico y Minero de España (IGME)		Gabardiella / Lusera*
Fig. 17N	<i>Pseudolacazina hottigeri</i>	G 13	L 52	Instituto Geológico y Minero de España (IGME)		Gabardiella / Lusera*
Fig. 17O	<i>Pseudolacazina hottigeri</i>	G 10	L 49	Instituto Geológico y Minero de España (IGME)		Gabardiella / Lusera*
Fig. 17P	<i>Pseudolacazina hottigeri</i>	G 18	L 65	Instituto Geológico y Minero de España (IGME)		Gabardiella / Lusera*
Fig. 17Q	<i>Pseudolacazina hottigeri</i>	G 16	L 61	Instituto Geológico y Minero de España (IGME)		Gabardiella / Lusera*
Fig. 17R	<i>Pseudolacazina hottigeri</i>	I 30	A 54	Instituto Geológico y Minero de España (IGME)		Isuela / Arguis*
Fig. 17S	<i>Perilaculina cf. raincourtii</i>	I 28	A 52	Instituto Geológico y Minero de España (IGME)		Isuela / Arguis*
Fig. 17T	<i>Perilaculina cf. raincourtii</i>	G 24	L 82	Instituto Geológico y Minero de España (IGME)		Gabardiella / Lusera*
Fig. 17U	<i>Perilaculina cf. raincourtii</i>	I 30	A 54	Instituto Geológico y Minero de España (IGME)		Isuela / Arguis*
Fig. 17V	<i>Perilaculina cf. raincourtii</i>	I 28	A 52	Instituto Geológico y Minero de España (IGME)		Isuela / Arguis*
Fig. 17W	<i>Perilaculina cf. raincourtii</i>	SC 22	Sc-3	Natural Science Museum of the University of Zaragoza	MPZ 2020/530	Sierra Caballera

## APPENDIX I. Continued.

Specimen	Species	Sample name in this work	Sample name in the repository	Repository	Catalogue numbers	Stratigraphic Section
Fig. 17X	<i>Periloculina cf. raincourtii</i>	SC 23	Sc-5	Natural Science Museum of the University of Zaragoza	MPZ 2020/533	Sierra Caballera
Fig. 18A	<i>Alveolina ospiensis</i>	G 3	L 36	Instituto Geológico y Minero de España (IGME)		Gabardiella / Lusera*
Fig. 18B	<i>Alveolina ospiensis</i>	G 3	L 36	Instituto Geológico y Minero de España (IGME)		Gabardiella / Lusera*
Fig. 18C	<i>Alveolina ospiensis</i>	G 3	L 36	Instituto Geológico y Minero de España (IGME)		Gabardiella / Lusera*
Fig. 18D	<i>Alveolina ospiensis</i>	G 3	L 36	Instituto Geológico y Minero de España (IGME)		Gabardiella / Lusera*
Fig. 18E	<i>Alveolina ospiensis</i>	G 3	L 36	Instituto Geológico y Minero de España (IGME)		Gabardiella / Lusera*
Fig. 19A	<i>Alveolina decastrai</i>	G 1	L 21	Instituto Geológico y Minero de España (IGME)		Gabardiella / Lusera*
Fig. 19A'	<i>Alveolina munieri</i>	I 17	A 40	Instituto Geológico y Minero de España (IGME)		Isuela / Arguis*
Fig. 19B	<i>Alveolina decastrai</i>	G 1	L 21	Instituto Geológico y Minero de España (IGME)		Gabardiella / Lusera*
Fig. 19B'	<i>Alveolina munieri</i>	I 20	A 43	Instituto Geológico y Minero de España (IGME)		Isuela / Arguis*
Fig. 19C	<i>Alveolina decastrai</i>	G 1	L 21	Instituto Geológico y Minero de España (IGME)		Gabardiella / Lusera*
Fig. 19C'	<i>Alveolina munieri</i>	I 16	A 39	Instituto Geológico y Minero de España (IGME)		Isuela / Arguis*
Fig. 19D	<i>Alveolina decastrai</i>	G 1	L 21	Instituto Geológico y Minero de España (IGME)		Gabardiella / Lusera*
Fig. 19D'	<i>Alveolina munieri</i>	I 20	A 43	Instituto Geológico y Minero de España (IGME)		Isuela / Arguis*
Fig. 19E	<i>Alveolina cremae</i>	G 1	L 20	Instituto Geológico y Minero de España (IGME)		Gabardiella / Lusera*
Fig. 19F	<i>Alveolina cremae</i>	G 1	L 21	Instituto Geológico y Minero de España (IGME)		Gabardiella / Lusera*
Fig. 19G	<i>Alveolina obtusa</i>	G 16	L 61	Instituto Geológico y Minero de España (IGME)		Gabardiella / Lusera*
Fig. 19H	<i>Alveolina levantina</i>	I 7	A 10	Instituto Geológico y Minero de España (IGME)		Isuela / Arguis*
Fig. 19I	<i>Alveolina levantina</i>	I 7	A 10	Instituto Geológico y Minero de España (IGME)		Isuela / Arguis*
Fig. 19J	<i>Alveolina obtusa</i>	G 16	L 61	Instituto Geológico y Minero de España (IGME)		Gabardiella / Lusera*
Fig. 19K	<i>Alveolina tenuis</i>	I 7	A 10	Instituto Geológico y Minero de España (IGME)		Isuela / Arguis*
Fig. 19L	<i>Alveolina boscii</i>	G 15	L 58	Instituto Geológico y Minero de España (IGME)		Gabardiella / Lusera*
Fig. 19M	<i>Alveolina boscii</i>	G 18	L 65	Instituto Geológico y Minero de España (IGME)		Gabardiella / Lusera*
Fig. 19N	<i>Alveolina tenuis</i>	I 7	A 10	Instituto Geológico y Minero de España (IGME)		Isuela / Arguis*
Fig. 19O	<i>Alveolina tenuis</i>	G 21	L 73	Instituto Geológico y Minero de España (IGME)		Gabardiella / Lusera*
Fig. 19P	<i>Alveolina tenuis</i>	G 17	L 63	Instituto Geológico y Minero de España (IGME)		Gabardiella / Lusera*
Fig. 19Q	<i>Alveolina boscii</i>	G 18	L 65	Instituto Geológico y Minero de España (IGME)		Gabardiella / Lusera*
Fig. 19R	<i>Alveolina boscii</i>	G 16	L 61	Instituto Geológico y Minero de España (IGME)		Gabardiella / Lusera*
Fig. 19S	<i>Alveolina boscii</i>	G 14	L 57	Instituto Geológico y Minero de España (IGME)		Gabardiella / Lusera*
Fig. 19T	<i>Alveolina boscii</i>	G 34	L 103	Instituto Geológico y Minero de España (IGME)		Gabardiella / Lusera*
Fig. 19U	<i>Alveolina boscii</i>	G 16	L 61	Instituto Geológico y Minero de España (IGME)		Gabardiella / Lusera*

## APPENDIX I. Continued.

Specimen	Species	Sample name in this work	Sample name in the repository	Repository	Catalogue numbers	Stratigraphic Section
Fig. 19V	<i>Alveolina callosa</i>	G 3	L 36	Instituto Geológico y Minero de España (IGME)		Gabardiella / Lusera*
Fig. 19W	<i>Alveolina stipes</i>	G 4	L 37	Instituto Geológico y Minero de España (IGME)		Gabardiella / Lusera*
Fig. 19X	<i>Alveolina tenuis</i>	I 13	A 27	Instituto Geológico y Minero de España (IGME)		Isuela / Arguis*
Fig. 19Y	<i>Alveolina callosa</i>	G 3	L 36	Instituto Geológico y Minero de España (IGME)		Gabardiella / Lusera*
Fig. 19Z	<i>Alveolina callosa</i>	SC 12	SC2-17	Natural Science Museum of the University of Zaragoza	MPZ 2020/525	Sierra Caballera
Fig. 20A	<i>Alveolina fusiformis</i>	I 20	A 43	Instituto Geológico y Minero de España (IGME)		Isuela / Arguis*
Fig. 20B	<i>Alveolina fusiformis</i>	O 7	O5-8	Natural Science Museum of the University of Zaragoza	MPZ 2020/512	La Osqueta
Fig. 20C	<i>Alveolina fusiformis</i>	I 22	A 46	Instituto Geológico y Minero de España (IGME)		Isuela / Arguis*
Fig. 20D	<i>Alveolina fusiformis</i>	O 3	O5-4	Natural Science Museum of the University of Zaragoza	MPZ 2020/510	La Osqueta
Fig. 20E	<i>Alveolina fusiformis</i>	I 20	A 43	Instituto Geológico y Minero de España (IGME)		Isuela / Arguis*
Fig. 20F	<i>Alveolina fusiformis</i>	I 22	A 46	Instituto Geológico y Minero de España (IGME)		Isuela / Arguis*
Fig. 20G	<i>Alveolina fusiformis</i>	P 12	Pe-19	Natural Science Museum of the University of Zaragoza	MPZ 2020/514	La Peña
Fig. 20H	<i>Alveolina fusiformis</i>	Lassere, Bastennes (Hottinger, 1974)	Plate 52.5			
Fig. 20I	<i>Alveolina fusiformis</i>	Brassempouy, Bastennes	Plate 52.2			
Fig. 20J	<i>Alveolina fusiformis</i>	Brassempouy, Bastennes	Plate 52.3			
Fig. 20K	<i>Alveolina fusiformis</i>	Lassere, Bastennes (Hottinger, 1974)	Plate 52.4			
Fig. 20L	<i>Alveolina fusiformis</i>	Lassere, Bastennes (Hottinger, 1974)	Plate 52.6			
Fig. 20M	<i>Alveolina fusiformis</i>	E 52	Es-52	Natural Science Museum of the University of Zaragoza	MPZ 2020/492	La Foz de Escatele
Fig. 20N	<i>Alveolina aff. fragilis</i>	P 32	P-33	Natural Science Museum of the University of Zaragoza	MPZ 2020/519	La Peña
Fig. 20O	<i>Alveolina aff. fragilis</i>	SF 6	SF-8	Natural Science Museum of the University of Zaragoza	MPZ 2020/544	San Felices
Fig. 20P	<i>Alveolina aff. fragilis</i>	E 15	Es2-16	Natural Science Museum of the University of Zaragoza	MPZ 2020/485	La Foz de Escatele
Fig. 20Q	<i>Alveolina aff. elongata</i>	SC 53	Sc-40	Natural Science Museum of the University of Zaragoza	MPZ 2020/542	Sierra Caballera
Fig. 20R	<i>Alveolina aff. elongata</i>	SF 6	SF-8	Natural Science Museum of the University of Zaragoza	MPZ 2020/543	San Felices
Fig. 20S	<i>Alveolina aff. elongata</i>	V 10	Vi-11	Natural Science Museum of the University of Zaragoza	MPZ 2020/546	Villalangua
Fig. 20T	<i>Alveolina aff. elongata</i>	O 3	O5-4	Natural Science Museum of the University of Zaragoza	MPZ 2020/509	La Osqueta
Fig. 21A	<i>Spiralina austriaca</i>	I 23	A 47	Instituto Geológico y Minero de España (IGME)		Isuela / Arguis*
Fig. 21B	<i>Spiralina austriaca</i>	G 50	L 126	Instituto Geológico y Minero de España (IGME)		Gabardiella / Lusera*
Fig. 21C	<i>Sivasina egribucakensis</i>	G 27	L 88	Instituto Geológico y Minero de España (IGME)		Gabardiella / Lusera*

## APPENDIX I. Continued.

Specimen	Species	Sample name in this work	Sample name in the repository	Repository	Catalogue numbers	Stratigraphic Section
Fig. 21D	<i>Penarchaia</i> sp.	G 28	L 91	Instituto Geológico y Minero de España (IGME)		Gabardiella / Lusera*
Fig. 21E	<i>Penarchaia</i> sp.	G 37	L 107	Instituto Geológico y Minero de España (IGME)		Gabardiella / Lusera*
Fig. 21F	<i>Penarchaia</i> sp.	G 42	L 117	Instituto Geológico y Minero de España (IGME)		Gabardiella / Lusera*
Fig. 21G	<i>Penarchaia</i> sp.	G 43	L 118	Instituto Geológico y Minero de España (IGME)		Gabardiella / Lusera*
Fig. 21H	<i>Orbitalites complanatus</i>	G 25	L 83	Instituto Geológico y Minero de España (IGME)		Gabardiella / Lusera*
Fig. 21I	<i>Orbitalites complanatus</i>	I 50	A 87	Instituto Geológico y Minero de España (IGME)		Isuela / Arguis*
Fig. 21J	<i>Orbitalites minimus</i>	P 5	Pe-10b	Natural Science Museum of the University of Zaragoza	MPZ 2020/521	La Peña
Fig. 21K	<i>Orbitalites minimus</i>	E 21	Es-16	Natural Science Museum of the University of Zaragoza	MPZ 2020/487	La Foz de Escalate
Fig. 21L	<i>Orbitalites complanatus</i>	SC 23	Sc-5	Natural Science Museum of the University of Zaragoza	MPZ 2020/532	Sierra Caballera
Fig. 21M	<i>Orbitalites complanatus</i>	G 30	L 96	Instituto Geológico y Minero de España (IGME)		Gabardiella / Lusera*
Fig. 21N	<i>Orbitalites catentinensis</i>	SC 30	Sc-13	Natural Science Museum of the University of Zaragoza	MPZ 2020/534	Sierra Caballera
Fig. 22A	<i>Haddonia heissigi</i>	I 37	A 69	Instituto Geológico y Minero de España (IGME)		Isuela / Arguis*
Fig. 22B	<i>Haddonia heissigi</i>	I 37	A 69	Instituto Geológico y Minero de España (IGME)		Isuela / Arguis*
Fig. 22C	<i>Haddonia heissigi</i>	G 6	L 41	Instituto Geológico y Minero de España (IGME)		Gabardiella / Lusera*
Fig. 22D	<i>Coskinalina cf. perpera</i>	G 2	L 23	Instituto Geológico y Minero de España (IGME)		Gabardiella / Lusera*
Fig. 22E	<i>Coskinalina cf. perpera</i>	G 1	L 21	Instituto Geológico y Minero de España (IGME)		Gabardiella / Lusera*
Fig. 22F	<i>Coskinalina roberti</i>	I 28	A 52	Instituto Geológico y Minero de España (IGME)		Isuela / Arguis*
Fig. 22G	<i>Coskinalina roberti</i>	I 31	A 55	Instituto Geológico y Minero de España (IGME)		Isuela / Arguis*
Fig. 22H	<i>Coskinalina roberti</i>	I 31	A 55	Instituto Geológico y Minero de España (IGME)		Isuela / Arguis*
Fig. 22I	<i>Coskinalina roberti</i>	I 24	A 48	Instituto Geológico y Minero de España (IGME)		Isuela / Arguis*
Fig. 22J	<i>Coskinalina roberti</i>	I 33	A 58	Instituto Geológico y Minero de España (IGME)		Isuela / Arguis*
Fig. 22K	<i>Coskinalina roberti</i>	I 50	A 86	Instituto Geológico y Minero de España (IGME)		Isuela / Arguis*
Fig. 22L	<i>Coskinalina roberti</i>	I 41	A 73	Instituto Geológico y Minero de España (IGME)		Isuela / Arguis*
Fig. 22M	<i>Coskinalina roberti</i>	I 38	A 70	Instituto Geológico y Minero de España (IGME)		Isuela / Arguis*
Fig. 22N	<i>Coskinalina roberti</i>	I 48	A 82	Instituto Geológico y Minero de España (IGME)		Isuela / Arguis*
Fig. 22O	<i>Coskinalina roberti</i>	I 42	A 74	Instituto Geológico y Minero de España (IGME)		Isuela / Arguis*
Fig. 22P	<i>Coskinalina roberti</i>	I 45	A 78	Instituto Geológico y Minero de España (IGME)		Isuela / Arguis*
Fig. 22Q	<i>Coskinalina roberti</i>	P 10	Pe-17	Natural Science Museum of the University of Zaragoza	MPZ 2020/513	La Peña
Fig. 22R	<i>Coskinalina roberti</i>	I 50	A 86	Instituto Geológico y Minero de España (IGME)		Isuela / Arguis*
Fig. 22S	<i>Coskinalina roberti</i>	I 45	A 78	Instituto Geológico y Minero de España (IGME)		Isuela / Arguis*
Fig. 22T	<i>Coskinalina roberti</i>	I 42	A 74	Instituto Geológico y Minero de España (IGME)		Isuela / Arguis*

## APPENDIX I. Continued.

Specimen	Species	Sample name in this work	Sample name in the repository	Repository	Catalogue numbers	Stratigraphic Section
Fig. 23A	Gavelinellidae indet.	G 40	L 112	Instituto Geológico y Minero de España (IGME)		Gabardiella / Lusera*
Fig. 23B	Gavelinellidae indet.	G 39	L 111	Instituto Geológico y Minero de España (IGME)		Gabardiella / Lusera*
Fig. 23C	Gavelinellidae indet.	G 40	L 112	Instituto Geológico y Minero de España (IGME)		Gabardiella / Lusera*
Fig. 23D	Gavelinellidae indet.	G 40	L 112	Instituto Geológico y Minero de España (IGME)		Gabardiella / Lusera*
Fig. 23E	Gavelinellidae indet.	G 38	L 110	Instituto Geológico y Minero de España (IGME)		Gabardiella / Lusera*
Fig. 23F	Gavelinellidae indet.	G 39	L 111	Instituto Geológico y Minero de España (IGME)		Gabardiella / Lusera*
Fig. 23G	<i>Fabiania cassis</i>	E 41	Es-39	Natural Science Museum of the University of Zaragoza	MPZ 2020/491	La Foz de Escalete
Fig. 23H	<i>Fabiania cassis</i>	I 33	A 58	Instituto Geológico y Minero de España (IGME)		Isuela / Arguis*
Fig. 23I	<i>Fabiania cassis</i>	G 33	L 102	Instituto Geológico y Minero de España (IGME)		Gabardiella / Lusera*
Fig. 23J	<i>Fabiania cassis</i>	G 36	L 105	Instituto Geológico y Minero de España (IGME)		Gabardiella / Lusera*
Fig. 23K	<i>Halkyardia minima</i>	G 67	L 152	Instituto Geológico y Minero de España (IGME)		Gabardiella / Lusera*
Fig. 23L	<i>Halkyardia minima</i>	G 62	L 147	Instituto Geológico y Minero de España (IGME)		Gabardiella / Lusera*
Fig. 23M	<i>Halkyardia minima</i>	SC 19	SC2-26	Natural Science Museum of the University of Zaragoza	MPZ 2020/529	Sierra Caballera
Fig. 23N	<i>Halkyardia minima</i>	G 48	L 123	Instituto Geológico y Minero de España (IGME)		Gabardiella / Lusera*
Fig. 24A	<i>Gyroidinella levis</i>	SC 1	SC2-2b	Natural Science Museum of the University of Zaragoza	MPZ 2020/524	Sierra Caballera
Fig. 24B	<i>Gyroidinella levis</i>	G 7	L 44	Instituto Geológico y Minero de España (IGME)		Gabardiella / Lusera*
Fig. 24C	<i>Gyroidinella levis</i>	I 4	A 5	Instituto Geológico y Minero de España (IGME)		Isuela / Arguis*
Fig. 24D	<i>Gyroidinella eoacaenica</i>	G 36	L 105	Instituto Geológico y Minero de España (IGME)		Gabardiella / Lusera*
Fig. 24E	<i>Gyroidinella eoacaenica</i>	G 36	L 105	Instituto Geológico y Minero de España (IGME)		Gabardiella / Lusera*
Fig. 24F	<i>Gyroidinella eoacaenica</i>	G 33	L 102	Instituto Geológico y Minero de España (IGME)		Gabardiella / Lusera*
Fig. 24G	<i>Gyroidinella magna</i>	G 45	L 120	Instituto Geológico y Minero de España (IGME)		Gabardiella / Lusera*
Fig. 24H	<i>Gyroidinella magna</i>	G 23	L 81	Instituto Geológico y Minero de España (IGME)		Gabardiella / Lusera*
Fig. 24I	<i>Gyroidinella magna</i>	G 58	L 139	Instituto Geológico y Minero de España (IGME)		Gabardiella / Lusera*
Fig. 24J	<i>Gyroidinella magna</i>	V 8	Vi-9	Natural Science Museum of the University of Zaragoza	MPZ 2020/550	Villalangua
Fig. 24K	<i>Gyroidinella magna</i>	G 23	L 81	Instituto Geológico y Minero de España (IGME)		Gabardiella / Lusera*
Fig. 24L	<i>Gyroidinella magna</i>	G 26	L 85	Instituto Geológico y Minero de España (IGME)		Gabardiella / Lusera*
Fig. 24M	<i>Gyroidinella magna</i>	G 24	L 82	Instituto Geológico y Minero de España (IGME)		Gabardiella / Lusera*
Fig. 24N	<i>Karobkovella grosserugosa</i>	SC 53	SC-40	Natural Science Museum of the University of Zaragoza	MPZ 2020/541	Sierra Caballera
Fig. 24O	<i>Karobkovella grosserugosa</i>	G 71	L 156	Instituto Geológico y Minero de España (IGME)		Gabardiella / Lusera*
Fig. 24P	<i>Karobkovella grosserugosa</i>	SC 53	SC-40	Natural Science Museum of the University of Zaragoza	MPZ 2020/540	Sierra Caballera
Fig. 24Q	<i>Victoriella conoidea</i>	I 54	A 95	Instituto Geológico y Minero de España (IGME)		Isuela / Arguis*

## APPENDIX I. Continued.

Specimen	Species	Sample name in this work	Sample name in the repository	Repository	Catalogue numbers	Stratigraphic Section
Fig. 24R	<i>Korabkovella grosserugosa</i>	G 39	L 111	Instituto Geológico y Minero de España (IGME)		Gabardiella / Lusera*
Fig. 24S	<i>Korabkovella grosserugosa</i>	SC 53	Sc-40	Natural Science Museum of the University of Zaragoza	MPZ 2020/539	Sierra Caballera
Fig. 25A	<i>Solenomeris cf. agormani</i>	G 50	L 126	Instituto Geológico y Minero de España (IGME)		Gabardiella / Lusera*
Fig. 25B	<i>Solenomeris cf. agormani</i>	I 33	A 58	Instituto Geológico y Minero de España (IGME)		Isuela / Arguis*
Fig. 25C	<i>Solenomeris cf. agormani</i>	V 10	Vi-11	Natural Science Museum of the University of Zaragoza	MPZ 2020/545	Villalangua
Fig. 25D	<i>"Gypsina" moussaviani</i>	G 38	L 110	Instituto Geológico y Minero de España (IGME)		Gabardiella / Lusera*
Fig. 25E	<i>"Gypsina" moussaviani</i>	I 47	A 81	Instituto Geológico y Minero de España (IGME)		Isuela / Arguis*
Fig. 25F	<i>"Gypsina" moussaviani</i>	G 50	L 126	Instituto Geológico y Minero de España (IGME)		Gabardiella / Lusera*
Fig. 25G	<i>"Gypsina" moussaviani</i>	G 30	L 96	Instituto Geológico y Minero de España (IGME)		Gabardiella / Lusera*
Fig. 25H	<i>Sphaerogypsina globulus</i>	P 25	P-19	Instituto Geológico y Minero de España (IGME)		La Peña
Fig. 25I	<i>Sphaerogypsina globulus</i>	G 59	L 140	Natural Science Museum of the University of Zaragoza	MPZ 2020/517	Gabardiella / Lusera*
Fig. 25J	<i>Asterigerina ratula</i>	SC 19	Sc2-26	Natural Science Museum of the University of Zaragoza	MPZ 2020/528	Sierra Caballera
Fig. 25K	<i>Asterigerina ratula</i>	SC 19	Sc2-26	Natural Science Museum of the University of Zaragoza	MPZ 2020/527	Sierra Caballera
Fig. 25L	<i>Asterigerina ratula</i>	SC 1	Sc2-2b	Natural Science Museum of the University of Zaragoza	MPZ 2020/523	Sierra Caballera
Fig. 25M	<i>Asterigerina ratula</i>	SC 16	Sc2-22c (lámina delgada)	Natural Science Museum of the University of Zaragoza	MPZ 2020/526	Sierra Caballera
Fig. 25N	<i>Asterigerina ratula</i>	G 41	L 116	Instituto Geológico y Minero de España (IGME)		Gabardiella / Lusera*
Fig. 25O	<i>Asterigerina ratula</i>	G 41	L 116	Instituto Geológico y Minero de España (IGME)		Gabardiella / Lusera*
Fig. 25P	<i>Planolindrina ?</i>	G 69	L 154	Instituto Geológico y Minero de España (IGME)		Gabardiella / Lusera*
Fig. 25Q	<i>Linderina cf. brugesi</i>	SC 40	Sc-23	Natural Science Museum of the University of Zaragoza	MPZ 2020/536	Sierra Caballera
Fig. 25R	<i>Linderina cf. brugesi</i>	G 48	L 123	Instituto Geológico y Minero de España (IGME)		Gabardiella / Lusera*
Fig. 25S	<i>Linderina cf. brugesi</i>	G 64	L 149	Instituto Geológico y Minero de España (IGME)		Gabardiella / Lusera*
Fig. 25T	<i>Planolindrina ?</i>	G 62	L 147	Instituto Geológico y Minero de España (IGME)		Gabardiella / Lusera*
Fig. 25U	<i>Planolindrina ?</i>	I 38	A 70	Instituto Geológico y Minero de España (IGME)		Isuela / Arguis*
Fig. 25V	<i>Rotarbinella hersoni</i>	G 71	L 156	Instituto Geológico y Minero de España (IGME)		Gabardiella / Lusera*
Fig. 25W	<i>Chapmanina gassinensis</i>	SC 23	Sc-5 (lámina delgada)	Natural Science Museum of the University of Zaragoza	MPZ 2020/531	Sierra Caballera
Fig. 26A	<i>Rotalia trochialiformis</i>	I 4	A 5	Instituto Geológico y Minero de España (IGME)		Isuela / Arguis*
Fig. 26B	<i>Rotalia trochialiformis</i>	SC 1	Sc2-2b	Natural Science Museum of the University of Zaragoza	MPZ 2020/522	Sierra Caballera
Fig. 26C	<i>Rotalia trochialiformis</i>	SC 32	Sc-15	Natural Science Museum of the University of Zaragoza	MPZ 2020/535	Sierra Caballera
Fig. 26D	<i>Rotalia trochialiformis</i>	I 51	A 88	Instituto Geológico y Minero de España (IGME)		Isuela / Arguis*
Fig. 26E	<i>Rotalia trochialiformis</i>	G 48	L 123	Instituto Geológico y Minero de España (IGME)		Gabardiella / Lusera*
Fig. 26F	<i>Rotalia trochialiformis</i>	I 54	A 95	Instituto Geológico y Minero de España (IGME)		Isuela / Arguis*

## APPENDIX I. Continued.

Specimen	Species	Sample name in this work	Sample name in the repository	Repository	Catalogue numbers	Stratigraphic Section
Fig. 26G	<i>Rotalia trochialiformis</i>	G 23	L 81	Instituto Geológico y Minero de España (IGME)		Gabardiella / Lusera*
Fig. 26H	<i>Medocia blayensis</i>	G 58	L 139	Instituto Geológico y Minero de España (IGME)		Gabardiella / Lusera*
Fig. 26I	<i>Medocia blayensis</i>	G 60	L 141	Instituto Geológico y Minero de España (IGME)		Gabardiella / Lusera*
Fig. 26J	<i>Medocia blayensis</i>	150	A 88	Instituto Geológico y Minero de España (IGME)		Isuela / Arguis*
Fig. 26K	<i>Medocia blayensis</i>	150	A 87	Instituto Geológico y Minero de España (IGME)		Isuela / Arguis*
Fig. 26L	<i>Medocia blayensis</i>	150	A 86	Instituto Geológico y Minero de España (IGME)		Isuela / Arguis*
Fig. 26M	<i>Medocia blayensis</i>	G 16	L 60	Instituto Geológico y Minero de España (IGME)		Gabardiella / Lusera*
Fig. 26N	<i>Medocia blayensis</i>	150	A 86	Instituto Geológico y Minero de España (IGME)		Isuela / Arguis*
Fig. 26O	<i>Medocia blayensis</i>	150	A 86	Instituto Geológico y Minero de España (IGME)		Isuela / Arguis*
Fig. 26P	<i>Medocia blayensis</i>	112	A 26	Instituto Geológico y Minero de España (IGME)		Isuela / Arguis*
Fig. 26Q	<i>Neorotalia lithamnica</i>	G 3	L 36	Instituto Geológico y Minero de España (IGME)		Isuela / Arguis*
Fig. 26R	<i>Neorotalia lithamnica</i>	12	A 2	Instituto Geológico y Minero de España (IGME)		Gabardiella / Lusera*
Fig. 26S	<i>Neorotalia lithamnica</i>	G 19	L 68	Instituto Geológico y Minero de España (IGME)		Isuela / Arguis*
Fig. 27A	<i>Assilina spira abarardi</i>	G 5	L 38	Instituto Geológico y Minero de España (IGME)		Gabardiella / Lusera*
Fig. 27B	<i>Assilina spira abarardi</i>	G 5	L 38	Instituto Geológico y Minero de España (IGME)		Gabardiella / Lusera*
Fig. 27C	<i>Assilina spira abarardi</i>	G 5	L 38	Instituto Geológico y Minero de España (IGME)		Gabardiella / Lusera*
Fig. 27D	<i>Assilina spira abarardi</i>	G 5	L 38	Instituto Geológico y Minero de España (IGME)		Gabardiella / Lusera*
Fig. 27E	<i>Assilina spira abarardi</i>	G 5	L 38	Instituto Geológico y Minero de España (IGME)		Gabardiella / Lusera*
Fig. 27F	<i>Assilina spira abarardi</i>	G 5	L 38	Instituto Geológico y Minero de España (IGME)		Gabardiella / Lusera*
Fig. 27G	<i>Assilina spira abarardi</i>	G 5	L 38	Instituto Geológico y Minero de España (IGME)		Gabardiella / Lusera*
Fig. 27H	<i>Assilina spira abarardi</i>	G 5	L 38	Instituto Geológico y Minero de España (IGME)		Gabardiella / Lusera*
Fig. 27I	<i>Assilina spira abarardi</i>	G 5	L 38	Instituto Geológico y Minero de España (IGME)		Gabardiella / Lusera*
Fig. 27J	<i>Assilina spira abarardi</i>	G 5	L 38	Instituto Geológico y Minero de España (IGME)		Gabardiella / Lusera*
Fig. 27K	<i>Assilina spira abarardi</i>	G 5	L 38	Instituto Geológico y Minero de España (IGME)		Gabardiella / Lusera*
Fig. 27L	<i>Assilina spira abarardi</i>	G 5	L 38	Instituto Geológico y Minero de España (IGME)		Gabardiella / Lusera*
Fig. 28A	<i>Nummulites lehnerei</i>	G 5	L 38	Instituto Geológico y Minero de España (IGME)		Gabardiella / Lusera*
Fig. 28A'	<i>Nummulites beneharnensis</i>	118	A 41	Instituto Geológico y Minero de España (IGME)		Isuela / Arguis*
Fig. 28B	<i>Nummulites lehnerei</i>	G 5	L 38	Instituto Geológico y Minero de España (IGME)		Gabardiella / Lusera*
Fig. 28B'	<i>Nummulites beneharnensis</i>	118	A 41	Instituto Geológico y Minero de España (IGME)		Isuela / Arguis*
Fig. 28C	<i>Nummulites lehnerei</i>	G 5	L 38	Instituto Geológico y Minero de España (IGME)		Gabardiella / Lusera*
Fig. 28C'	<i>Nummulites crassus</i>	SM 4	SM-6	Serra-Kiel collection. Department of Earth and Ocean Dynamics, University of Barcelona (UB)		Santa Marina

## APPENDIX I. Continued.

Specimen	Species	Sample name in this work	Sample name in the repository	Repository	Catalogue numbers	Stratigraphic Section
Fig. 28D	<i>Nummulites lehneri</i>	G 5	L 38	Instituto Geológico y Minero de España (IGME)		Gabardella / Lusera*
Fig. 28D'	<i>Nummulites crassus</i>	SM 4	SM-6	Serra-Kiel collection. Department of Earth and Ocean Dynamics, University of Barcelona (UB)		Santa Marina
Fig. 28E	<i>Nummulites lehneri</i>	G 5	L 38	Instituto Geológico y Minero de España (IGME)		Gabardella / Lusera*
Fig. 28E'	<i>Nummulites crassus</i>	SM 4	SM-6	Serra-Kiel collection. Department of Earth and Ocean Dynamics, University of Barcelona (UB)		Santa Marina
Fig. 28F	<i>Nummulites lehneri</i>	G 5	L 38	Instituto Geológico y Minero de España (IGME)		Gabardella / Lusera*
Fig. 28F'/Fig. 33K	<i>Nummulites crassus</i>	SM 4	SM-6	Serra-Kiel collection. Department of Earth and Ocean Dynamics, University of Barcelona (UB)		Santa Marina
Fig. 28G	<i>Nummulites lehneri</i>	G 5	L 38	Instituto Geológico y Minero de España (IGME)		Gabardella / Lusera*
Fig. 28G'	<i>Nummulites crassus</i>	SM 4	SM-6	Serra-Kiel collection. Department of Earth and Ocean Dynamics, University of Barcelona (UB)		Santa Marina
Fig. 28H	<i>Nummulites lehneri</i>	G 5	L 38	Instituto Geológico y Minero de España (IGME)		Gabardella / Lusera*
Fig. 28H'/Fig. 33L	<i>Nummulites crassus</i>	SM 4	SM-6	Serra-Kiel collection. Department of Earth and Ocean Dynamics, University of Barcelona (UB)		Santa Marina
Fig. 28I	<i>Nummulites lehneri</i>	G 5	L 38	Instituto Geológico y Minero de España (IGME)		Gabardella / Lusera*
Fig. 28I'	<i>Nummulites crassus</i>	SM 4	SM-6	Serra-Kiel collection. Department of Earth and Ocean Dynamics, University of Barcelona (UB)		Santa Marina
Fig. 28J	<i>Nummulites lehneri</i>	G 5	L 38	Instituto Geológico y Minero de España (IGME)		Gabardella / Lusera*
Fig. 28J'	<i>Nummulites crassus</i>	SM 4	SM-6	Serra-Kiel collection. Department of Earth and Ocean Dynamics, University of Barcelona (UB)		Santa Marina
Fig. 28K	<i>Nummulites lehneri</i>	G 5	L 38	Instituto Geológico y Minero de España (IGME)		Santa Marina
Fig. 28K'	<i>Nummulites crassus</i>	SM 4	SM-6	Serra-Kiel collection. Department of Earth and Ocean Dynamics, University of Barcelona (UB)		Gabardella / Lusera*
Fig. 28L	<i>Nummulites lehneri</i>	G 5	L 38	Instituto Geológico y Minero de España (IGME)		Santa Marina
Fig. 28L'/Fig. 33M	<i>Nummulites crassus</i>	SM 4	SM-6	Serra-Kiel collection. Department of Earth and Ocean Dynamics, University of Barcelona (UB)		Gabardella / Lusera*
Fig. 28M/ Fig. 33E	<i>Nummulites aspermontis</i>	I 8	A 11	Instituto Geológico y Minero de España (IGME)		Isuela / Arguis*
Fig. 28M'/ Fig. 33N	<i>Nummulites taverletensis</i>	SM 4	SM-6	Serra-Kiel collection. Department of Earth and Ocean Dynamics, University of Barcelona (UB)		Santa Marina
Fig. 28N	<i>Nummulites aspermontis</i>	I 8	A 11	Instituto Geológico y Minero de España (IGME)		Isuela / Arguis*
Fig. 28N'	<i>Nummulites taverletensis</i>	SM 4	SM-6	Serra-Kiel collection. Department of Earth and Ocean Dynamics, University of Barcelona (UB)		Santa Marina
Fig. 28O	<i>Nummulites aspermontis</i>	I 8	A 11	Instituto Geológico y Minero de España (IGME)		Isuela / Arguis*
Fig. 28O'/ Fig. 33Q	<i>Nummulites taverletensis</i>	SM 4	SM-6	Serra-Kiel collection. Department of Earth and Ocean Dynamics, University of Barcelona (UB)		Santa Marina
Fig. 28P	<i>Nummulites aspermontis</i>	I 8	A 11	Instituto Geológico y Minero de España (IGME)		Isuela / Arguis*
Fig. 28P'	<i>Nummulites taverletensis</i>	SM 4	SM-6	Serra-Kiel collection. Department of Earth and Ocean Dynamics, University of Barcelona (UB)		Santa Marina
Fig. 28Q	<i>Nummulites aspermontis</i>	I 8	A 11	Instituto Geológico y Minero de España (IGME)		Isuela / Arguis*
Fig. 28Q'/ Fig. 33O	<i>Nummulites taverletensis</i>	SM 4	SM-6	Serra-Kiel collection. Department of Earth and Ocean Dynamics, University of Barcelona (UB)		Santa Marina
Fig. 28R'	<i>Nummulites aturicus</i>	SC 39	Sc-N1	Serra-Kiel collection. Department of Earth and Ocean Dynamics, University of Barcelona (UB)		Sierra Caballera
Fig. 28R'/ Fig. 33D	<i>Nummulites aspermontis</i>	I 8	A 11	Instituto Geológico y Minero de España (IGME)		Isuela / Arguis*
Fig. 28S	<i>Nummulites aspermontis</i>	I 8	A 11	Instituto Geológico y Minero de España (IGME)		Isuela / Arguis*

## APPENDIX I. Continued.

Specimen	Species	Sample name in this work	Sample name in the repository	Repository	Catalogue numbers	Stratigraphic Section
Fig. 285'	<i>Nummulites aturicus</i>	SC 39	Sc-N1	Serra-Kiel collection. Department of Earth and Ocean Dynamics, University of Barcelona (UB)		Sierra Caballera
Fig. 28T	<i>Nummulites aspermontis</i>	I 8	A 11	Instituto Geológico y Minero de España (IGME)		Isuela / Arguis*
Fig. 28T'/Fig. 33Y	<i>Nummulites aturicus</i>	SC 39	Sc-N1	Serra-Kiel collection. Department of Earth and Ocean Dynamics, University of Barcelona (UB)		Sierra Caballera
Fig. 28U	<i>Nummulites aspermontis</i>	I 8	A 11	Instituto Geológico y Minero de España (IGME)		Isuela / Arguis*
Fig. 28U'	<i>Nummulites aturicus</i>	SC 50	Sc-36	Serra-Kiel collection. Department of Earth and Ocean Dynamics, University of Barcelona (UB)		Sierra Caballera
Fig. 28V	<i>Nummulites benehamensis</i>	I 18	A 41	Instituto Geológico y Minero de España (IGME)		Isuela / Arguis*
Fig. 28V'	<i>Nummulites aturicus</i>	SC 50	Sc-36	Serra-Kiel collection. Department of Earth and Ocean Dynamics, University of Barcelona (UB)		Sierra Caballera
Fig. 28W	<i>Nummulites benehamensis</i>	I 18	A 41	Instituto Geológico y Minero de España (IGME)		Isuela / Arguis*
Fig. 28W'	<i>Nummulites aturicus</i>	SC 39	Sc-N1	Serra-Kiel collection. Department of Earth and Ocean Dynamics, University of Barcelona (UB)		Sierra Caballera
Fig. 28X	<i>Nummulites benehamensis</i>	I 18	A 41	Instituto Geológico y Minero de España (IGME)		Isuela / Arguis*
Fig. 28X'	<i>Nummulites aturicus</i>	SC 50	Sc-36	Serra-Kiel collection. Department of Earth and Ocean Dynamics, University of Barcelona (UB)		Sierra Caballera
Fig. 28Y	<i>Nummulites benehamensis</i>	I 18	A 41	Instituto Geológico y Minero de España (IGME)		Isuela / Arguis*
Fig. 28Z	<i>Nummulites benehamensis</i>	I 18	A 41	Instituto Geológico y Minero de España (IGME)		Isuela / Arguis*
Fig. 28Z'	<i>Nummulites aturicus</i>	SC 50	Sc-36	Serra-Kiel collection. Department of Earth and Ocean Dynamics, University of Barcelona (UB)		Sierra Caballera
Fig. 29A'/Fig. 33G'	<i>Nummulites perforatus</i>	SM 6	SM-7	Serra-Kiel collection. Department of Earth and Ocean Dynamics, University of Barcelona (UB)		Santa Marina
Fig. 29A'/Fig. 33R	<i>Nummulites aff. deshayesi</i>	I 52	A 91	Instituto Geológico y Minero de España (IGME)		Isuela / Arguis*
Fig. 29B	<i>Nummulites aff. deshayesi</i>	I 52	A 91	Instituto Geológico y Minero de España (IGME)		Isuela / Arguis*
Fig. 29B'/Fig. 33E'	<i>Nummulites perforatus</i>	SM 6	SM-7	Serra-Kiel collection. Department of Earth and Ocean Dynamics, University of Barcelona (UB)		Santa Marina
Fig. 29C'	<i>Nummulites perforatus</i>	SM 6	SM-7	Serra-Kiel collection. Department of Earth and Ocean Dynamics, University of Barcelona (UB)		Santa Marina
Fig. 29C'/Fig. 33S	<i>Nummulites aff. deshayesi</i>	I 52	A 91	Instituto Geológico y Minero de España (IGME)		Isuela / Arguis*
Fig. 29D'	<i>Nummulites perforatus</i>	SM 6	SM-7	Serra-Kiel collection. Department of Earth and Ocean Dynamics, University of Barcelona (UB)		Santa Marina
Fig. 29D'/Fig. 33U	<i>Nummulites aff. deshayesi</i>	I 52	A 91	Instituto Geológico y Minero de España (IGME)		Isuela / Arguis*
Fig. 29E	<i>Nummulites aff. deshayesi</i>	E 30	Es-27	Serra-Kiel collection. Department of Earth and Ocean Dynamics, University of Barcelona (UB)		La Foz de Escalate
Fig. 29F	<i>Nummulites aff. deshayesi</i>	E 30	Es-27	Serra-Kiel collection. Department of Earth and Ocean Dynamics, University of Barcelona (UB)		La Foz de Escalate
Fig. 29G	<i>Nummulites aff. deshayesi</i>	SC 38	Sc-21	Serra-Kiel collection. Department of Earth and Ocean Dynamics, University of Barcelona (UB)		Sierra Caballera
Fig. 29H	<i>Nummulites aff. deshayesi</i>	E 30	Es-27	Serra-Kiel collection. Department of Earth and Ocean Dynamics, University of Barcelona (UB)		La Foz de Escalate
Fig. 29I	<i>Nummulites aff. deshayesi</i>	E 30	Es-27	Serra-Kiel collection. Department of Earth and Ocean Dynamics, University of Barcelona (UB)		La Foz de Escalate
Fig. 29J	<i>Nummulites aff. deshayesi</i>	E 30	Es-27	Serra-Kiel collection. Department of Earth and Ocean Dynamics, University of Barcelona (UB)		La Foz de Escalate
Fig. 29K	<i>Nummulites aff. deshayesi</i>	E 30	Es-27	Serra-Kiel collection. Department of Earth and Ocean Dynamics, University of Barcelona (UB)		La Foz de Escalate
Fig. 29L	<i>Nummulites aff. deshayesi</i>	SC 38	Sc-21	Serra-Kiel collection. Department of Earth and Ocean Dynamics, University of Barcelona (UB)		Sierra Caballera
Fig. 29M'/Fig. 33Z	<i>Nummulites deshayesi</i>	I 54	A 95	Instituto Geológico y Minero de España (IGME)		Isuela / Arguis*
Fig. 29N	<i>Nummulites deshayesi</i>	SC 50	Sc-36	Serra-Kiel collection. Department of Earth and Ocean Dynamics, University of Barcelona (UB)		Sierra Caballera

## APPENDIX I. Continued.

Specimen	Species	Sample name in this work	Sample name in the repository	Repository	Catalogue numbers	Stratigraphic Section
Fig. 290/Fig. 33B'	<i>Nummulites deshayesi</i>	I 54	A 95	Instituto Geológico y Minero de España (IGME)		Isuela / Arguis*
Fig. 29P/Fig. 33A'	<i>Nummulites deshayesi</i>	I 54	A 95	Instituto Geológico y Minero de España (IGME)		Isuela / Arguis*
Fig. 29Q	<i>Nummulites deshayesi</i>	SC 50	Sc-36	Serra-Kiel collection. Department of Earth and Ocean Dynamics, University of Barcelona (UB)		Sierra Caballera
Fig. 29R	<i>Nummulites deshayesi</i>	SC 50	Sc-36	Serra-Kiel collection. Department of Earth and Ocean Dynamics, University of Barcelona (UB)		Sierra Caballera
Fig. 29S	<i>Nummulites deshayesi</i>	SM 5	SM-5	Serra-Kiel collection. Department of Earth and Ocean Dynamics, University of Barcelona (UB)		Santa Marina
Fig. 29T	<i>Nummulites deshayesi</i>	SC 50	Sc-36	Serra-Kiel collection. Department of Earth and Ocean Dynamics, University of Barcelona (UB)		Sierra Caballera
Fig. 29U	<i>Nummulites deshayesi</i>	SC 50	Sc-36	Serra-Kiel collection. Department of Earth and Ocean Dynamics, University of Barcelona (UB)		Sierra Caballera
Fig. 29V/Fig. 33D'	<i>Nummulites perforatus</i>	SM 6	SM-7	Serra-Kiel collection. Department of Earth and Ocean Dynamics, University of Barcelona (UB)		Santa Marina
Fig. 29W	<i>Nummulites perforatus</i>	SM 6	SM-7	Serra-Kiel collection. Department of Earth and Ocean Dynamics, University of Barcelona (UB)		Santa Marina
Fig. 29X/Fig. 33F'	<i>Nummulites perforatus</i>	SM 6	SM-7	Serra-Kiel collection. Department of Earth and Ocean Dynamics, University of Barcelona (UB)		Santa Marina
Fig. 29Y/Fig. 33H'	<i>Nummulites perforatus</i>	SM 6	SM-7	Serra-Kiel collection. Department of Earth and Ocean Dynamics, University of Barcelona (UB)		Santa Marina
Fig. 29Z	<i>Nummulites perforatus</i>	SM 6	SM-7	Serra-Kiel collection. Department of Earth and Ocean Dynamics, University of Barcelona (UB)		Santa Marina
Fig. 30A	<i>Nummulites bousiaci</i>	SM 2	SM-3	Serra-Kiel collection. Department of Earth and Ocean Dynamics, University of Barcelona (UB)		Santa Marina
Fig. 30B	<i>Nummulites bousiaci</i>	SM 2	SM-3	Serra-Kiel collection. Department of Earth and Ocean Dynamics, University of Barcelona (UB)		Santa Marina
Fig. 30C	<i>Nummulites bousiaci</i>	SM 2	SM-3	Serra-Kiel collection. Department of Earth and Ocean Dynamics, University of Barcelona (UB)		Santa Marina
Fig. 30D	<i>Nummulites aff. bullatus</i>	I 52	A 91	Instituto Geológico y Minero de España (IGME)		Santa Marina
Fig. 30E	<i>Nummulites aff. bullatus</i>	I 52	A 91	Instituto Geológico y Minero de España (IGME)		Isuela / Arguis*
Fig. 30F	<i>Nummulites aff. bullatus</i>	I 52	A 91	Instituto Geológico y Minero de España (IGME)		Isuela / Arguis*
Fig. 30G	<i>Nummulites migliurinus</i>	I 18	A 41	Instituto Geológico y Minero de España (IGME)		Isuela / Arguis*
Fig. 30H	<i>Nummulites migliurinus</i>	I 18	A 41	Instituto Geológico y Minero de España (IGME)		Isuela / Arguis*
Fig. 30I	<i>Nummulites praediscorbinus</i>	I 7	A 10	Instituto Geológico y Minero de España (IGME)		Isuela / Arguis*
Fig. 30J	<i>Nummulites praediscorbinus</i>	I 7	A 10	Instituto Geológico y Minero de España (IGME)		Isuela / Arguis*
Fig. 30K	<i>Nummulites praepuschi</i>	M 24	Mu-5	Natural Science Museum of the University of Zaragoza	MPZ 2020/504	Murillo de Gállego
Fig. 30L	<i>Nummulites praepuschi</i>	M 24	Mu-5	Natural Science Museum of the University of Zaragoza	MPZ 2020/503	Murillo de Gállego
Fig. 30M	<i>Nummulites praepuschi</i>	M 24	Mu-5	Natural Science Museum of the University of Zaragoza	MPZ 2020/502	Murillo de Gállego
Fig. 30N	<i>Nummulites praepuschi</i>	M 24	Mu-5	Natural Science Museum of the University of Zaragoza	MPZ 2020/501	Murillo de Gállego
Fig. 30O	<i>Nummulites praepuschi</i>	M 24	Mu-5	Natural Science Museum of the University of Zaragoza	MPZ 2020/500	Murillo de Gállego
Fig. 30P	<i>Nummulites praepuschi</i>	M 24	Mu-5	Natural Science Museum of the University of Zaragoza	MPZ 2020/499	Murillo de Gállego
Fig. 30Q	<i>Nummulites praepuschi</i>	M 24	Mu-5	Natural Science Museum of the University of Zaragoza	MPZ 2020/498	Murillo de Gállego
Fig. 30R	<i>Nummulites praepuschi</i>	M 24	Mu-5	Natural Science Museum of the University of Zaragoza	MPZ 2020/497	Murillo de Gállego
Fig. 30S	<i>Nummulites beaumonti</i>	E 40	Es-38	Natural Science Museum of the University of Zaragoza	MPZ 2020/489	La Foz de Escalate

## APPENDIX I. Continued.

Specimen	Species	Sample name in this work	Sample name in the repository	Repository	Catalogue numbers	Stratigraphic Section
Fig. 30T	<i>Nummulites beaumonti</i>	P 29	P-25	Natural Science Museum of the University of Zaragoza	MPZ 2020/518	La Peña
Fig. 30U	<i>Nummulites beaumonti</i>	I 50	A 86	Instituto Geológico y Minero de España (IGME)		Isuela / Arguis*
Fig. 30V	<i>Nummulites biarrizensis</i>	CF 5	CF-20	Natural Science Museum of the University of Zaragoza	MPZ 2020/484	Campo Fenero
Fig. 30W	<i>Nummulites biarrizensis</i>	CF 5	CF-20	Natural Science Museum of the University of Zaragoza	MPZ 2020/483	Campo Fenero
Fig. 33A	<i>N. beneharnensis</i>	I 18	A 41	Instituto Geológico y Minero de España (IGME)		Isuela / Arguis*
Fig. 33B	<i>N. beneharnensis</i>	I 18	A 41	Instituto Geológico y Minero de España (IGME)		Isuela / Arguis*
Fig. 33C	<i>N. beneharnensis</i>	I 18	A 41	Instituto Geológico y Minero de España (IGME)		Isuela / Arguis*
Fig. 33C'	<i>N. deshayesi</i>	I 54	A 95	Instituto Geológico y Minero de España (IGME)		Isuela / Arguis*
Fig. 33F	<i>N. aspermontis</i>	I 8	A 11	Instituto Geológico y Minero de España (IGME)		Isuela / Arguis*
Fig. 33G	<i>Nummulites lehneri</i>	G 5	L 38	Instituto Geológico y Minero de España (IGME)		Gabardiella / Lusera*
Fig. 33H	<i>Nummulites lehneri</i>	G 5	L 38	Instituto Geológico y Minero de España (IGME)		Gabardiella / Lusera*
Fig. 33I	<i>Nummulites lehneri</i>	G 5	L 38	Instituto Geológico y Minero de España (IGME)		Gabardiella / Lusera*
Fig. 33J	<i>N. crassus</i>	SM 4	SM-6	Serra-Kiel collection. Department of Earth and Ocean Dynamics, University of Barcelona (UB)		Santa Marina
Fig. 33P	<i>N. tovertetensis</i>	SM 4	SM-6	Serra-Kiel collection. Department of Earth and Ocean Dynamics, University of Barcelona (UB)		Santa Marina
Fig. 33T	<i>N. aff. deshayesi</i>	I 52	A 91	Instituto Geológico y Minero de España (IGME)		Isuela / Arguis*
Fig. 33V	<i>Nummulites aturicus</i>	SC 39	SC-N1	Serra-Kiel collection. Department of Earth and Ocean Dynamics, University of Barcelona (UB)		Sierra Caballera
Fig. 33W	<i>Nummulites aturicus</i>	SC 39	SC-N1	Serra-Kiel collection. Department of Earth and Ocean Dynamics, University of Barcelona (UB)		Sierra Caballera
Fig. 33X	<i>Nummulites aturicus</i>	SC 39	SC-N1	Serra-Kiel collection. Department of Earth and Ocean Dynamics, University of Barcelona (UB)		Sierra Caballera

\* Stratigraphic section names employed on the IGME repositories.

---

## APPENDIX II

---

### SYSTEMATICS OF LARGER BENTHIC FORAMINIFERA

**Phylum** Foraminifera EICHWALD, 1830

**Class** Tubothalamea PAWLOWSKI, HOLZMANN, JAROSLAW & TYSZKA, 2013

**Order** Miliolida DELAGE & HÉROUARD, 1896

**Superfamily** Milioloidea Ehrenberg, 1839

**Family** Hauerinidae Schwager, 1876

**Subfamily** Miliolinellinae Vella, 1957

GENUS *Idalina* SCHLUMBERGER & MUNIER-CHALMAS, 1884

Type species *Idalina antiqua* SCHLUMBERGER & MUNIER-CHALMAS, 1884

*Idalina berthelini* SCHLUMBERGER, 1905

*Idalina osquetaensis* n. sp. SERRA-KIEL & SILVA-CASAL

**Superfamily** Alveolinoidea EHRENBERG, 1839

**Family** Fabulariidae EHRENBERG, 1839

GENUS *Fabularia* DEFRANCE, 1820

Type species: *Fabularia discolites* DEFRANCE in BRONN, 1825

*Fabularia roselli* CAUS, 1979

*Fabularia ovata* de Roissy, 1805

GENUS *Pseudolacazina* CAUS, 1979

Type species: *Pseudolacazina hottingeri* CAUS, 1979

*Pseudolacazina hottingeri* CAUS, 1979

GENUS *Periloculina* MUNIER-CHALMAS & SCHLUMBERGER, 1885

Type species: *Periloculina zitteli* MUNIER-CHALMAS & SCHLUMBERGER, 1885

*Periloculina* cf. *raincourti* SCHLUMBERGER, 1905

**Family** Alveolinidae EHRENBERG, 1839

GENUS *Alveolina* D'ORBIGNY, 1826

Type species: *Oryzaria boscii* DeFrance in Bronn, 1825

*Alveolina ospiensis* DROBNE, 1977

*Alveolina decastroi* DI SCOTTO, 1966

*Alveolina cremae* CHECCHIA-RISPOLI, 1905

*Alveolina obtusa* MONTANARI, 1964

*Alveolina boscii* DEFRANCE, 1825

*Alveolina levantina* HOTTINGER, 1960

*Alveolina tenuis* HOTTINGER, 1960

*Alveolina callosa* HOTTINGER, 1960

*Alveolina stipes* HOTTINGER, 1960

*Alveolina munieri* HOTTINGER, 1960

*Alveolina fusiformis* SOWERBY, 1850

*Alveolina* aff. *fragilis* HOTTINGER, 1960

*Alveolina* aff. *elongata* D'ORBIGNY, 1828

**Family** Peneroplidae SCHULTZE, 1854

GENUS *Spirolina* LAMARCK, 1804

Type species: *Spirolina cylindracea* LAMARCK, 1804  
*Spirolina austriaca* D'ORBIGNY, 1834

GENUS *Sivasina* SIREL & ÖZGEN-ERDEM, 2013

Type species: *Sivasina egribucakensis* SIREL & ÖZGEN-ERDEM, 2013  
*Sivasina egribucakensis* SIREL & ÖZGEN-ERDEM, 2013

GENUS *Penarchaias* HOTTINGER, 2007

Type species: *Peneroplis glynnjonesi* HENSON, 1950  
*Penarchaias* sp.

**Family:** Soritidae EHRENBERG, 1839  
**Subfamily:** Soritinae EHRENBERG, 1839

GENUS *Orbitolites* LAMARCK, 1801

Type species: *Orbitolites complanatus* LAMARCK, 1801  
*Orbitolites minimus* HENSON, 1950  
*Orbitolites complanatus* LAMARCK, 1801  
*Orbitolites cotentinensis* LEHMANN, 1961

**Class** Globothalamea PAWLOWSKI *et al.*, 2013

**Order** "Textulariida" Delage & Hérouard, 1896 *partim*

**Superfamily** Coscinophragmatacea THALMANN, 1951

**Family** Haddoniidae CHAPMAN, 1898

GENUS *Haddonia* CHAPMAN, 1898

Type species: *Haddonia torresiensis* CHAPMAN, 1898  
*Haddonia heissigi* HAGN, 1968

**Superfamily** ATAXOPHRAGMIOIDEA SCHWAGER, 1877

**Family** COSKINOLINIDAE MOULLADE, 1965

GENUS *Coskinolina* Stache, 1875

Type species: *Coskinolina liburnica* Stache, 1875  
*Coskinolina* cf. *perpera* HOTTINGER & DROBNE, 1980  
*Coskinolina roberti* SCHLUMBERGER, 1905

**Order** ROTALIIDA DELAGE AND HÉROUARD, 1896

**Superfamily** CHILOSTOMELLACEA BRADY, 1881

**Family** GAVELINELLIDAE HOFKER, 1956

Gavelinellidae indet.

**Superfamily** Planorbuloidea SCHWAGER, 1877

**Family** Cymbaloporidae CUSHMAN, 1927

**Subfamily** Fabianinae DELOFFRE AND HAMAOU, 1973

GENUS *Fabiania* SILVESTRI, 1924

Type species: *Patella (Cymbolia) cassis* Oppenheim, 1896  
*Fabiania cassis* Oppenheim, 1896

**Subfamily** Halkyardiinae KUDO, 1931

GENUS *Halkyardia* HERON-ALLEN AND EARLAND, 1918

Type species: *Cymbalopora radiata* VON HAGENOW VAR. MINIMA LIEBUS, 1911  
*Halkyardia minima* LIEBUS, 1911

**Family** Victoriellinae CHAPMAN AND CRESPIN, 1939

GENUS *Gyroidinella* LE CALVEZ, 1949

Type species: *Gyroidinella magna* LE CALVEZ, 1949

*Gyroidinella levis* GRIMSDALE, 1952

*Gyroidinella eocaenica* SACAL AND DEBOURLE, 1957

*Gyroidinella magna* LE CALVEZ, 1949

GENUS: *Korobkovella* HAGN AND OHMERT, 1971

Type species: *Truncatulina grosserugosa* GÜMBEL, 1870

*Korobkovella grosserugosa* GÜMBEL, 1870

GENUS: *Victoriella* CHAPMAN AND CRESPIN, 1971

Type species: *Victoriella conoidea* RUTTEN, 1914

*Victoriella conoidea* RUTTEN, 1914

**Superfamily** Acervulinoidea SCHULTZE, 1854

**Family** Acervulinidae SCHULTZE, 1854

GENUS *Solenomeris* DOUVILLÉ, 1924

Type species: *Solenomeris ogormani* DOUVILLÉ, 1924

*Solenomeris* cf. *ogormani* DOUVILLÉ, 1924

GENUS *Gypsina* CARTER, 1877

Type species: *Polytrema planum* CARTER, 1877

"*Gypsina*" *moussaviani* BRUGNATTI & UNGARO, 1987

GENUS *Sphaerogypsina* GALLOWAY, 1933

Type species: *Cerriopora globulus* REUSS, 1848

*Sphaerogypsina globulus* REUSS, 1848

**Superfamily** Asterigerinacea D'ORBIGNY, 1839

**Family** Asterigerinidae D'ORBIGNY, 1839

GENUS *Asterigerina* D'ORBIGNY, 1839

Type species: *Asterigerina carinata* D'ORBIGNY, 1839

*Asterigerina rotula* KAUFFMAN, 1867

**Superfamily** Orbitoideoidea SCHWAGER, 1876

**Family** Linderinidae LOEBLICH & TAPPAN, 1986

GENUS *Linderina* SCHLUMBERGER, 1893

Type species: *Linderina brugesi* SCHLUMBERGER, 1893

*Linderina brugesi* SCHLUMBERGER, 1893

**Superfamily** Planorbulinacea SCHWAGER, 1877

**Family** Planorbulinidae SCHWAGER, 1877

GENUS *Planolinderina* FREUDENTHAL, 1969

Type species: *Planolinderina escornebovensi* FREUDENTHAL, 1969

*Planolinderina?* FREUDENTHAL, 1969

**Superfamily** Rotalioidea EHRENBERG, 1839

**Family Rotaliidae EHRENBERG, 1839****Subfamily Rotaliinae EHRENBERG, 1839**GENUS *Rotorbinella* BANDY, 1944

Type species: *Rotorbinella colliculus* Bandy, 1944  
*Rotorbinella hensoni* SMOUT, 1954

GENUS *Rotalia* LAMARCK, 1804

Type species: *Rotalites trochidiformis* LAMARCK, 1804  
*Rotalia trochidiformis* (LAMARCK, 1804)

GENUS *Medocia* PARVATI, 1971

Type species: *Medocia blayensis* PARVATI, 1971  
*Medocia blayensis* PARVATI, 1971

**Family Chapmaninidae THALMANN, 1938**GENUS *Chapmanina* SILVESTRI, 1905

Type species: *Chapmanina gassinensis* SILVESTRI, 1905  
*Chapmanina gassinensis* SILVESTRI, 1905

Taxa Excluded from the Family Rotaliidae by HOTTINGER (2014)

GENUS *Neorotalia* Bermúdez, 1952

Type species: *Rotalia mexicanai* NUTALL, 1928  
*Neorotalia lithamnica* (UHLIG, 1886)

**Family Nummulitidae DE BLAINVILLE, 1825****Subfamily Nummulitinae DE BLAINVILLE, 1825**GENUS *Assilina* D'ORBIGNY, 1839

Type species: *Assilina depressa* D'ORBIGNY, 1850  
*Assilina spira abrardi* SCHAUB, 1981

GENUS *Nummulites* LAMARCK, 1801

Type species: *Camerina laevigata* BRUGUIÈRE, 1792  
*Nummulites lehneri* SCHAUB, 1981  
*Nummulites aspermontis* SCHAUB, 1981  
*Nummulites beneharnensis* DE LA HARPE, 1926  
*Nummulites crassus* BOUBÉE, 1831  
*Nummulites taverdetensis* REGUANT & CLAVELL, 1967  
*Nummulites aturicus* JOLY & LEYMERIE, 1848  
*Nummulites* aff. *deshayesi* D'ARCHIAC & HAIME, 1853  
*Nummulites deshayesi* D'ARCHIAC & HAIME, 1853  
*Nummulites perforatus* (MONTFORT, 1808)  
*Nummulites boussaci* ROZLOZNIK, 1924  
*Nummulites* aff. *bullatus* AZZAROLI, 1952  
*Nummulites migiurtinus* AZZAROLI, 1952  
*Nummulites praediscorbinus* SCHAUB, 1981  
*Nummulites praepuschi* SCHAUB, 1981  
*Nummulites beaumonti* D'ARCHIAC & HAIME, 1853  
*Nummulites biarritzensis* D'ARCHIAC & HAIME, 1853